Cardiovascular Data Analytics for Real Time Patient Monitoring

Ragheed Dawood Salim Allami, M. Sc.

This thesis is submitted in total fulfilment of the requirements for the degree of Doctor of Philosophy

Faculty of Science and Technology
Federation University
PO Box 663
University Drive, Mount Helen
Ballarat, Victoria 3353
Australia

November 2017

Principal Supervisor
Associate Prof. Andrew Stranieri

Associate Supervisors
A/Prof. Herbert F. Jelinek
Dr. Venki Balasubramanian

Abstract

Improvements in wearable sensor devices make it possible to constantly monitor physiological parameters such as electrocardiograph (ECG) signals for long periods. Remote patient monitoring with wearable sensors has an important role to play in health care, particularly given the prevalence of chronic conditions such as cardiovascular disease (CVD)—one of the prominent causes of morbidity and mortality worldwide. Approximately 4.2 million Australians suffer from long-term CVD with approximately one death every 12 minutes.

The assessment of ECG features, especially heart rate variability (HRV), represents a non-invasive technique which provides an indication of the autonomic nervous system (ANS) function. Conditions such as sudden cardiac death, hypertension, heart failure, myocardial infarction, ischaemia, and coronary heart disease can be detected from HRV analysis. In addition, the analysis of ECG features can also be used to diagnose many types of life-threatening arrhythmias, including ventricular fibrillation and ventricular tachycardia. Non-cardiac conditions, such as diabetes, obesity, metabolic syndrome, insulin resistance, irritable bowel syndrome, dyspepsia, anorexia nervosa, anxiety, and major depressive disorder have also been shown to be associated with HRV.

The analysis of ECG features from real time ECG signals generated from wearable sensors provides distinctive challenges. The sensors that receive and process the signals have limited power, storage and processing capacity. Consequently, algorithms that process ECG signals need to be lightweight, use minimal storage resources and accurately detect abnormalities so that alarms can be raised. The existing literature details only a few algorithms which operate within the constraints of wearable sensor networks.

This research presents four novel techniques that enable ECG signals to be processed within the limitations of resource constraints on devices to detect some key abnormalities in heart function.

- The first technique is a novel real-time ECG data reduction algorithm, which detects and transmits only those key points that are critical for the generation of ECG features for diagnoses.
- The second technique accurately predicts the five-minute HRV measure using only three minutes of data with an algorithm that executes in real-time using minimal computational resources.

- The third technique introduces a real-time ECG feature recognition system that can be applied to diagnose life threatening conditions such as premature ventricular contractions (PVCs).
- The fourth technique advances a classification algorithm to enhance the performance of automated ECG classification to determine arrhythmic heart beats based on noisy ECG signals.

The four novel techniques are evaluated in comparison with benchmark algorithms for each task on the standard MIT-BIH Arrhythmia Database and with data generated from patients in a major hospital using Shimmer3 wearable ECG sensors. The four techniques are integrated to demonstrate that remote patient monitoring of ECG using HRV and ECG features is feasible in real time using minimal computational resources.

The evaluation show that the ECG reduction algorithm is significantly better than existing algorithms that can be applied within sensor nodes, such as time-domain methods, transformation methods and compressed sensing methods. Furthermore, the proposed ECG reduction is found to be computationally less complex for resource constrained sensors and achieves higher compression ratios than existing algorithms.

The prediction of a common HRV measure, the five-minute standard deviation of inter-beat variations (SDNN) and the accurate detection of PVC beats was achieved using a Count Data Model, combined with a Poisson-generated function from three-minute ECG recordings. This was achieved with minimal computational resources and was well suited to remote patient monitoring with wearable sensors. The PVC beats detection was implemented using the same count data model together with knowledge-based rules derived from clinical knowledge.

A real-time cardiac patient monitoring system was implemented using an ECG sensor and smartphone to detect PVC beats within a few seconds using artificial neural networks (ANN), and it was proven to provide highly accurate results. The automated detection and classification were implemented using a new wrapper-based hybrid approach that utilized t-distributed stochastic neighbour embedding (t-SNE) in combination with self-organizing maps (SOM) to improve classification performance. The t-SNE-SOM hybrid resulted in improved sensitivity, specificity and accuracy compared to most common hybrid methods in the presence of noise. It also provided

a better, more accurate identification for the presence of many types of arrhythmias from the ECG recordings, leading to a more timely diagnosis and treatment outcome.

Declaration

Except where explicit references are made, the text of this work contains no material submitted previously, or extracted in whole or in part from any other academic award. No other person's work has been relied upon or utilized without due acknowledgement in the main text and bibliography of the work.

Ragheed Allami
Faculty of Science and Technology
Federation University
27 November 2017

List of Publications

- Allami, R., Stranieri, A., Balasubramanian, V. & Jelinek, H. F. (2017). A count data model for heart rate variability forecasting and premature ventricular contraction detection. *Signal, Image and Video Processing*, 11, 1427-1435.

- Allami, R., Stranieri, A., Balasubramanian, V. & Jelinek, H. F. (2016). A genetic algorithm-neural network wrapper approach for bundle branch block detection. *Proceedings of the Computing in Cardiology Conference (CinC)* (pp. 461-464). Vancovor, Canada, IEEE.

- Allami, R., Stranieri, A., Balasubramanian, V. & Jelinek, H. F. (2016). ECG Reduction for Wearable Sensor. *Proceedings of the 12th International Conference on Signal-Image Technology & Internet-Based Systems (SITIS)* (pp. 520-525). Naples, Italy, IEEE.

Acknowledgements

I would like to express my substantial gratitude to my principal supervisor, Andrew Stranieri, for his valuable guidance and tremendous support. He has been a constant inspiration throughout my Ph.D. journey. I have learned many things from Prof. Stranieri such as research skills, writing skills, and hard work. If it were not for his guidance and motivation, it would not have been possible for me to reach the hill of doctoral level research work in a foreign country and with a lot of family commitments. I would also like to thank my associate supervisors, Dr. Venki Balasubramanian and Dr. Herbert Jelinek, for their guidance and support. Special thanks are due to Senior Cardiologist Dr. Hazim Allawi and his staff from Ibn Alnafees Hospital in Baghdad for being actively involving in this PhD project, providing real time ECG data, classifying ECG data, medical knowledge and terminologies related to cardiology. Also, I would like to thank the expert cardiologist Dr. Saheb Al-Daher from Australia for his valuable recommendations, classifying ECG segments and providing specialist knowledge, as well as the staff at the research services and the Faculty of Science and Technology for their consistent support and the good research environment provided by the school.

I would also like to extend my sincerest thanks and appreciation to the Ministry of Higher Education & Scientific Research and the University of Technology in Iraq for making this academic project a reality.

A special thanks to my parents who sacrificed a lot for me. Without them, I would not be at this stage in my life. Their prayers have always helped me. Last but not least, thanks to my dearest wife and great love Zina for her unwavering support and patience. I got my strength to continue my PhD thesis from my family and their kind words which encouraged me to reach this stage.

Statement of Ethics Approval

Approval to use existing data and access completely de-identified data gathered and supplied by Ibn Alnafees Hospital in Baghdad, Iraq (responsible for gaining consent of the patients for the use of their data) has been granted.

Principal Researcher:	A/Prof Andrew Stranieri
Other/Student Researcher/s:	Mr Ragheed Allami Dr Venki Balasubramanian Dr Herbert Jelinek Dr Hazim Allawi
School/Section:	**Faculty of Science and Technology**
Project Number:	**A16-011**
Project Title:	**Cardiovascular Analysis for Real Time Patient Monitoring.**
For the period:	01/11/2016 **to** 30/03/2018

Please quote the project number in all correspondence regarding this application.

REPORTS TO HREC:

An annual report for this project must be submitted to the Ethics Officer on:
1 November 2017

A final report for this project must be submitted to the Ethics Officer on:
30 April 2018

These report forms can be found on:
http://federation.edu.au/research-and-innovation/research-support/ethics/human-ethics/human-ethics3

Ethics Officer
1 November 2016

Table of Contents

List of Figures

List of Abbreviations

Amplitude Zone Time Epoch Coding	AZTEC
Artificial Neural Network	ANN
Atrial Premature Contraction	APC
Atrioventricular	AV
Autonomic Nervous System	ANS
Baseline Wander	BW
Best Matching Unit	BMU
Bundle Branch Block	BBB
Cardiovascular disease	CVD
Cascade Forward Neural Network	CFNN
Code Compose Studio	CCS
Compressed sensing	CS
Compression Ratio	CR
Coordinate Reduction Time Encoding System	CORTES
Discrete Wavelet Transformation	DWT
Electrocardiograph	ECG
Electromyogram	EMG
First Order Interpolator	FOI
First Order Predictor	FOP
Genetic Algorithm	GA
Heart Rate Variability	HRV
High Frequency	HF
Low Frequency	LF
Multi-Layer Perceptron	MLP
Parasympathetic Nervous System	PNS

Percentage Root Mean Square Difference	PRD
Premature Ventricular Contraction	PVC
Principal Component Analysis	PCA
Root Mean Square Error	RMSE
Root Mean Square of Successive Differences	RMSSD
Self-Organizing Maps	SOM
Standard deviation of normal to normal	SDNN
Stochastic Neighbour Embedding	SNE
Support Vector Machine	SVM
Symbolic Dynamics	SDyn
Sympathetic Nervous System	SNS
t-distributed Stochastic Neighbour Embedding	t-SNE
Turning Point	TP
Ultra Low Frequency	ULF
Very Low Frequency	VLF
Zero Order Interpolator	ZOI
Zero Order Predictor	ZOP

CHAPTER 1

1 Introduction

1.1 Background and Motivation

Chronic diseases are those that may not be directly life threatening in the short-term but must be managed and controlled, often for many years, using a great deal of health sector resources. Chronic conditions represent common causes of disability and death around the world as disease pathology progresses (Australia Institute of Health and Welfare, 2015). Cardiovascular diseases (CVDs) are one of the more prominent chronic diseases in many countries. Each year, the American Heart Association (AHA) publishes statistics on heart diseases, stroke, and other vascular diseases and their risk factors. Recently, the AHA showed that mortality rates reached 40.6% due to cardiovascular diseases (Rodríguez-Liñares, Lado, Vila, Méndez, & Cuesta, 2014). Heart diseases represent approximately 7.2 million deaths around the world (Heart Foundation, 2016). For instance, approximately 4.2 million Australians have long-term heart diseases and roughly every 12 minutes one of them dies from cardiovascular diseases (Heart Foundation, 2016).

Since the cost of treatment has a considerable impact on a country's economy, the improvement of effective techniques for the early detection and prevention of CVD is crucial for minimizing the burden of treatment in heart disease (Martis, Prasad, Chakraborty, & Ray, 2014b). Continuous monitoring can help patients manage chronic conditions (Hamine, Gerth, Faulx, Green, & Ginsburg, 2015) more effectively. The improvement of wearable sensor devices in recent years makes it possible to constantly monitor physiological parameters such as electrocardiograph (ECG) over long intervals (Lou et al., 2013).
Mobile health care can accomplish the aim of continuously monitoring patients' physiological status using indicators such as body temperature, electrocardiograph (ECG) and respiration rate.

Ranck (2014) has estimated that there will be 170 million wearable devices for measuring medical indicators such as ECG, HRV and body temperature, in the world, by 2017. Many of these devices are likely to be operated by hospitals to monitor the progress of discharged patients at home in order to identify disease progression or anomalies in a timely manner and achieve real cost savings in an era of increasing healthcare costs with the inability of government capacity to meet the gap. Some early examples of field trials and prototypes with the use of wearable devices are emerging for

diabetes complications (Habib, Biswas, Akter, Saha, & Ali, 2010), and early detection of heart failure, arrhythmias and depression (Huang , Huang, & Liu, 2014; Nguyen, Lou, Caelli, Venkatesh, & Phung, 2014).

In a body area wireless sensor network (BAWSN) the wearable sensors are found on the top of the body that can transmit vital health data using a wireless protocol such as Bluetooth, ZigBee or Wi-Fi to a nearby base station, which is often a smartphone or a tablet. In addition, the vital health data are received by healthcare applications (HA) that are required to process the data in order to raise alarms or perform other actions if the patient's health deteriorates.

Figure 1.1 a illustrates a patient wearing an ECG sensor, an electromyographic (EMG) sensor and an accelerometer taken from Balasubramanian and Stranieri (2014) at Federation University.

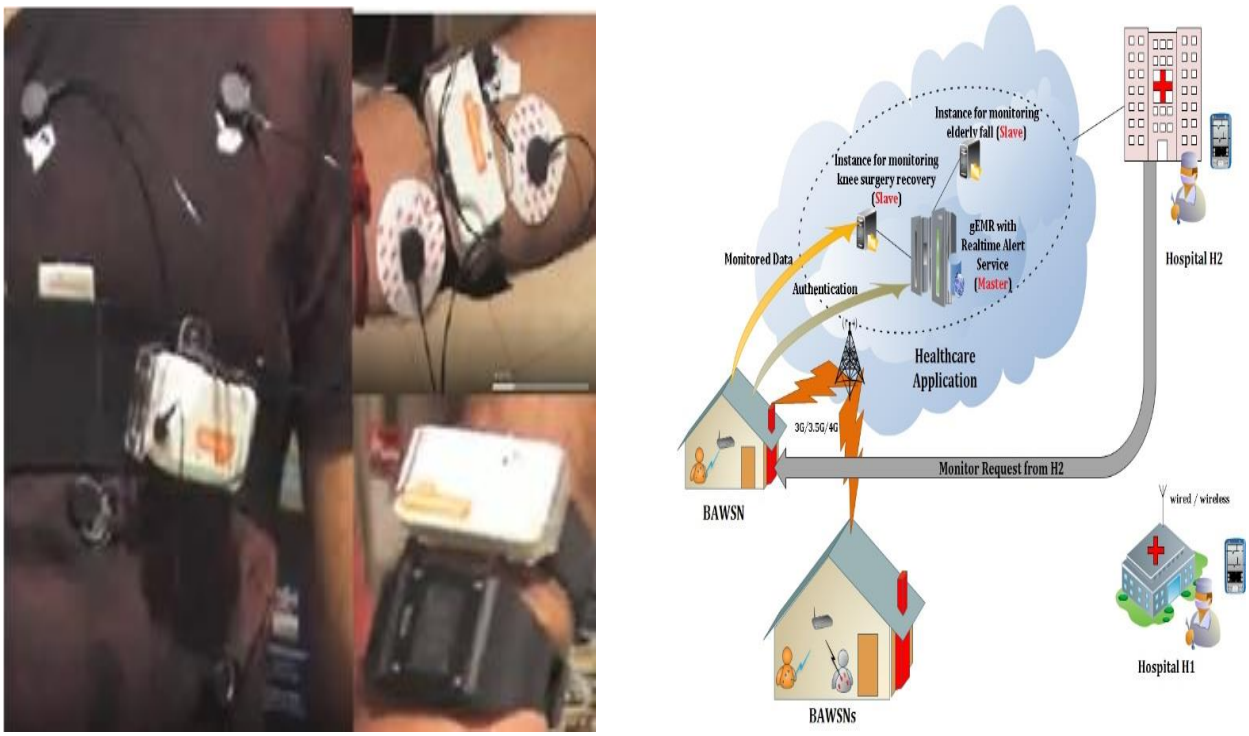

(a) (b)

Figure 1.1 a. A patient wearing Shimmer ECG devices on the chest, EMG in the forearm and an accelerometer in the wrist (a). Figure 1.1b. Schematic of a patient monitoring architecture. Reproduced with permission from Balasubramanian and Stranieri (2014).

The sensors illustrated in Figure 1.1a are programmable sensors from Shimmer3 (Shimmer, 2015) that can stream data in real time to a mobile device that executes a program to analyse the data, port it to Cloud repositories and raise alarms if necessary (Figure 1.1b).

Real-time monitoring systems require continuous and reliable processing of health data (Laplante & Ovaska, 2011). They require algorithms that continuously process the received health data from the devices that have limited battery and memory capacity (Islam, Mamun, & Rahman, 2014; Laplante & Ovaska, 2011; Mukhopadhyay, Mitra, & Mitra, 2012). For real-time processing in tele-monitoring systems, the time required to analyse the biological data should be less than the time required to collect that data, during continuous streaming of data from the sensor device (Sufi & Khalil, 2008). Furthermore, the transmission of data from sensors to mobile devices with Bluetooth or Zigbee protocols, especially in the presence of other transmission protocols, is known to be very noisy and consume more demanding of power (Gough, 2011; Islam et al., 2014; Shin, Park, & Kwon, 2007). Signals from body area wireless sensors of nearby patients, Wi-Fi access points, mobile phone transmissions all contribute to interference so the data is lost or corrupted (Islam et al., 2014; Mukhopadhyay et al., 2012).

Table 1.1 represents the standards measurements of wireless communication techniques that are commonly used with sensors and mobile phones (Lee, 2016).

Table 1.1. Wireless communication standards

Technique	**Range**	**Data Rate**	**Power consumption**
Zigbee	10-75 m	20-250 kbps	30mW
Bluetooth	10-100 m	1-3 Mbps	2.5-100mW
Wi-Fi (802.11g)	200 m	54Mbps	1W

The automated detection and classification of arrhythmias is important for prompt, accurate diagnosis and treatment to reduce morbidity and mortality. Irregular heartbeats and presence of noise impede cardiologists in detection of arrhythmias. In addition, visual analysis of long term biosignals such as ECG consumes time and may cause misdiagnosis or produce inaccurate diagnosis of the heart rhythm (Goldberger, Goldberger, & Shvilkin, 2017).

Noise and data transmission losses are likely to heavily affect wearable ECG sensors because of interference from other portable devices. Existing arrhythmia classification methods were tested on noise-free or carefully chosen and often clean ECG signals, which produced accurate classification results (Elhaj, Salim, Harris, Swee, & Ahmed, 2016). However, these methods may not provide the same high accuracy in the presence of a noisy ECG.

The current research was concerned with identifying and developing algorithms for remote patient monitoring that reduce the data needed to be transmitted so that the sensor and mobile device battery life can be extended. The research was also concerned with developing algorithms that forecast HRV minutes in to the future, and are able to execute with minimal storage and processing capacity. In

addition, the thesis focused on developing advanced machine learning algorithm for reliable and robust analysis of ECG signals for the automatic classification and detection of various cardiac arrhythmias.

Most of the algorithms focused on in this research involve the analysis of heart function using new approaches for ECG signal and heart rate variability (HRV) analysis. The next section demonstrates ECG features, then HRV analysis will be further explained.

1.2 Basic ECG Components

An ECG is a non-invasive technique to read the electrical function of the heart over an interval of time by placing electrodes on the body. It is commonly used for diagnosis of cardiovascular diseases due to its simplicity and non-invasive nature (Goldberger et al., 2017). A normal ECG beat/cycle, called Normal Sinus Rhythm (NSR), as shown in Figure 1.2, can be illustrated by a signature waveform.

Figure 1.2 depicts an ECG signature waveform composed of five peaks and troughs P, Q, R, S, and T. Each wave is generated by a physiological event of the heart where the P wave reflects the depolarisation of the atria muscle; it has a duration of 0.08–0.11 seconds in a healthy heart. The Q, R, S points represent the QRS complex that derives from the depolarisation of the ventricular muscle with a normal duration of 0.06–0.10 seconds. The T wave indicates the repolarisation of the ventricular muscle that normally has a duration of 0.20 seconds (Rai, Trivedi, & Shukla, 2013). ECG signals obtained from three to ten leads, where electrical activity is typically measured 1000 times per second. Consequently, an ECG signal generates large streams of data and requires large space on storage devices to be kept in digital form (Task Force of the European Society of Cardiology, 1996).

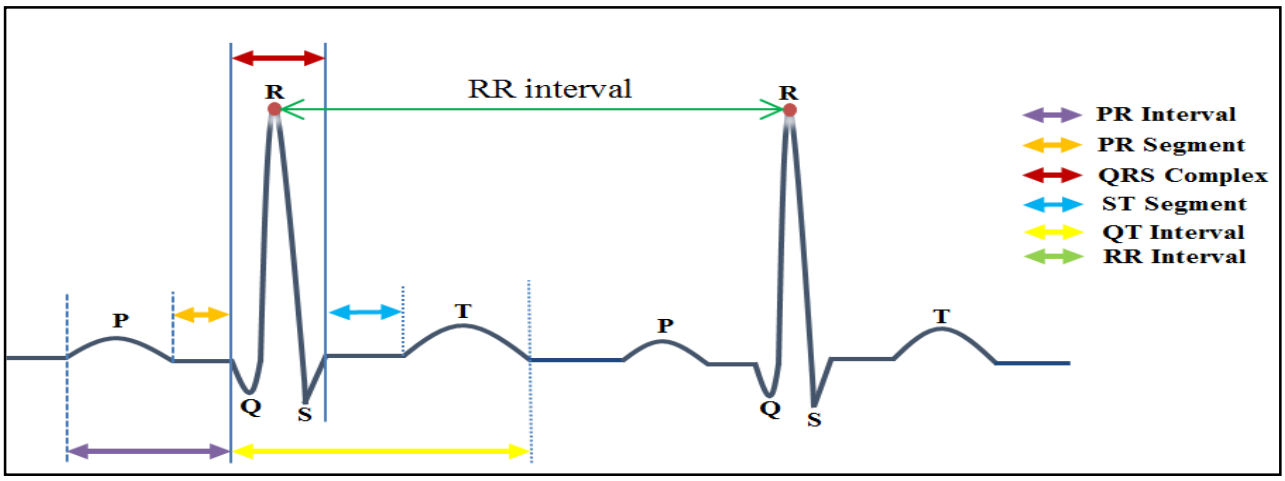

Figure 1.2. ECG signal diagnostic features

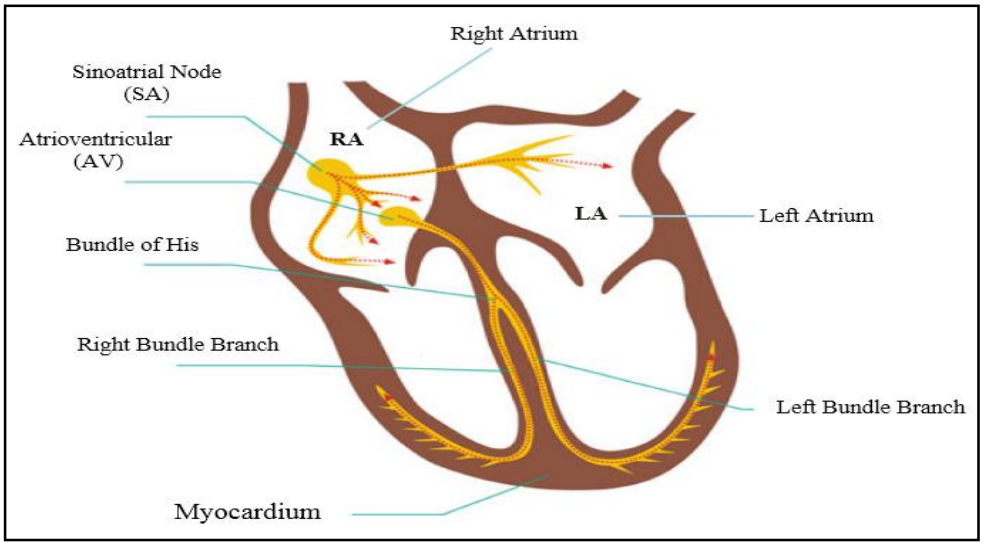

Figure 1.3. Electrical conduction system of the heart (Wasilewski & Poloński, 2012)

Many heart arrhythmias can be detected from ECG waves, segments, and intervals. The P wave starts with the first deflection from baseline and ends when the wave meets the baseline once again. The P wave strongly suggests that the atria have followed through with a contraction

The PR segment is the section between the end of the P wave and the starting of the QRS complex. It represents the electrical conductivity through the slow atrioventricular (AV) junction (Reed, Robertson, & Addison, 2005)

The PR interval starts at the end of the P wave to the start of the QRS complex. It produces clues to both the location of the originating impulse and the integrity of the conduction tracks of the heart. The PR interval measures the AV node efficiency. Also, it assesses the duration taken for an electrical impulse to travel from the sinus node to the AV node. PR intervals longer than 0.2 seconds are usually diagnosed to be symptoms of first degree heart block, while PR intervals shorter than 0.12 seconds could be considered as tachyarrhythmia (Goldberger et al., 2017).

The QRS complex represents the tracks of ventricular depolarisation. Early depolarisation produces a small downward deflection called the Q wave. A normal Q wave is narrow and small in amplitude. Following depolarisation of the interventricular septum, ventricular depolarisation then progresses from the endocardium through to the epicardium across both ventricles generating the R and S waves. The R wave is the first positive deflection of the QRS complex. The S wave follows the R wave and continues below the baseline or isoelectric line. Abnormal ventricular depolarisation can produce QRS complexes that often have altered characteristics. The QRS complex width represents an

important diagnostic feature and indicates the location of the originating electrical impulse for ventricular contraction. The morphology of the QRS complex is often used to diagnose different heart diseases (Gacek & Pedrycz, 2011; Rodríguez-Liñares et al., 2014).

The QT interval reflects the full ventricular cycle of depolarisation and repolarisation. It represents the interval from the starting of the QRS complex to the end of the T wave. The QT interval is less than half the RR interval. It is highly variable, depending on gender, age, heart rate and the influence of drugs. A prolonged QT interval longer than 0.45 seconds is an indicator of ventricular tachyarrhythmia, which is a risk factor of sudden death (Gertsch, 2008).

The PR segment and ST segment are both isoelectric in that no electrical activity can be collected from the surface electrodes over this period. Hence, there is no wave deflection visible on the ECG waves. The ST segment reflects depolarisation of the ventricles. This segment can reveal insufficient blood supply to the heart, also called ischemia, when it is depressed or elevated from the isoelectric line. This shift from the isoelectric is created by the changes in electrical current flow properties of the dead conductive cells, because of ischemia from coronary blockage. ST segment elevation refers to myocardial infarction, while ST segment depression represents coronary ischemia, which may be produced by overdose of substance or coronary blockage, e.g. digoxin or potassium (Gregg, Zhou, Lindauer, Helfenbein, & Giuliano, 2008).

1.3 Heart Rate Variability

One of the most promising analyses to assess heart activity is heart rate variability (Task Force 1996; ChuDuc, NguyenPhan, & NguyenViet, 2013). HRV is a physiological event that describes the changes in time between successive heartbeats, which is controlled by the autonomic nervous system (ANS) and endocrine activity (Miličević, 2005). The ANS consists of the parasympathetic nervous system (PNS) and the sympathetic nervous system (SNS). The PNS initiates a slow diastolic depolarisation of heart tissues, which decreases the heart rate. The SNS initiates a quick diastolic depolarisation of heart tissues, which increases the heart rate, and the balance of these two systems ensures the integrity of the heart rate and its variability (Johnson & Loewy, 1990).

The assessment of HRV represents a simple and non-invasive technique that can be exploited to provide an indication of ANS function (Widjaja, Vlemincx, & Van Huffel, 2012). In cardiac patients, for example, a reduction in HRV can be associated with sudden cardiac death, hypertension, heart failure, myocardial infarction, ischemia and coronary heart disease (Jarrin, McGrath, Giovanniello, Poirier, & Lambert, 2012; Rodríguez-Liñares et al., 2011) and in non-cardiac patients it can indicate

cardiac rhythm changes associated with diabetes, obesity, metabolic syndrome, insulin resistance, irritable bowel syndrome, dyspepsia, anorexia nervosa, anxiety, risk of mortality and major depressive disorder (Jarrin et al., 2012).

HRV estimations are calculated from ECG information. Most effectively, inter-beat intervals or the time from normal ECG peak of the beat (the R peak) to the next normal R peak is called the RR or NN (normal to normal) interval, which is typically measured in milliseconds (Kranjec, Beguš, Geršak, & Drnovšek, 2014) and illustrated in Figure 1.2. The R peak is the largest upward deflection of a normal ECG as shown in Figure 1.2 and indicates depolarisation of the ventricles (Reed et al., 2005). RR interval/ RR data can be calculated from short-term or long-term ECG records. Short-term measurement is normally based on at least five minutes of recording. Long-term measurement is normally for several hours up to 24 hours and longer (Khandoker, Karmakar, Brennan, Palaniswami, & Voss, 2013). The next section describes the problem in more detail and advances specific research aims.

1.4 Thesis Contribution

Although ECG data, and particularly HRV, is promising for remote patient monitoring systems, the majority of algorithms that analyse HRV have not been developed for real time processing of signals, robustness to noise or minimal computational requirements. Fang, Huang, and Tseng (2013) and Elgendi (2013) have identified that approaches to process ECG signals that rely on smaller datasets and execute faster are required for remote patient monitoring because they require low complex resources. In this research, new algorithms for ECG transmission, ECG classification, and HRV analysis have been advanced and evaluated against existing approaches to assess the extent to which the new algorithms are suited for remote patient monitoring and arrhythmias detection.
The project's overriding aim is to advance a new approach to remote patient monitoring by:

1. Advancing an algorithm for reducing ECG signals to compress the amount of data that needs to be transmitted.
2. Advancing a new real-time algorithm that forecasts HRV measures minutes into the future so HRV can be analysed ahead of time.
3. Advancing new techniques that detect and classify arrhythmias from normal beats based on noisy or free noise signals.

The new ECG reduction method depends on analysing a simple statistical algorithm we referred to as Max_Min with a sliding window technique that directly selects only those key points on an ECG

signal in the time domain, which are critical for the maintenance of ECG signal quality and generation of accurate ECG diagnostic features.

The advanced forecasting algorithm relies on data models known as "count data" systems. Count data is statistical data, which represents the number of data occurrences over a specified interval or event (Cameron & Trivedi, 2013). The count data model has emerged as a powerful statistical tool in many fields such as machine learning, pattern recognition, data mining, medical, and bioinformatics (Bakhtiari & Bouguila, 2014; Tu & Koh, 2017). In medical investigations, count data is often measured using binomial or Poisson models, which are discrete probability distributions (Sloane & Morgan, 1996; Tang, He, & Tu, 2012). A binomial model represents the discrete probabilities of each of the possible numbers that appear in a known sample set. It forecasts the number of successes in a given number of trials (Cameron & Trivedi, 2013). A Poisson model represents a common approach to process count data. It is a statistical model, which refers to the number of discrete events that are observed in a given interval of time or space such as the number of phone calls in 24 hours. It also estimates the range of spread around a known average rate of occurrence (Winkelmann, 2013).

The detection of a premature ventricular contraction rhythm depends on a count data model and a rule-based system generated from clinical experiences. A rule-based system provides rules that are used to represent facts as a set of if-then statements known as production rules or if-then rules (Grosan & Abraham, 2011). More details on the count data model and rule-based system are explained in Chapter 3 and Chapter 4.

A novel method for the accurate classification of cardiac arrhythmia to identifying various types of arrhythmia based on ECG features is proposed in this thesis. This work applied the most common methods of ECG-based cardiac arrhythmia classification by evaluating the signal pre-processing, heart beat segmentation, feature extraction and machine learning algorithms. Four different combined structures including genetic algorithm (GA) with artificial neural network (ANN), principal component analysis (PCA) with ANN, GA-SVM (support vector machine), and PCA-SVM were formed by engaging two filtering techniques that are widely used with ECG signal namely Haar wavelet and Butterworth FIR to render the obscure complexities in the noisy ECG signal. Furthermore, a new arrhythmia classification technique is introduced by combining t-distributed stochastic neighbour embedding (t-SNE) with self-organizing maps (SOM). The t-SNE visualises high-dimensional data by providing each data sample a position in a two or three-dimensional map (Maaten & Hinton, 2008). This approach is a modification of the stochastic neighbour embedding (SNE) (Hinton & Roweis, 2003). The SOM algorithm is an example of an unsupervised machine

learning technique and is commonly exploited for structure visualisation of high dimensional data. The location of points in a two-dimensional grid aims to reflect the similarities between the corresponding patterns in a multidimensional space (Kohonen, 1982). The SOM is widely applied to classification and clustering problems in many fields such as data exploration in industry, finance, natural sciences, medical and linguistics (Kim & Mazumder, 2017; Kolasa, Długosz, Talaśka, & Pedrycz, 2017). It allows for visualisation of relationships between patterns in a multidimensional space. More information on the t-SNE and SOM is found in Chapter 5.

1.5 Research Questions

As illustrated above, the research aims to advance a new approach to remote patient monitoring. The following research questions will be addressed to meet each aim:

Q1. How can ECG be reduced with minimal computational resources for battery driven devices so that key ECG indicators can be readily extracted and battery life extended?

Q2. How can short duration HRV indicators be predicted minutes ahead of their occurrence within the constraints of remote patient monitoring?

Q3. How can a life-threating rhythm (PVC) be detected using HRV features within the constraints of remote patient monitoring?

Q4. How can many types of arrhythmias be classified using ECG features within the presence of remote patient monitoring noise?

As aforementioned, the thesis aims to advance a novel technique to remote patient monitoring. Each of the sub-aims of this research will be discussed in the following sections prior to the description of HRV measurements and arrhythmias detection.

1.6 ECG Reduction/Compression

ECG datasets become so large quickly that (Padhy, Sharma, & Dandapat, 2016) and (Sufi & Khalil, 2011b) have raised the need for data reduction/compression techniques to be developed for ECG streams so that functionalities such as ambulatory recording systems, ECG signal storage, ECG signal transmission over digital telecommunication or wireless networks, become practically feasible. Furthermore, many wearable ECG devices (e.g. Shimmer ECG Sensor) have recently emerged that

deploy the Bluetooth protocol to stream ECG data to a mobile device for transmission to servers for online storage. These devices require ECG reduction/compression and simple algorithms to maintain ECG key points and calculate ECG in real time because of inherent limitations of battery-operated devices, including memory, processor capacity and power-consumption constraints. Along a similar vein, Elgendi (2013) and Fang et al. (2013) have identified that approaches to process ECG signals that rely on smaller datasets and execute faster are required for remote patient monitoring.

ECG compression methods encode the ECG data to compress the amount of ECG data that needs to be stored or transmitted. Also, they require to decode/reconstruct the compressed ECG data to extract the raw ECG data, while ECG reduction methods reduce the amount of ECG data by selecting the important ECG data and omitting the remaining. Thus, they do not require a reconstruction process to extract the raw data that leads to the consumption of reduced computational resources and power for battery-driven devices. In general, ECG reduction/compression techniques are grouped into three categories; direct time domain techniques, transform techniques and parameter techniques (Jalaleddine, Hutchens, Strattan, & Coberly, 1990; Rossi et al., 2002). Direct time domain techniques have lower complexity than transform and parameter techniques. Consequently these algorithms can be easily executed in mobile devices (Rossi et al., 2002). Direct time domain algorithms apply simple interpolation techniques, which usually harness previous information to predict future samples (Jalaleddine et al., 1990). Recently, a compressed sensing (CS) algorithm has been introduced as a powerful method to compress ECG signal. CS collects only the sparse samples in a particular domain. A signal has sparse description if small samples of its coefficients represent a major percentage of the energy (Craven, McGinley, Kilmartin, Glavin, & Jones, 2015). In fact, the CS algorithm acquires important coefficients/non zero samples and applies mathematical methods such as L1 optimisation to retrieve the raw data during reconstruction. Nonetheless, few investigations have simulated CS on the Shimmer ECG sensor in order to decrease power consumption (Craven et al., 2015).

This thesis introduces a new ECG reduction algorithm, which has been tested clinically and on test samples. It was implemented on the ECG sensor node, maintained all ECG key points/diagnostic features and extended the sensor battery life significantly. This algorithm was compared with existing real time ECG compression/reduction methods that can execute on the Shimmer ECG sensor.

High performance and low complexity compression and ECG measurement schemes for medical signals are crucial in applications related to mobile healthcare and real-time patient monitoring.

1.7 Forecasting HRV Minutes into the Future

The Task Force (1996) recommends that HRV analysis should be calculated over five minutes for a short-term analysis. Many researchers have attempted to estimate the five-minute HRV in a shorter time than the Task Force recommended. For example, Smith, Owen, and Reynolds (2013a) provided a survey including the methods used to analyse HRV for less than a 60-second period. The survey comprised assessments of frequency domain, time domain and nonlinear parameters. The authors indicated that these parameters require validation from clinics before they can be applied to short-term HRV measurement. Chang and Lin (2005) compared three-minute with five-minute HRV analysis. This research indicated that HRV indices can accurately be calculated from three minutes except the all-important SDNN parameter. Recently, many investigations (Chen, Yao, Yin, & Li, 2017; Jelinek, Adam, Krones, & Cornforth, 2017; Khandoker, Jelinek, & Palaniswami, 2009) have approved the Chang and Lin (2005) finding.

In this thesis, an algorithm that can accurately predict the five-minute SDNN parameter from three minutes of data is advanced. The key advantage of the proposed algorithm is an accurate prediction of many HRV, including SDNN indices from three minutes of data. The algorithm executes so quickly that it can be revised in real time as each new data point is sensed. Furthermore, many investigations proposed that the SDNN/RMSSD ratio can be used as surrogate for the LF/HF parameter (Antônio, Cardoso, & De Abreu, 2014; Brisinda, Venuti, Iantorno, Efremov, & Cataldi, 2014). Recently, numerous studies reported that SDNN/RMSSD achieved higher accuracy results than LF/HF (Billman, 2013; Holper, Seifritz, & Scholkmann, 2016), which means that if the SDNN index can be predicted from three minutes, it can help to analyse HRV only from time domain parameters, especially in real time monitoring platforms in three minutes. In addition, HRV parameters (Time domain parameters) can be executed on battery driven devices because existing methods that are used to calculate HF and LF require high computational resources.

HRV is typically assessed in the short-term or long-term. Reed et al. (2005) demonstrated that existing HRV methods require all RR data be available over a five-minute analysis (period for a short analysis) or 24 hours (for a long analysis). In addition, existing algorithms are computationally complex so it can be expected to use a high level of computational resources in order to assess HRV. More details on the forecasting method are demonstrated in Chapter 3.

1.8 Arrhythmia Classification

Arrhythmias are heart pulses that become either too slow (bradycardia), or too fast (tachycardia), and/or abnormal. There are various patterns of arrhythmias, some of which are harmless, whereas others produce critical health conditions. On the one hand, ventricular arrhythmias are fatal. On the other hand, atrial arrhythmias are less life-threating, but atrial fibrillation raises the risk of stroke (Qu, Hu, Garfinkel, & Weiss, 2014).

Premature ventricular contraction (PVC) is a serious cardiovascular condition that can lead to life-threatening conditions. The instant recognition of life-threatening cardiac arrhythmias is a challenging problem of clinical significance (Li et al., 2014; Liu et al., 2012; Liu et al., 2010).

Although, several studies employed RR data to classify and detect PVC beats (Nabil & Reguig, 2015), approaches that are sufficiently accurate and can execute rapidly for fast real-time PVC detection have proven to be elusive.

We provide a new PVC arrhythmia detection method that employs three-minute RR data to reliably detect PVC beats in a simple and fast way within the constraints of remote patient monitoring. Moreover, it detects PVC beats from non-PVC beats, using intelligent data mining methods in a few seconds. The third thesis question regarding arrhythmia detection within the limitation of battery operated devices is addressed in Chapter 4.

Numerous studies used different linear and nonlinear techniques generated from ECG features to recognise arrhythmias, e.g. artificial neural network (ANN) methods, discrete wavelet transformation (DWT) methods, principal component analysis (PCA) method, linear discrimination analysis (LDA) method, independent component analysis (ICA) method, support vector machine (SVM) algorithm, genetic algorithm (GA), and self organisation method (SOM). Furthermore, some investigations combined the above techniques to enhance the classification accuracy. For instance, Martis, Acharya, and Min (2013) combined PCA, LDA and ICA with ANN and SVM. Also, (Allami, Stranieri, Balasubramanian, & Jelinek, 2016b) proposed a wrapper hybrid technique, GA-ANN to detect and classify bundle branch block (BBB) arrhythmia. A (BBB) is a delay or obstruction along electrical impulse pathways of the heart manifesting in a prolonged QRS interval usually greater than 120ms. The automated detection and classification of a BBB is important for prompt, accurate diagnosis and treatment to reduce morbidity and mortality.

These methods require more complex computations processing than HRV arrhythmia detection methods because they consist of three main stages, namely feature extraction, feature selection, and classifier construction (Wang, Chiang, Hsu, & Yang, 2013). The current state-of-the-art methods of ECG-based automated abnormalities heartbeat classification have been surveyed by presenting ECG signal pre-processing, heartbeat segmentation techniques, feature description methods, and learning algorithms. More details on the linear and nonlinear methods are described in Chapter 5.

One of the main aims of this research was to develop advanced machine learning algorithms for reliable and robust analysis of ECG signals for timely detection of various cardiac arrhythmias. In this thesis, the construction of optimised classification models and their performance in detection of various arrhythmias are reported. In addition, a new classification method that can enhance and speed the classification accuracy is proposed. This significant improvement of cardiac arrhythmia classification, which is exhibited by the new ECG beat classifier improves the efficiency of cardiovascular monitoring in a clinical setting. Heart rate variability measurements and ECG features have been widely used to detect arrhythmias. These HRV measurements are outlined in the next sub-section.

1.9 Heart Rate Variability Measurements

Time domain and frequency domain evaluations represent the most common linear methods for HRV analysis. Time domain measurements rely on statistical methods, and frequency domain measurements depend on power spectrum density (Ong et al., 2008). Due to the sophistication of the heart control function, it is unlikely that HRV can be entirely explained using linear techniques. Consequently, many nonlinear techniques have been used to identify the properties of the beat-to-beat variability (Tarvainen, Niskanen, Lipponen, Ranta-Aho, & Karjalainen, 2014). The next section illustrates linear (Time and Frequency domain) and nonlinear (e.g. entropy methods) HRV measurements.

1.9.1 Time domain methods

Time domain techniques are applied directly to a series of successive RR items. The simplest is the mean value of RR cycles or, similarly, the mean HR. Several indices have been applied to assess the variability of RR cycles:

SDNN (the standard deviation of normal to normal RR cycles) represents the overall (both long-term and short-term) variation within the RR interval series (Niskanen, Tarvainen, Ranta-Aho, & Karjalainen, 2004). Low values usually refer to possible disease and low heart rate variability

(Khandoker et al., 2013). A healthy heart has a SDNN value of 141+/−39ms for 24-hour measurements (Task Force, 1996). In Chapter 3, the SDNN is estimated using a count data model.

SDANN (the standard deviation of the average RR cycles) assesses five-minute segments over a 24-hour recording to measure the autonomic influence on HRV (Niskanen et al., 2004). A healthy heart has an SDANN value of 127+/−35ms (Task Force, 1996).

RMSSD (the root mean square of successive differences of the RR cycles) has been used as a measure of the short-term variability (Niskanen et al., 2004). A healthy heart has an RMSSD value of 27+/−12ms (Task Force, 1996).

NN50 (the number of successive cycles differing by more than 50ms) is a short-term HRV measurement (Niskanen et al., 2004), while pNN50 is the segment of NN50 intervals as a proportion of the complete value of NN intervals (Niskanen et al., 2004).

SDNN and SDANN measure both the sympathetic and parasympathetic activity of the heart rate, whereas RMSSD and pNN50 reflect the parasympathetic function (Task Force, 1996).

The time domain measures of HRV typically require algorithms that are less complex than frequency domain measures, which are discussed next, and require resource intensive transformations. This makes time domain methods more suited to remote patient monitoring than those in the frequency domain.

1.9.2 Frequency domain methods

The frequency domain techniques involve a power spectra assessment computed for the RR cycle sequence. The spectrum assessments are then divided into three main bands in case of short-term (generally five minutes) HRV recordings as (Carvalho et al., 2003; Xhyheri, Manfrini, Mazzolini, Pizzi, & Bugiardini, 2012):
HF band: high frequency bin (0.15–0.4 Hz) refers to the parasympathetic tone.
LF band: low frequency bin (0.04–0.15 Hz) refers to the sympathetic tone or autonomic balance.
VLF band: very low frequency bin (0.0033–0.04 Hz) remains uncertain and is generally treated as slow physiological influences such as endocrine.

The ratio between HF and LF is applied to measure the fractional distribution between the two systems and is a significant pointer of sympathovagal balance.

Ultra low frequency (ULF) is obtained if long-term data (24 hours or more are under estimation.

Frequency domain features are all calculated in standard units known as absolute values of power (ms^2); LF and HF can also be computed in normal units although the normalisation tends to underestimate their values in total power changes. SDNN and SDANN indexes correspond to ULF power; RMSSD and pNN50 to HF power and LF and VLF power to SDNN index (Carvalho et al., 2003; Xhyheri et al., 2012).

1.9.3 Nonlinear methods

Measurements other than time or frequency domain methods have been implemented for HRV (Tarvainen et al., 2014). These measurements include:

Entropy measures (e.g., sample entropy, compression entropy, and approximate entropy).
Poincare plot (Kamen & Tonkin, 1995).

Fractal measures (e.g. detrended fluctuation analysis, multifractal analysis, and power-law correlation) (Glass, Lerma, & Shrier, 2011).

Symbolic dynamics (SDyn) (Kurths et al., 1995). SDyn measurement is applied to analyse the coarse-grained dynamics of HR fluctuations based on symbolisation and probability distribution.

All linear and nonlinear HRV methods require at least five minutes or 24hours, which will be further explained, to detect heart dysfunction. Hence, they consume more power when applied for continuous cardiac monitoring systems, using battery driven devices such as ECG sensor and smartphone devices. Also, some of them need visual analysis such as Poincare plot.

1.10 Detection of Arrhythmia

There are several mechanisms of arrhythmia, including abnormal/enhanced automaticity, re-entry and conduction delays (Nabil & Reguig, 2015). Ectopic or premature beats can be generated from the atrial, junctional or ventricular regions of the heart. The most salient feature of a premature beat is one that occurs earlier than expected in the cardiac cycle and has a morphology different than the normal underlying rhythm. The morphological changes are key points in identifying arrhythmia.

The detection of cardiac arrhythmia involves the site of its origin and its rate. Arrhythmias are widely different and may be normal, symptomatic, life threatening or, in some cases, fatal. Hence, automatic arrhythmia classification is critical in clinical cardiology. It is achieved by analysing ECG features (diagnostic features).

Recently, a major investigation of published algorithms has concluded that decreased 24-hour SDNN is an important independent predictor of arrhythmic events following myocardial infarction (Khandoker et al., 2013). The SDNN parameter, linear and non-linear parameters, extracted from HRV, will be discussed in the next section.

1.10.1 Arrhythmia detection using HRV

The central issue in arrhythmia detection using HRV involves the selection of HRV indicators that can be used to accurately detect abnormal from normal sequences. In this research, we do not search for new HRV indicators but rather look for simple algorithms that can execute in real time on data streaming from wearable sensors, because SDNN is extensively used clinically and relatively easy to calculate. It also has good prospects to be an accurate indicator for arrhythmia detection. For the current research count RR data was employed and SDNN and mean equations developed that can classify ECGs in real-time using less time than the standard time.

1.10.1.1 Time domain indicators

Standard deviation of normal to normal beats (SDNN) is a simple yet powerful time domain indicator that has proven to be important clinically (Malliani, Lombardi, & Pagani, 1994). Murray, Ewing, Campbell, Neilson, and Clarke (1975) discovered that SDNN was decreased in diabetic patients without the normal cardiovascular indicators of autonomic neuropathy. Kleiger, Miller, Bigger, and Moss (1987) used SDNN to predict which patients survived following an acute myocardial infarction (AMI). Both Murray et al. (1975) and Kleiger et al. (1987) elucidated the decrease in HRV as an indicator of reduced parasympathetic activity. Wolf, Varigos, Hunt, and Sloman (1978) illustrated that patients with a low value of short-term HRV had a poor prediction after AMI. In the late 1980s, the Multicenter Post-Infarction Project (MPIP) approved the expected value of decreased HRV by measuring long-term SDNN over 24 hours following AMI (Kleiger et al., 1987). Vaage-Nilsen, Rasmussen, Jensen, Simonsen, and Mortensen (2001) assessed 24-hour tachograms using SDNN of 103 patients one week following an AMI. The study concluded that SDNN analysed for the day time period one week after AMI was under 30 minutes while during the night time SDNN was under 18 minutes. Moreover, SDNN during daylight hours was stable for 1.5 years after AMI whereas in healthy men, SDNN was remarkably decreased. SDNN during the night time, one month after AMI, was usually also decreased. Therefore, the authors found during the night time a gradual recovery of

parasympathetic preponderance starting early after AMI and during daylight hours and a continuous irregular sympathetic preponderance for sixteen months after AMI.

A ten-year observational investigation by ATRAMI (Autonomic Tone and Reflexes after Myocardial Infarction) for patients after multicenter post-infarction project (MPIP) verified that decreased SDNN in the long term is connected with a higher relative risk of 3.2 for mortality during 21 months of observation. Thus, SDNN was suggested as a simple measure to analyse the sympathovagal balance. SDNN provides an assessment of overall HRV but, as an index of variations in sympathovagal balance, it is limited (La Rovere et al., 1998). Huikuri and Stein (2013) relied on SDNN for prognosis of cardiac patients. It is worth noting that research based on HRV from a 24-hour ECG signal and two years risk for sudden cardiac death has used mean RR data, SDNN, and other parameters for long and short term recording to explain the relationship between sudden death and disturbance of ANS function (Algra, Tijssen, Roelandt, Pool, & Lubsen, 1993).

Findings from SDNN studies demonstrate that if the SDNN for 24 hours can be calculated and the SDNN for days, months, and years be estimated, then sudden cardiac death risk can be predicted using only 24-hour measurements. However, there is currently a great deal of research involved in searching for indicators of HRV other than SDNN surveyed by (Khandoker et al., 2013).

1.10.1.2 Frequency domain indicators

Many methods can be applied to measure the range, centre frequency, and amplitude of the fluctuant factors invisible in the variability wave. A majority of research has used either autoregressive approach (AR) or fast Fourier transformation (FFT). The AR method automatically provides the range, centre frequency, and related power of fluctuant factors without requiring a priori selection. The FFT is simplest to calculate but needs a priori decision of the number and frequency range of the bands of interest. The benefit of the AR method is that only a short section of data is required for an efficient spectral calculation (Malliani et al., 1994). These methods require complex calculation processes and consume a large amount of power and storage for microprocessors homecare devices that are used to monitor HRV (Lee & Chiu, 2010).

1.10.1.3 Wavelet technique

Many studies have employed Wavelet techniques for HRV analysis to describe HR rhythms. The study introduced by Ashkenazy et al. (1998) applied Multi-resolutional Wavelet transformation of RR intervals. They succeeded in distinguishing between healthy and subjects with CVD. The authors concluded that fluctuations in normal subjects were greater than in patients. However, wavelet algorithms require high computational time not suited for real-time recording and analysis. Linear

methods possibly cannot fully illustrate HRV because of the complex control system of the heart. Accordingly, HRV has been measured by using various nonlinear methods to fully capture the characteristics of the beat-to-beat variability.

1.10.1.4 Nonlinear algorithms

Investigation of nonlinear dynamics (NLD) algorithms has been reviewed by (Voss, Schulz, Schroeder, Baumert, & Caminal, 2009). The authors have classified methods obtained from NLD for measuring HRV into four groups. The first group is fractal measurements. It consists of three algorithms (power-law correlation, detrended fluctuation analysis (DFA), and multifractal analysis). These methods assess self-affinity of heartbeat fluctuations over multiple time scales. The second group are entropy measurements, which include approximate entropy, sample entropy, multiscale entropy, Renyi entropy and compression entropy. This group of measures determines the regularity/irregularity or randomness of heartbeat fluctuations. The third group of NLD measures is symbolic dynamics (DSyn). DSyn is applied to analyse the coarse-grained dynamics of HR fluctuations based on symbolisation. The final method noted here is the Poincaré plot representation, which measures the heartbeat dynamics based on a simplified phase space embedding. These methods introduced supplementary information and assisted classical time and frequency domain assessments of HRV.

1.10.1.5 Symbolic dynamics

Kurths et al. (1995) presented symbolic dynamics algorithm for the HRV assessment as an index for risk stratification of sudden cardiac death. The SDyn method aims to explain the overall short-time dynamics of beat-to-beat variability. The first step converts the time series into a symbol sequence of 4 symbols with the alphabet A= (0, 1, 2, and 3) to categorise the dynamic variations within that time series. Three successive symbols from the alphabet describe the symbol strings by 64 different word patterns. The probability distribution of each single word within a word series is then measured. These short-term oscillations are generally produced by vagal and baroreflex functions (Voss et al., 2009).

Further support for applying SDyn can be found in the work of Porta et al. (2001), where the development the SDyn algorithm has been proposed to decrease RR data. The number of RR data was reduced to 300 beats and samples of length three (L=3) were built. Besides, the range of the RR series was divided into six levels from 0 to 5 (Guzzetti et al., 2005). Samples with L=3 were classified, without any loss, into four groups. The first group includes samples with no variation (0V), the second includes samples with one variation (1V), the penultimate group includes samples with two like variations (2LV), and finally the last group includes samples with two unlike variations (2UV).

While Voss et al. (2010) used a new SDyn method known as segment symbolic dynamics (SSD). The aim was to compare SSD parameters with time-frequency domain and nonlinear parameters to measure the compatibility of the SSD algorithm for risk stratification in patients with ischemic heart failure. For computing SSD, a 30-min RR intervals window was segmented into one minute overlapping windows. Word and symbol transformations were applied for each window. Also, probabilities of word type occurrences were measured. Results indicated that the SSD algorithm improved significantly the risk stratification for ischaemic cardiomyopathy patients.

Loss of information detail and outliers (ectopic beats and noise) and the selection of symbol strings represent the main limitations of the SDyn algorithm (Porta et al. 2001). Therefore, it consumes more time and requires complex computational resources for remote sensing and automated analysis.

1.10.1.6 Heartprints

A novel method has been proposed by Glass et al. (2011) for a better understanding of heartbeat behaviour in risk stratification. The dynamical properties of ventricular premature complexes (PVC) over 24 hours were measured in an effort to understand the underlying mechanisms of ventricular arrhythmias and the arrhythmias that occur in individual patients. Two dimensional density plots, known as Heartprints were suggested to record dynamical characteristics of premature ventricular complexes in Holter recordings. Heartprints display distinctive features in individual patients over 24 hour epochs. However, this method requires visual evaluation from specialists and is therefore not suitable for automated analysis at this stage.

Other approaches have been used to detect HRV patterns such as nonlinear complexity measures, wavelet transform and sophisticated artificial neural networks (Vu et al., 2010). However, these approaches may not always be technically feasible for real-time processing of HRV data from wearable sensors and mobile devices due to high computational resources and power consumption

1.11 Intellectual Contribution and Significance

The major contributions of this PhD research are:
One of the main contributions of this research is a simple and computationally inexpensive algorithm for real time ECG reduction. A novel ECG reduction algorithm that can be applied was proposed within ECG sensor node to increase sensor battery life significantly.

A second contribution is the advancement of a new real-time algorithm that forecasts HRV measures minutes into the future so HRV can be analysed ahead of time.

A third contribution is to build a real diagnosis system based on ECG sensor and mobile phone that can detect arrhythmia in a simple and fast manner.

A fourth contribution is the advancing a new algorithm that detects many types of arrhythmias from normal beats in the presence of noise.

Therefore, this PhD research contributes at building a new ECG analysis method in real time to assist people and clinicians with measuring HRV and detect arrhythmias quickly and easily enough to deploy on wearable devices.

1.12 Organisation of Thesis

This introductory chapter provides background information related to cardiovascular remote patient monitoring application, its real-time reduction and detection. Also, it explains existing problems and clarifies the motivation behind the research undertaken. Furthermore, it lists the research questions and significant contributions of this PhD thesis.
The rest of this paper is organised as follows:

Chapter 2 explains different techniques for real time ECG signal reduction/compression, answering the first research question. It also demonstrates how the proposed method can be executed within wearable ECG sensor node. In addition, the chapter reports the experimental results and cardiologists results.

The analysis of advancing a new real-time algorithm that predicts HRV measures minutes into the future is represented in Chapter 3. The analysis of the results and observations on these HRV measures are also illustrated in this chapter.

Chapter 4 details a novel life-threatening arrhythmia detection algorithm. It also demonstrates how the proposed real cardiac monitoring system can be implemented within wearable ECG sensor node and mobile phone. In addition, it represents experimental results.

Chapter 5 describes different techniques for the automated arrhythmias detection and classification a new wrapper based hybrid technique compared to the existing hybrid methods in the presence of noise, answering the third research question. It also details how the proposed technique can be improved classification performance and accuracy. Moreover, it illustrates the experimental results.

Finally, Chapter 6 concludes the project. The limitations of the study presented in this thesis and the directions for future research are explained in this chapter.

1.13 Chapter Summary

In this chapter, cardiovascular disease is introduced and the importance of real-time ECG reduction and early detection of heart disease are described. The challenges inherent in the implementation real-time cardiac monitoring system based on battery operated devices are outlined. In addition, the need for automated detection and classification techniques in order to help patients and cardiologists to increase the arrhythmias detection accuracy, sensitivity and reduce the workload are detailed. ECG features play a pivotal role in the prediction and classification accuracy. Novel ECG signal reduction, prediction and classification techniques are proposed in this PhD project. The research questions and the contributions of this thesis are then listed followed by the organisation of the thesis. The next chapter answers the first question of this thesis.

CHAPTER 2

2 ECG Reduction for Wearable Sensor

By utilising simple algorithms with a sliding window that can boost the compression ratio to a higher level with limited computational resources, simpler, faster and more effective ECG reduction technique can be achieved. The concept is to reduce the ECG at body area side (i.e. on patient's ECG sensor), before transmission to a portable device (e.g. a Smart phone). Hence, the scheme of the reduction technique requires special investigation with the aim being to decrease the number of operations. This chapter reports on a new reduction technique to reduce the amount of ECG data that needs to be transmitted in real time from the body sensor to a Smart phone with a Bluetooth or Zigbee protocol.

In this chapter, first of all, current real-time ECG compression/reduction algorithms that can be implemented within ECG wearable sensors are described. Secondly, the objective of reduction/compression and the causes for selecting a novel ECG compression/reduction technique are provided. Then, the proposed reduction technique is explained in detail, with examples from a standard database and body sensor databases. In the results section of this chapter, signal quality, performance and power consumption are compared with respect to current compression techniques. The cardiologists' evaluation of the proposed ECG reduction technique is also illustrated in the results section. Finally, the discussion and chapter summery is provided prior to the chapter conclusion.

Why ECG reduction/compression is important for wearable sensors?

Advances in wearable ECG sensor technology in recent years has changed the way ECG signals are collected, stored and processed (Lee, Chen, Hsiao, & Tseng, 2007; Scully et al., 2012). This can lead to reductions in the use of Holter devices in favour of real-time, continuous monitoring (Oresko 2010). Secondly, ECG sensors generate large streams of data that easily exhaust storage of mobile devices and need high bandwidth capacity for transmission. Some applications are required to process and store ECG recordings for one or more days (Elgendi, Eskofier, Dokos, & Abbott, 2014). ECG data collected from a patient at sampling rate 500Hz with 16-bit resolution for 24 hours can easily reach up to 6.5 GB. Thus, in order to transmit this huge data using standard wireless techniques such as Wi-Fi and Bluetooth, requires a dedicated limited speed of 631 kbps as in Equation 2.1.

$$Required\ transmission\ speed = \frac{size\ of\ data}{transmission\ time} = \frac{6.5\ \text{GB}}{24\ \text{hours}} = 631\ \text{kbps} \quad (2.1)$$

Few telemedicine services provide this transmission speed (Sufi, Fang, Khalil, & Mahmoud, 2009). During the streaming of huge ECG data, a reduction/compression method can be used to reduce bandwidth and transmission requirement for faster transmission on minimum bandwidth wireless link. ECG reduction/compression technique also adds value to home or hospital telecare monitoring systems; they are usually based on mobile devices, by increasing their battery life as described in Chapter 1.

Trials of the ECG reduction algorithm advanced here were applied to the MIT-BIH Arrhythmia (Mark & Moody, 1997) and Shimmer3 ECG databases. The MIT-BIH Arrhythmia database was used for testing and the Shimmer3 dataset was used for measuring the generalisation capability performance of the method and evaluation of the proposed techniques in a real-time transmission context. Both datasets will be described in this chapter. The ECG reduction results on the MIT-BIH Arrhythmia database was published in a peer reviewed conference (Allami, Stranieri, Balasubramanian, & Jelinek, 2016a)

2.1 ECG Data Reduction/Compression Background and Related Work

The current ECG reduction/compression methods can be grouped under two main approaches: lossless and lossy. Lossless algorithms can reconstruct the raw signal from compressed signal without any data loss. In contrast, lossy algorithms can retrieve an estimated version of the raw signal. Lossy compression methods possibly provide higher compression ratios than lossless algorithms with minimal changes between raw data and compressed data (Ibaida, Al-Shammary, & Khalil, 2014).

Lossy compression algorithms are commonly used to reduce/compress ECG signal (Ibaida et al., 2014; Sufi & Khalil, 2011a). They are mainly grouped into three categories: direct methods (reduction methods), transformational methods and parameter/feature methods. Transformational methods employ transformations processing such as discrete cosine transform (DCT) (Lee & Buckley, 1999), fast Fourier transform (FFT) (Reddy & Murthy, 1986), and discrete wavelet transform (DWT) (Rajoub, 2002). The rationale underpinning transformational methods represent the signal in a suitable transform domain and select the number of transform coefficients to be streamed, in place of the raw samples.

Parameter/feature methods use neural networks, vector quantisation and pattern matching (Cárdenas-Barrera & Lorenzo-Ginori, 1999; Maglaveras, Stamkopoulos, Diamantaras, Pappas, & Strintzis, 1998). Their rationale is to process the temporal series to obtain some knowledge to forecast the signal behaviour. Many parameter/feature methods require the detection of the QRS complex first, for the extraction of features, prior to the deployment of pattern recognition or machine learning methods (Ibaida, 2014; Sufi et al., 2009).

In general, all the transformational and parameter/feature algorithms are designed for PC-based environments that have high memory requirements, processer capacities and I/O ports. Unlike mobile devices that have limited hardware resources, challenge the execution of transformational and parameter/feature algorithms on mobile phone (Sufi, 2011).

Direct methods reduce/compress the ECG signal directly in the time-domain without any pre-processing. Direct algorithms extract a subset of significant points simply and swiftly by utilising the information of previous points (usually using prediction methods) or employing the information of both future and previous points (usually using interpolation methods) (Jalaleddine et al., 1990). Therefore, they are efficient in terms of compression ratio and fast processing. They directly detect and eliminate redundant points from the raw signal and some of them provide minimum distortion (Ranjeet, Kumar, & Pandey, 2011). This makes direct methods more suited for remote patient monitoring than transformational and parameter/feature methods. Also, they can be simply executed on mobile devices (Ranjeet, Kumar, & Pandey, 2013; Rossi et al., 2002). Although other methods achieve higher compression ratios than direct methods, they consume more time, power and computational resources to be suitable for deployment with wearable sensors devices (Francescon et al., 2015; Jalaleddine et al., 1990).

ECG data reduction/compression using a lossy method provides a distorted version of the original data. Hence, the quality of reconstructed data should be evaluated using subjective and objective measures. Subjective evaluation is achieved visually by cardiologists (Chen, Hsieh, & Yuan, 2004; Huang, 2004; Zigel, Cohen, & Katz, 2000). Objective evaluation is commonly achieved using four fundamental measures; signal reconstruction error, compression ratio, compression performance and root mean square error. The compression ratio (CR) describes the effectiveness of an ECG compression method. The percentage root mean square difference (PRD) is a computation of error due to signal infidelity. This measures the distortion between the original and the reconstructed signal (Huang, 2004; Ibaida et al., 2014). Root mean square error (RMSE) is calculated from actual and expected measurements (Hyndman & Athanasopoulos, 2014).

Why is a novel ECG reduction/compression required for wearable sensors?

Firstly, most existing ECG compression/reduction algorithms are computationally expensive. In addition, they are designed and evaluated on PC environments and some of them on mobile phone environments (Sufi, 2011). Furthermore, almost all the current ECG compression/reduction algorithms are evaluated based on objective evaluation. Subjective evaluations have hardly ever been carried out.

Secondly, ECG signals from wearable sensors processed on battery-driven devices require algorithms to execute rapidly in real-time, due to limitations in processor capability, power and memory (Elgendi et al., 2014). Therefore, there is increasing attention on the advancement of simple algorithms that reduce the data signals streamed so that wearable sensors battery life can be extended. In addition, the large datasets and limited processing capacity of devices near the sensors results in the need to consider near, or real-time reduction of large ECG data sets for critical operations in ambulatory recording systems, ECG signal storage systems and for ECG signal transmission over wireless networks (Francescon et al., 2015; Padhy et al., 2016). Moreover, any reduction in ECG signals should not impede clinicians' diagnostic assessments (Mamaghanian, Khaled, Atienza, & Vandergheynst, 2011).

Most existing ECG data reduction algorithms are designed to reduce information size while maintaining significant information, so that the ECG wave can be reconstructed from the reduced form as intact as possible (Moody, Soroushian, & Mark, 1987). Critically, any ECG data reduction algorithm should preserve the essential features (diagnostic features) of the ECG signal (P, QRS, T) waves as these peaks and troughs as well as the calculated intervals (i.e. QT interval) are used for the clinical interpretation of the ECG (Lee, Kim, & Lee, 2011; Zigel et al., 2000). However, some existing ECG compression methods discussed below are not entirely lossless but result in changed diagnostic features.

Lastly, algorithms that aim to reduce existing compression algorithms that achieve considerable compression by applying computationally resource intensive transformations are difficult to deploy on wearable devices, which are constrained by power and memory limitations. In contrast, many reduction algorithms cannot be reversed to re-create the original signal but they reproduce important features (diagnostic features) of the signal only. Moreover, many existing reduction algorithms require a block of ECG data and cannot reduce a signal incrementally as it arrives from wearable

devices so that the need to store the entire stream can be obviated. In addition, most current compression algorithms need extra processing on the compressed ECG in order to reconstruct the origin data that leads to consume more time and power, especially in case of resource constraint mobile devices, where reconstruction time could be long.

In this chapter, a simple, yet effective ECG data reduction algorithm where the signal cannot be reconstructed as intact but nevertheless has a number of benefits is introduced. First, the compression ratio is higher than many existing real-time reduction methods. Also, most ECG diagnostic features, intervals and ECG waves can be detected from reduced data. Second, the algorithm can be applied on programmable ECG mobile sensors such as Shimmer3 ECG sensor and demonstrably increase the battery life. Finally, the reduction processing is computationally less expensive than current ECG data reduction/compression methods because the algorithm is simple and can execute every few milliseconds on data streaming in to devices or sensors.

To the best of our knowledge, this is the first time the efficacy of an ECG reduction algorithm has been assessed in a real-world system, based on subjective and objective evaluations, to reduce and stream ECG data with wearable ECG sensors. In the next section, direct and real-time ECG reduction/compression methods will be described more in depth.

2.1.1 Direct methods

Real-time ECG data reduction algorithms known as “lossy” methods are those where the reduced ECG signal usually cannot be reconstructed or recovered in an exact manner. Algorithms in this category include turning point (TP) (Mueller, 1977), amplitude zone time epoch coding (AZTEC) (Cox, Nolle, Fozzard, & Oliver, 1968), coordinate reduction time encoding system (CORTES) (Abenstein & Tompkins, 1982), and Fan/SAPA (Scan Along polygonal Approximation) (Singh, Kaur, & Singh, 2015).

2.1.1.1 Analysis of direct methods

Reduction of ECG signal does not require retaining all data points but rather only some points of the ECG data are essential (P, Q, R, S, T as illustrated in Figure 1.2 in chapter 1), and relevant intervals. The subtlety of the ECG signal may be ignored in favour of higher compression ratios (Jalaleddine et al., 1990; Ranjeet et al., 2011; Rossi et al., 2002). Hence, numerous types of compression/reduction methods that contain some errors have been applied to reduce ECG signals.

Many of the direct algorithms are based on interpolation or prediction techniques. Interpolation and prediction methods eliminate data redundancy by testing the successive value of neighbouring points.

Interpolation methods including first-order and zero-order interpolators (FOI, ZOI) utilise prior information of both previous and next values, whereas prediction methods such as first-order and zero-order predictors (FOP, ZOP) employ only prior information of some previous values (Jalaleddine et al., 1990).

The description of prediction and interpolation techniques is represented below. Polynomial predictor is a data compression algorithm in which a polynomial of order *j* is fitted via previously recognised data points and then extrapolated to predict subsequent points.

The polynomial predictor equation written as:

$$X'_n = X_{n-1} + Fx_{n-1} + F^2X_{n-1} + ... + F^jX_{n-1} \quad (2.2)$$

Where

X'_n = predicted sample point at time t_n

X_{n-1} = point value at one point period prior to t_n

$$FX_{n-1} = X_{n-1} - X_{n-2} \quad (2.3)$$

$$F^jX_{n-1} = F^{j-1}X_{n-1} - F^{j-1}X_{n-2} \quad (2.4)$$

When j=0 the polynomial predictor is called zero-order predictor (ZOP). ZOP algorithm predicts each data point in the same way as the previous one as illustrated in Equation 2.5 below:

$$X'_n = X_{n-1} \quad (2.5)$$

Most techniques apply the ZOP algorithm as a step technique or floating aperture. This method keeps a single data point and omits each successive point that remains within a tolerance band ± e, whose centre remains on the kept point and changes them with a horizontal line. When a point is outside the tolerance band, the new point is kept as depicts in Figure 2.1. This process is repeated until all data finish.

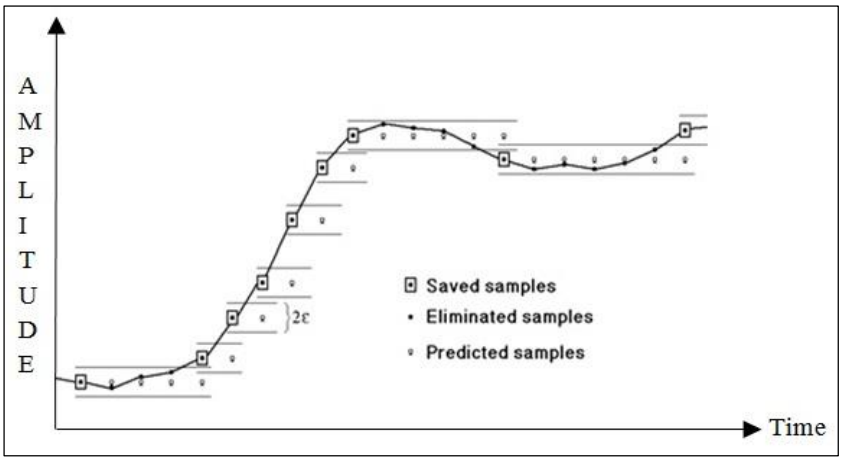

Figure 2.1. An example of the ZOP floating aperture algorithm (Jalaleddine et al., 1990)

The first-order predictor (FOP) algorithm applies a polynomial predictor with $j = 1$. Two previous samples have to be defined in the FOP algorithm as represented in the equation below.

$$X'_n = 2X_{n-1} + X_{n-2} \tag{2.6}$$

The FOP algorithm is similar to ZOP algorithm. Its difference lies in the way the forecasting line is drawn. Rather than a horizontal line, the two previous samples are used to generate a starting sample and a slope for the prediction. A tolerance band is still implemented, and when a data point remains outside the tolerance band, a new FOP is created (Lynch, 1985).

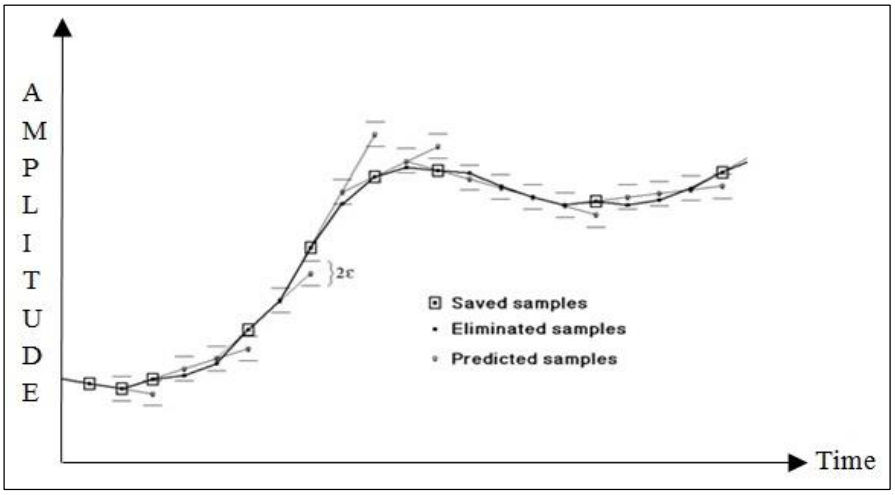

Figure 2.2. An example of the FOP algorithm (Jalaleddine et al., 1990)

Polynomial interpolator algorithm differs from polynomial predictor algorithm in that previous and next data points are employed to generate the forecasting polynomial. The zero-order interpolator (ZOI) algorithm adjusts the ZOP by allowing the horizontal line has height corresponding to the mean of a set of data rather than simply that of the first point. As illustrated in Figure 2.3, both algorithms (ZOI algorithm and ZOP algorithm) maintain all data points within a tolerance band around the

reconstructed data. ZOI algorithm achieves higher compression results because it choses data points more appropriately.

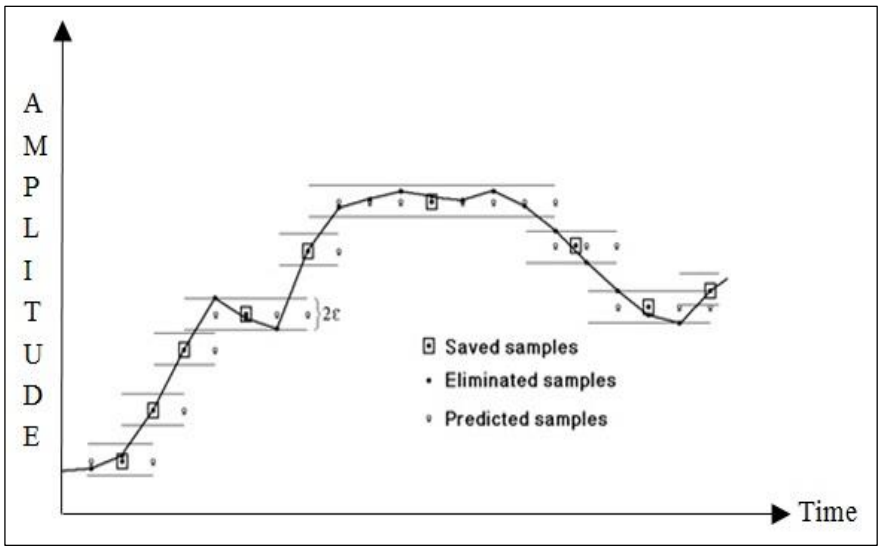

Figure 2.3. An example of the ZOI algorithm (Jalaleddine et al., 1990)

FOI algorithm uses two points to create a slope and line similar to FOP algorithm but it applies the ZOI idea in selecting two points that leads to an optimised compression ratio.

FOP algorithm with two degrees of freedom (FOI-2DF) is also called a two-sample projection algorithm. It keeps two successive data points and generates a line linking the points. If altering the line to pass via the third data point rather than the second still keeps the second data point within a tolerance bound around the line, a new line is drawn from the first point to the fourth rather than to the third as explained in Figure 2.4. This also applies to the *j*th point, when data points between the first and the *j*th remains outside the tolerance bound around the line. The line linking the first and (*j*-1)th sample proposes to be the best approximation and is kept. It has been regularly found to be the most successful of the FOI's (Kortman, 1967). However, the kept data refer to a height and a distance to the next kept point. When reconstructing the data, the line is drawn via the kept height and the next kept height, using this new height as starting point of the next line (Jalaleddine et al., 1990). The FOP requires many calculations and it also requires data look ahead.

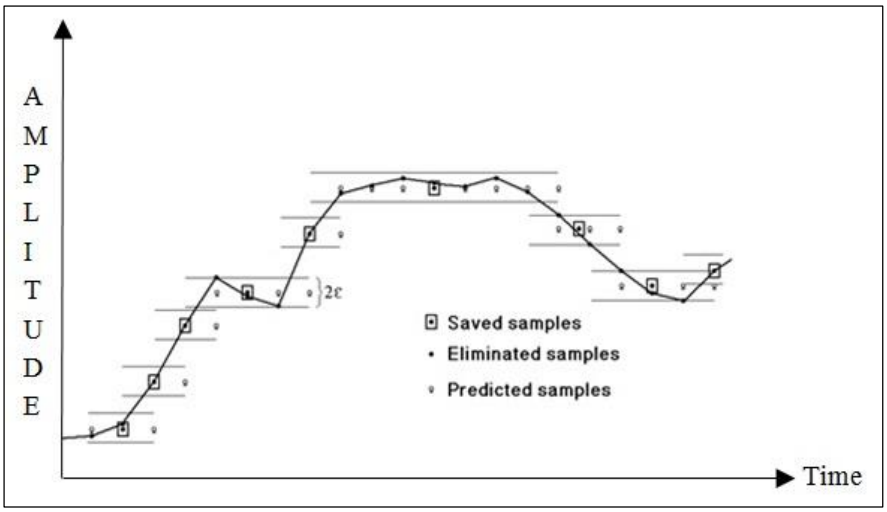

Figure 2.4. An example of the FOI-2DF algorithm (Jalaleddine et al., 1990)

Cox et al. (1968) introduced the AZTEC algorithm that changes a plain ECG signal into slopes and horizontal lines (plateaus). When a plateau of three points or more are formed then the slope is saved. The amplitude and length are saved while the horizontal lines use the zero-order interpolator method to reduce the data. The information saved from a slope is the length of the slope and its final amplitude. Although the AZTEC method realises on a high CR of about 10:1 (500 Hz sampled ECG with 12 bits resolution), it provides imprecise reconstruction of ECG waves because T and P waves have slow varying slopes. Also, the accuracy of the decompression ECG waves is often unacceptable to cardiologists due to the discontinuity (step-like quantization) that appears in the reconstructed ECG signal (Jalaleddine et al., 1990). In addition, it produces a PRD of 28 % and requires pre-processing to reduce an ECG signal.

The turning point method, proposed by Mueller (Mueller, 1977) reduces the sampling frequency of an ECG wave to 100 Hz and preserves the peak of the large amplitude QRS waves. The Turning point method operates by substituting each of three successive values with the two that best represent the slope of the three values. The second of the two stored values is used for the computation of the next two values. It uses the first value (V_0) as a reference value for the future iteration. The next two successive values represented as V_1 and V_2. The method keeps either V_1 or V_2, based on which value maintains the slope change of the raw data. Turning point maintains the essential aspects of the ECG data and supplies a CR of 2:1. However, it is sensitive to sampling rate and relevant clinical information is lost if a minimum or a maximum value is lost. Therefore, if one of the two values in the pair is a local minimum or a local maximum, then it is the other value in the pair that is eliminated (Horspool & Windels, 1994). In fact, the proposed method advanced in this study is similar to the

turning point method but it provides a higher CR and overcomes the local minimum and local maximum problem that may lead to missed diagnostic features.

The high precision of the turning point reduction technique and the superior CR of the AZTEC technique were merged into the CORTES method. (Abenstein & Tompkins, 1982) demonstrated the implementation analysis of the CORTES, AZTEC, and Turning Point methods for ECG's sampled at 200 Hz with PRD 7 and CR of 4.8:1.

Fan and SAPA methods represent an ECG data reduction algorithm which provides a CR of around 3:1 and PRD of nearly 4 (250 Hz sampled ECG). These two methods depend on a first-order interpolation with two degrees of freedom (FOI-2DF) algorithm. The Fan algorithm achieves the FOI-2DF without saving all the raw data samples between the last transmitted and the present sample (Singh et al., 2015). The real-time ECG data compression algorithms that can execute on wearable, programmable ECG sensor devices are explained next.

A real-time ECG data compression algorithm, +SLOPE, was introduced by (Tai, 1991). This algorithm processes some neighbouring patterns as a vector and expands the vector if the next pattern falls in a fan spanned by the vector and threshold angle. By this approach, +SLOPE constantly restricts linear parts of different slopes and lengths. Initially, the Slope algorithm reads the first three points (P1, P2, and P3). These three points are considered to be represented in a linear segment which expects to be increased by coming points. When P4 is coming, then it is tested with the threshold if P4> threshold then P4 is considered to be the first point of a new linear segment else, P4 adds to the current segment. The +SLOPE algorithm reproduces ECG signal well. However, the approach can lead to QRS misdetection and a CR of 4.8 and PRD of 7. The +SLOPE algorithm was tested on the MIT-BIH Arrhythmia database by (Tai, 1991).

A compression engine was introduced by Fang et al. (2013) for portable real-time ECG data monitoring to transfer ECG signal wirelessly and analyse heart rate variability in real-time. The compression engine achieves a compression ratio of approximately 2.5 by classifying every ECG sample based on prior samples with the Golomb-Rice k-parameter algorithm. The compression algorithm was evaluated on the MIT-BIH Arrhythmia database. The ECG signals were resampled to 256 Hz before being tested and achieved a compression ratio of approximately 2.5.

Sufi (2011) introduced an ECG algorithm based on genome sequences. The genome sequences ECG compression method was implemented with three ECG compression methods known as ZOP, SAPA

and Peak, for comparison, on a mobile phone platform for real-time ECG compression. The basic idea of the Sufi research is to stream ECG data from a wearable data to a patient mobile phone via Bluetooth or Wi-Fi in real time. The received ECG data compresses and transmits to a doctor's mobile phone via SMS or MMS in real time. The author reported the results of execution time, CR and PRD for all four methods. The ZOP method provides fastest execution time with CR of 3.7 and PRD of 2.6. The peak method required the highest execution time with CR of 6.6 and PRD of 2.1. The SAPA and genome sequences methods approximately recorded similar execution time with CR of 3, 3.9 and PRD of 4, and 0, respectively. Although the Peak method achieves high CR it consumes more time and computational resources to detect the QRS complex. Also, it is not ideal for diagnosis because it completely eliminates T waves, more details of the Peak method are represented in (Rossi et al., 2002) investigation.

The Sufi (2011) study was not implemented using real-time ECG data collected from a wearable ECG sensor. Rather, the study was evaluated based on 12 records obtained from MIT-BIH Arrhythmia database. In addition, it did not measure the power consumption of the mobile phone. Further, the SMS and MMS have limited size and are not suitable for real wearable ECG sensor that stream ECG data from 4 or 5 channels because it requires more power, processor capability and memory.

Modern real-time ECG compression methods that can be applied within wearable ECG sensors to reduce power consumption and reconstruct signal quality are described below.

2.2 Compressed Sensing for ECG Signal Compression

Compressed sensing (CS) is a recent compression method which imposes the sparsity of data in compression and reconstruction processes (Baraniuk, 2007). It applies simple linear transformation methods such as sensing matrix that relies on an implementation of Gaussian random distribution to reduce the amount of data and exploits the sparsity of the compressed data in the reconstruction process. The sparsity indicates that most of the input data are zeros (Zhang, Jung, Makeig, & Rao, 2013). On the other hand, the CS methods transmit only nonzero data. Recently, numerous investigations have implemented CS techniques for ECG compression and provided high CR (Craven et al., 2015; Parkale & Nalbalwar, 2017). However, an ECG signal is not sparse in its nature. Hence, traditional CS methods fail in the compression and reconstruction processes. Therefore, current studies have proposed more complex methods including machine learning, DWT, and DCT, etc. to solve non sparse ECG signal (Da Poian, Brandalise, Bernardini, & Rinaldo, 2016).

Nevertheless two studies proposed by (Da Poian et al., 2016; Mamaghanian et al., 2011) attempted to simulate/develop CS algorithms and thresholding based DWT algorithm directly on a Shimmer ECG wearable sensor. Those studies aimed to measure power reduction, CR, and signal quality. Mamaghanian et al. illustrated the advantage of CS in wearable ECG sensor for compression and collection of adult ECG data. The method was evaluated against the DWT algorithm in terms of power saving on Shimmer ECG node. The method was evaluated on standard records from the MIT-BIH Arrhythmia database. However, the ECG collection was not implemented in real-time on Shimmer ECG device. Instead, the ECG data was stored on the memory of Shimmer sensor and resampled at 256 Hz. The method utilized a sliding window size of 512 because of memory size restriction. The sliding window required two seconds to collect an ECG segment of 512 points at the sampling rate of 256 Hz. So, it consumed more time, where one minute of processing requires 30 seconds waiting plus the execution time of the algorithms. The authors reported that CS algorithm provided CR of about 2 or 51%, energy consumption of 7.29 mJ and increased battery life by 37%. DWT algorithm achieved CR of 3.7 or 73%, energy consumption of 9.86 mJ, and decreased battery life. Those results were based on one channel ECG segment size of 512 samples and very good reconstruction quality.

Last year, a study also compared the CS algorithm against DWT algorithm based on foetal ECG data (Da Poian et al., 2016). ECG data was also obtained from a standard database, Physionet Challenge database (Physionet, 2013). During the compression phase, the method utilised a sliding window size of 256 sampling at 1 kHz. Results represented that CS and DWT algorithms achieved CR of about 4 or 75 % and provided good signal quality. In addition, the results illustrated CS algorithm consumed less power (1.2 Joule) than the DWT algorithm (1.8 Joule). The authors indicated that DWT algorithm cannot be executed in real-time based on four channels ECG data recordings at a sampling rate 1 kHz due to limitation of memory size of sensor node. In the reconstruction stage, the study employed more complex technique called block sparse Bayesian learning, because existing CS techniques do not reconstruct high quality foetal ECG data from CS methods.

Both studies above that were implemented or simulated within Shimmer ECG sensors were based on standard ECG data obtained from Physionet databases (Physionet, 2015). Accordingly, the authors indicated that ECG collection stage was not implemented in real-time on Shimmer ECG node. In addition, the reading process was not real. The power consumption results, therefore, can be said to require more analysis (Craven et al., 2015). Also, there was buffering time/delay (2 seconds or 1 second) for a window to collect data. All above problems generate imprecise measurements of battery-life. CS methods require very complex computational techniques to reconstruct the raw signal.

Consequently, the study recommended to apply the reconstruction process based on a cloud server, especially for systems that use mobile devices for ambulatory monitoring (Craven et al., 2015).

All the methods above provide a CR that is less than the proposed method except the AZTEC method which produced a CR of 10 but does not retain all relevant clinical data. It typically misses P and T waves. Other approaches have a fixed CR whereas the proposed algorithm can be varied. So, it can provide CR of about 10 and in some cases miss P and T waves as well, when their amplitudes are low. Also, existing methods require more processing time and suffer from buffering problems when they execute on a wearable ECG sensor. In addition, they need to reconstruct the ECG signal that consumes more time and power for battery driven device. Sufi, Khalil, and Mahmood (2011) reported that cardiovascular detection based on compressed ECG data is quicker than reconstruction followed by detection. Therefore, they consume more time and energy than the proposed method advanced in this thesis. Each of the proposed algorithms will be discussed in the following sections prior to the description of experiment results.

2.3 Method Description

In this investigation, a sliding window in time-domain is analysed with a simple filter referred to as Maximum_Minimum (Max_Min) to reduce the amount of ECG data rapidly. The aim of the proposed algorithms is to reduce data points making sure that P, Q, R, S, and T are not removed so that the features useful for diagnostic purposes remain intact and energy consumption for wearable sensor is reduced as much as possible. In addition, the same procedures as proposed by other statistical methods such as mean and median were applied for comparison. The approach also enables variable compression ratios.

2.3.1 Proposed ECG reduction algorithm

The direct ECG data reduction algorithm proposed here implements real-time direct reduction. The algorithm reads and stores n consecutive raw ECG measurements. The algorithm then takes a stream of millivolt readings as input and operates in the same way regardless of the sampling rate.
The algorithm, described in Table 2.1 operates as follows.

The algorithm reads n consecutive +/- ve millivolt ECG readings. The maximum point of the samples in the window is identified. If this maximum is positive, it is retained in the reduced set and the other points are discarded. This ensures the P, R and T peaks are not discarded. If the maximum point is not positive, the minimum is identified and retained and the others are discarded. This ensures the Q and S troughs are not missed.

Algorithm 2.1: Proposed ECG reduction algorithm coding schema

Input: Plain ECG signal in +/- millivolts

Output: Reduced ECG signal +/- millivolts

Step 1: Window size (n)
Step 2: While ECG ≠ N Do
Step 3: Read n
Step 4: Max= Maximum sample in n
Step 5: Min= Minimum sample in n
Step 6: If Max>= 0 Then save Max
Else save Min
Step 7: End while
Step 8: Return to Step 2

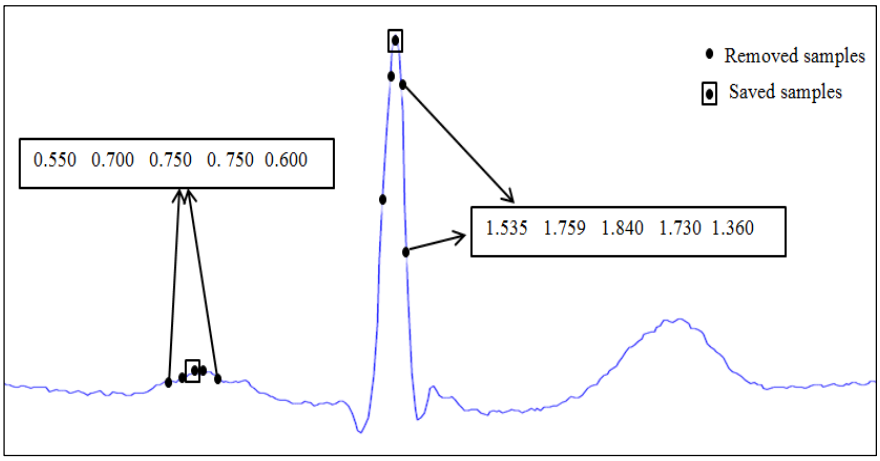

Figure 2.5. An example of proposed ECG reduction algorithm

It is noted that usually each window of size 5 consists of samples close to each other and some of the samples are repeated as depicted in Figure 2.5. In other words, they have low standard deviation. Therefore, the mean and median methods can be implemented to reduce ECG signal and achieve good results, especially for ECG signals that have high amplitudes.

2.3.2 Mean and median ECG reduction algorithm

The algorithms apply the same procedures listed in Algorithm 2.1. They read and store a window of *n* consecutive raw ECG samples. The mean of the samples is identified then only the mean is saved and other samples are discarded. The mean algorithm estimates the slop a sample, when it has been a

part of the selected samples as represented in Algorithm 2.2. It is similar to the Turning Point algorithm which only estimates the slope change sample and omits the other samples.

Algorithm 2.2: Mean ECG reduction algorithm coding schema

Input: Plain ECG signal in +/- millivolts

Output: Reduced ECG signal +/- millivolts

Step 1: Window size (n)
Step 2: While ECG ≠ N Do
Step 3: Read n
Step 4: M=Mean(n)
Step 5: Save M
Step 6: End while
Step 7: Return to Step 2

Median algorithm is the same as the mean algorithm except it uses median not mean as illustrated in Algorithm 2.2.

Mean and median algorithms preserve the essential aspects of the ECG data. However, they do not always retain the original peaks and troughs and the relevant clinical information is lost or estimated incorrectly if a window of size 5 composes of incoherent samples and the standard deviation of the sample is high. The proposed ECG reduction algorithm is virtually guaranteed to retain the original peaks and troughs as described in Figure 2.5.

2.4 Results

2.4.1 Experimental Results

The proposed algorithms were evaluated using the MIT-BIH Arrhythmia database (Mark & Moody, 1997) and Shimmer3 ECG database collected for the current study. The MIT-BIH Arrhythmia database is commonly used in ECG signal analysing because it includes different patterns of ECG signal and contains data from 48 ECG traces for 30 minutes from different patients. Furthermore, it has two channel ambulatory ECG recordings in digital format with an 11 bits and 360 Hz sampling rate. The Shimmer3 ECG dataset consists of 52 records (Normal and Abnormal) of 30 minutes real world ECG signals obtained from various patients at sampling rate 256 Hz. The Shimmer3 ECG dataset was collected during 2016–2017 and classified by experienced cardiologists at Ibn Alnafees Hospital in Baghdad, Iraq. A single Shimmer3 ECG sensor (matchbox size) strapped to the patients

received a signal from five electrodes attached to the chest. Patients were selected for the data collection by the attending registrar who applied the inclusion criteria: cognate, over 18 and under 75 years. We applied the proposed algorithms on both MIT-BIH Arrhythmia database and Shimmer3 ECG dataset.

2.4.1.1 Proposed ECG reduction results

Figure 2.6 depicts part of the raw ECG from Record no. 103 of the MIT-BIH Arrhythmia database. This record represents a Normal ECG. Figure 2.7 also illustrates a segment of record No. 103 but where only some of the samples have been selected for storage by the proposed ECG reduction algorithm described above in Algorithm 2.1 using a window of size 5. Figure 2.7 demonstrates that each peak and trough has been correctly identified. The algorithm provides a compression ratio of 5 and 1% PRD. Furthermore, it can be used with long and short term ECG signal at different sampling rates.

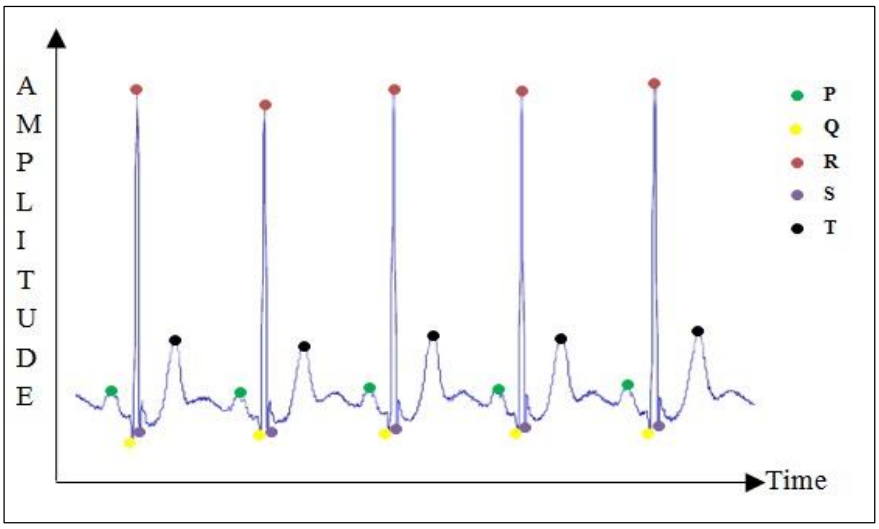

Figure 2.6. Segment of normal ECG for record no. 103 with raw samples

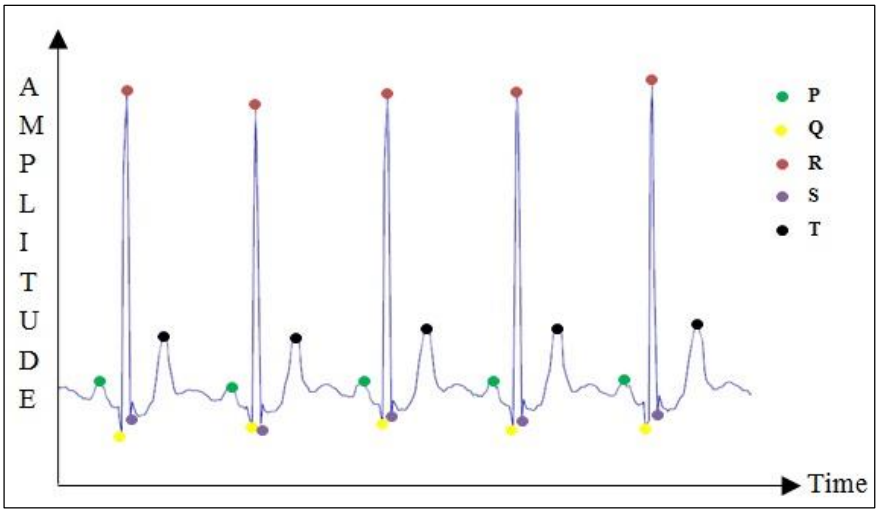

Figure 2.7. Segment of normal ECG for record no. 103 with reduced samples illustrates all ECG peaks and troughs are maintained after reduction process

Extra ECG examples readings from Shimmer3 ECG dataset are represented in below figures in order to illustrate that the proposed ECG reduction algorithm can be implemented in different ECG signals collected from wearable ECG sensor or traditional devices sampling at different rates.

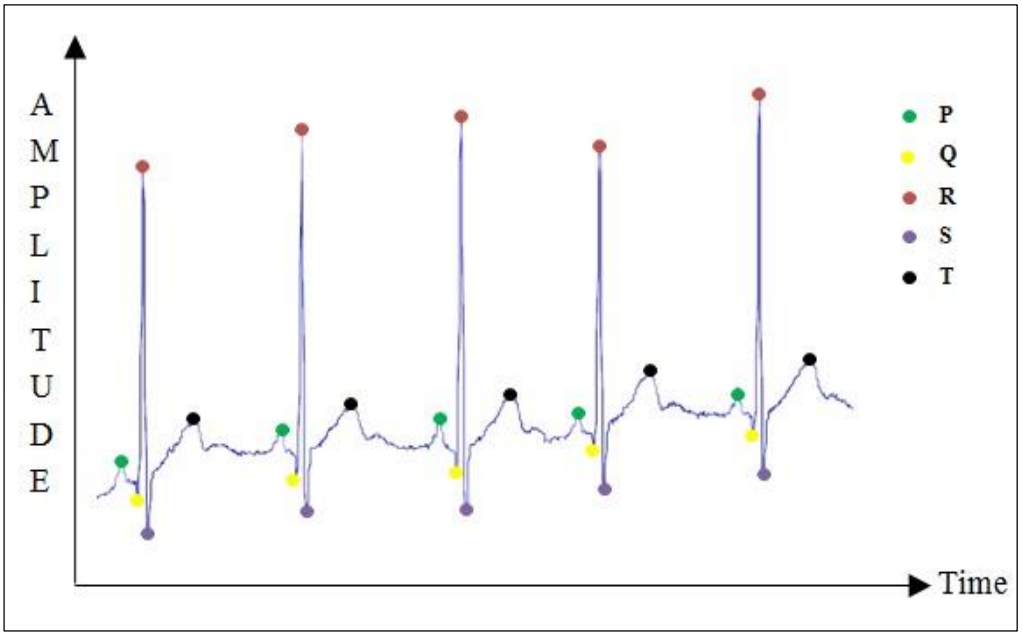

Figure 2.8. Segment of Normal ECG for record no. N001 with raw samples readings from Shimmer3 ECG dataset

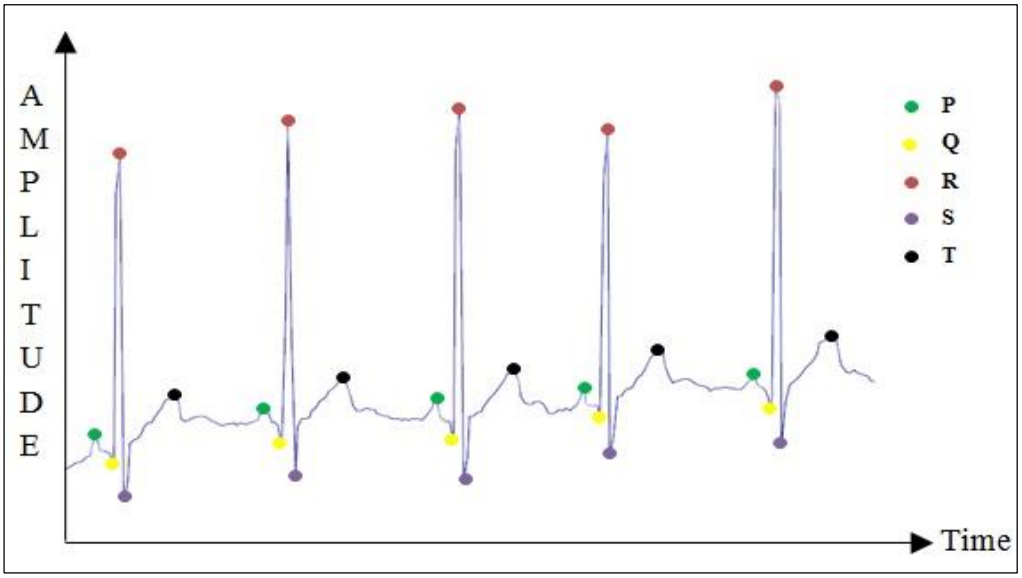

Figure 2.9. Segment of normal ECG for record no. N001 with reduced samples and a window of size 5 shows all ECG peaks and troughs are maintained after reduction process readings from Shimmer3 ECG dataset

The proposed ECG reduction algorithm can be acceptable to reduce a Normal ECG data when a window size was increased up to 15 because the reduced ECG signals maintained the diagnostic features and P,Q,R,S,T waves, especially R waves. For example, Figure 2.8 represents raw ECG signal with five ECG beats. When the proposed ECG reduction algorithm was applied to reduce the ECG signal using a window size of 15 the reduced ECG signal conserved for P,Q,S,T points and all R points as shown in Figure 2.10.

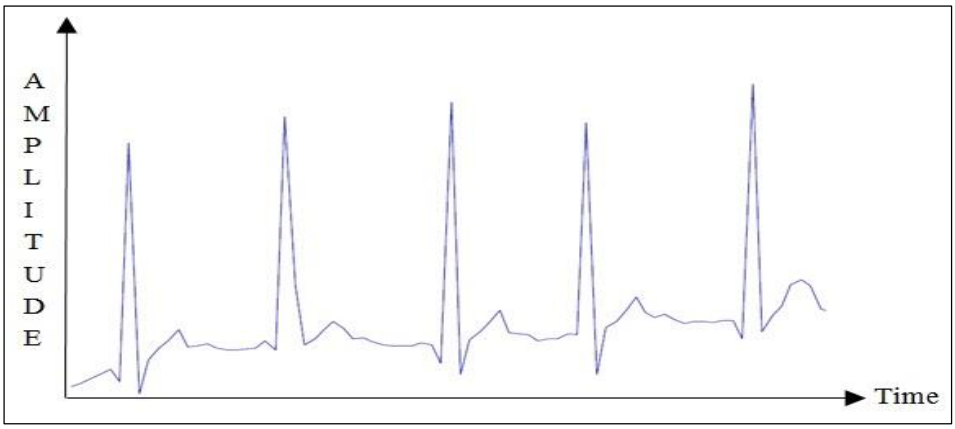

Figure 2.10. Segment of Normal ECG for record no. N001 readings from Shimmer3 ECG dataset with reduced samples and a window of size 15 illustrates some ECG peaks and troughs such as P and Q waves are missed after reduction process but the R and T waves are still saved

The proposed ECG reduction algorithm (Max_Min) provided very good signal quality when it was applied to all cardiovascular arrhythmias with window size set from 2 to 5. It did not change the morphology/shape of ECG signal waves (P, Q,R,S, T) and maintained all P or T waves when their amplitutes were too low such as in Atrial Flutter rhythm or Atrial Fibrilliation rhythm. Also, it included the P, R, T peaks as well as shown in Figure 2.11 and Figure 2.12 below, indicating that the automated detection algorithm to correctly detecting diagnostic features.

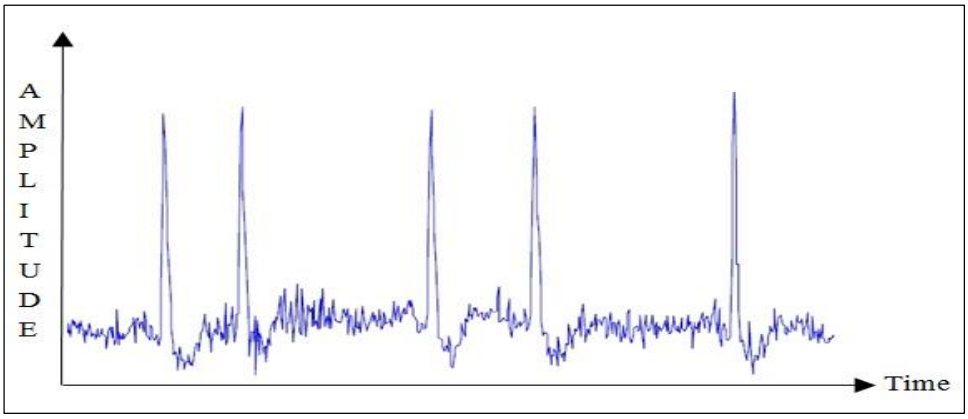

Figure 2.11. Segment of ECG for record no. 200 with raw AF samples reading from MIT-BIH Arrhythmia database

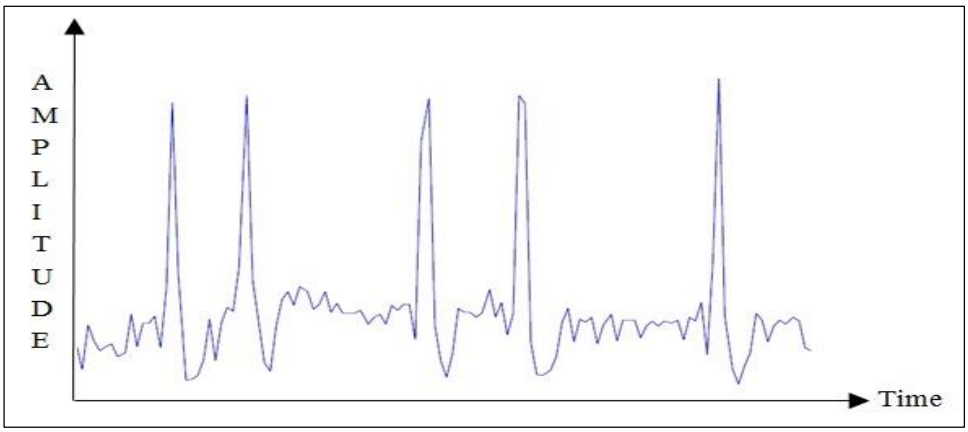

Figure 2.12. Segment of ECG for record no. 200 readings from MIT-BIH Arrhythmia database with reduced AF samples and a window of size 5 illustrates many ECG peaks and troughs are saved after reduction process

2.4.1.2 Mean ECG reduction algorithm results

Figure 2.13 depicts part of the raw ECG from record no. 103 readings of the MIT-BIH Arrhythmia database. This record represents a Normal ECG. Figure 2.14 also illustrates a segment of record no. 103 but where only some of the samples have been selected for storage by the mean ECG reduction algorithm described above in algorithm 2.2 using a window of size 5. Figure 2.14 illustrates that each peak and trough has been correctly retained. The mean algorithm provides a compression ratio of 5 and 2 PRD. Furthermore, it can be used with long and short term ECG signal at different sampling rates.

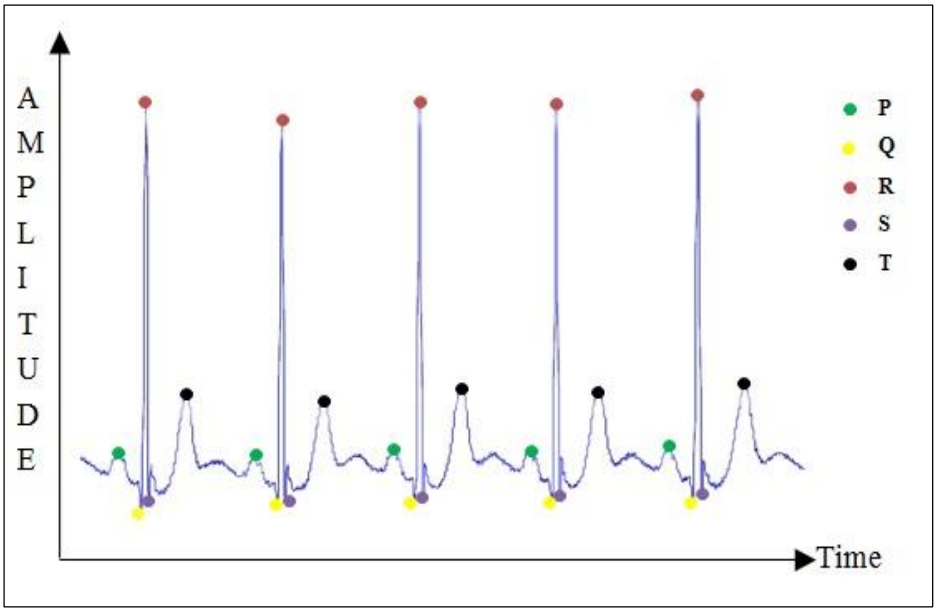

Figure 2.13. Segment of normal ECG for record No. 103 with raw samples

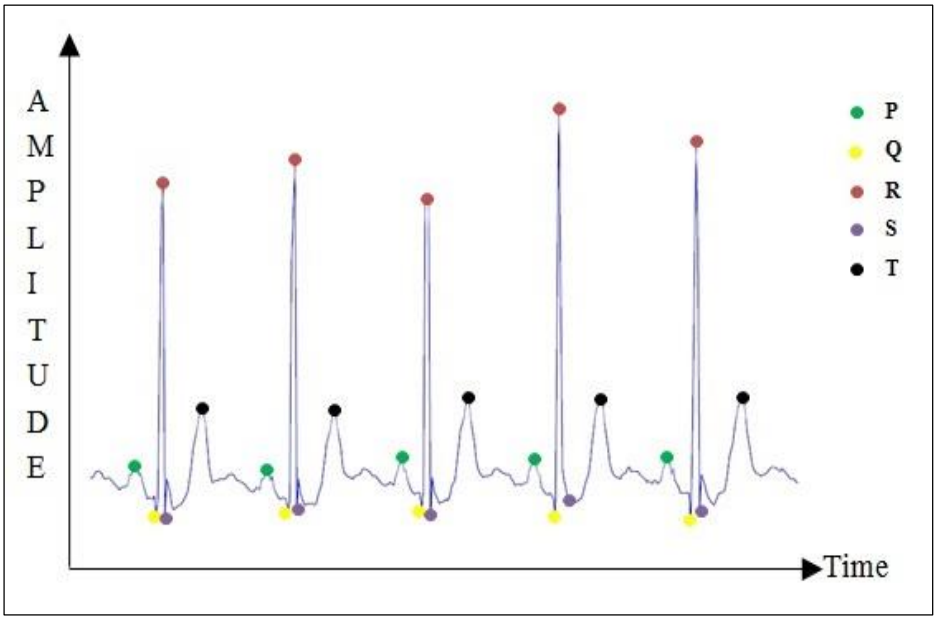

Figure 2.14. Segment of Normal ECG for record no. 103 with reduced samples illustrates all ECG peaks and troughs are maintained after reduction process

More ECG examples obtained from Shimmer3 ECG dataset are illustrated in the figures below.

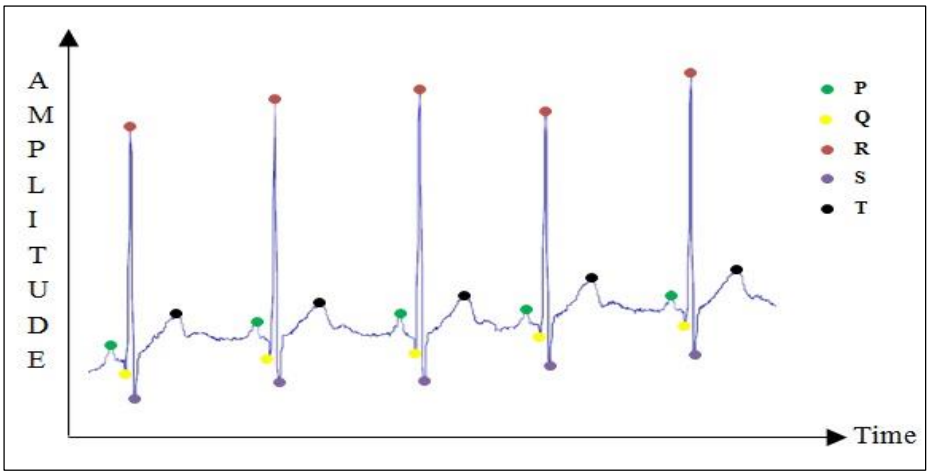

Figure 2.15. Segment of Normal ECG for record no. N001 with raw samples readings from Shimmer3 ECG dataset

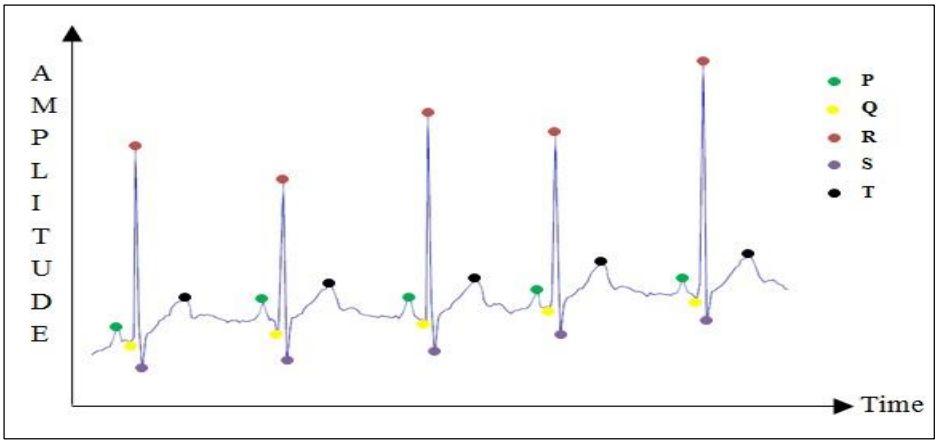

Figure 2.16. Segment of Normal ECG for record no. N001 with reduced samples using a window of size 5 illustrates all ECG peaks and troughs are maintained after reduction process readings from Shimmer3 ECG dataset

The mean ECG reduction algorithm was unable to reduce a Normal ECG data set when window size was increased up to 10 because the reduced ECG signals missed some P, Q, R, S, T waves and changed the ECG signals morphology. Figure 2.16 represents the raw ECG signals, which consist of five ECG beats when the mean ECG reduction algorithm was applied to reduce the ECG signals. With a window size of 10 the reduced ECG signals missed the first, fourth, and fifth beat and changed the ECG signals morphology as shown in Figure 2.17.

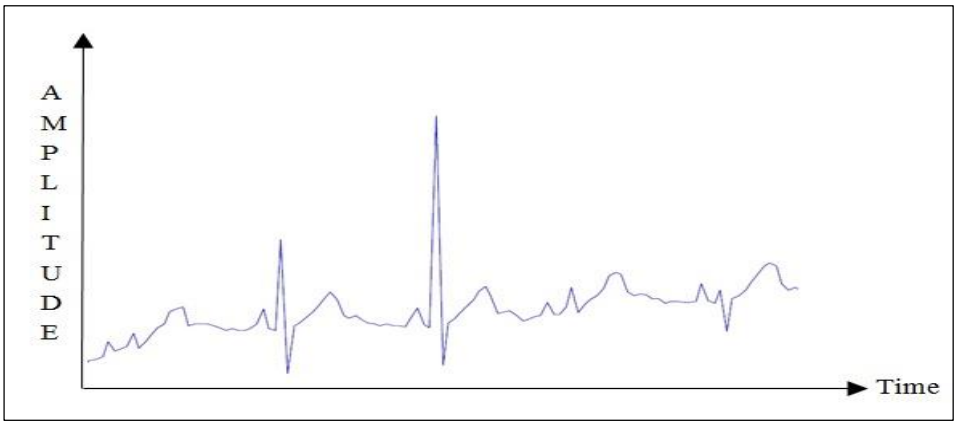

Figure 2.17. Segment of Normal ECG for record no. N001 readings from Shimmer3 ECG dataset with reduced samples and a window size of 10 illustrates some ECG peaks and troughs are missed after reduction process

The mean ECG reduction algorithm provided very good signal quality but only when it was applied to some cardiovascular arrhythmias such as PAC, Normal, and PVC rhythms with a window size from 2 to 5. In contrast, the mean ECG reduction algorithm changed the ECG signal rhythm and missed P or T or both (P, T) waves, particularly when their amplitudes were too low. For example, as shown in Figure 2.18, the original ECG signals comprised five ECG beats when the mean ECG reduction algorithm was employed to reduce the ECG signals with a window size of 5, whereupon the morphology of the reduced ECG signals changed significantly. Clearly, it represented the first, second, third and fourth beats very poorly and maintained only the fifth beat, as depicted in Figure 2.19 which caused the automated detection algorithms to fail in terms of detecting diagnostic features.

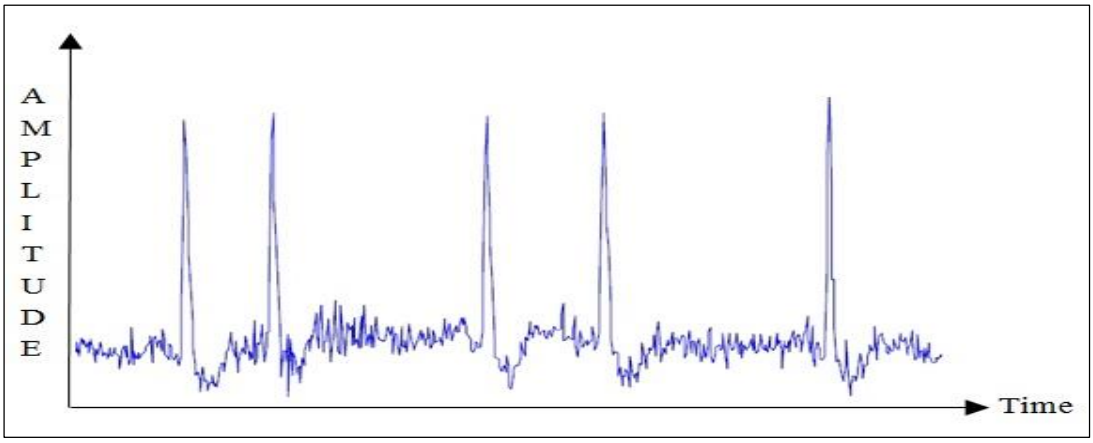

Figure 2.18. Segment of ECG for record no. 200 with raw AF samples reading from MIT-BIH Arrhythmia database

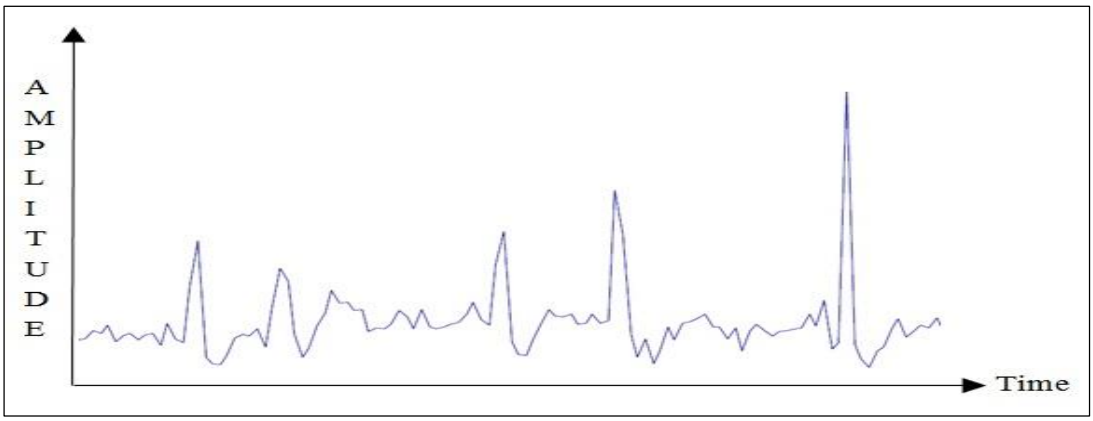

Figure 2.19. Segment of ECG for record no. 200 readings from MIT-BIH Arrhythmia database with reduced AF samples and a window size of 5 illustrates many ECG peaks and troughs are missed after reduction process

2.4.1.3 Median ECG reduction results

Figure 2.20 shows segment of the raw ECG from record no. 119 readings of the MIT-BIH Arrhythmia database. Figure 2.21 also depicts a part of record no. 119 but where only some of the samples have been selected for storage by the median ECG reduction algorithm using a window of size 5. Figure 2.21 illustrates that each peak and trough has been correctly estimated. The algorithm provides

a compression ratio of 5 and 3% PRD. Furthermore, it can be used with long and short term ECG signal at different sampling rates.

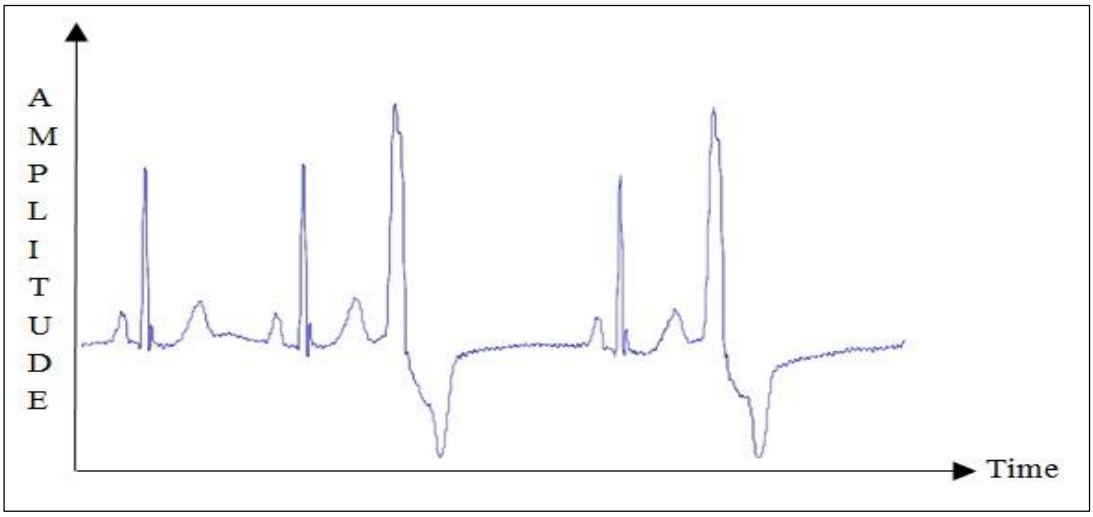

Figure 2.20. Segment of PVC ECG for record no. 119 with raw samples

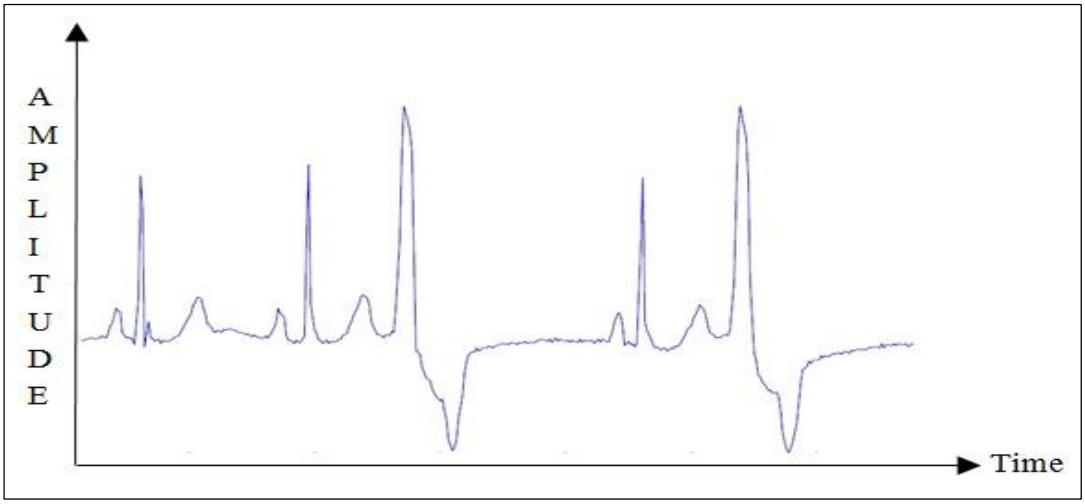

Figure 2.21. Segment of PVC ECG for record no. 119 with reduced samples illustrates all ECG peaks and troughs are maintained after reduction process.

More illustration segments, which support the meadian ECG reduction algorithm, extracted from Shimmer3 ECG dataset are represented in the figures below.

Figure 2.22. Segment of PVC ECG for record no. N007 with raw samples readings from Shimmer3 ECG dataset

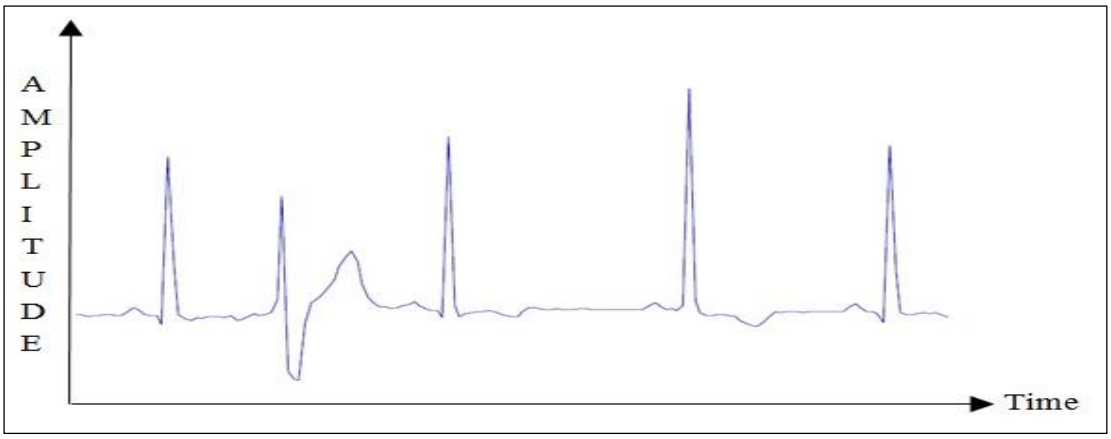

Figure 2.23. Segment of PVC ECG for record no. N007 with reduced samples and a window size of 5 illustrates all ECG peaks and troughs are maintained after reduction process readings from Shimmer3 ECG dataset

The median ECG reduction algorithm was unable to reduce PVC ECG data when the window size was increased to 8 because the reduced ECG signals eliminated the diagnostic features and changed the ECG signals' morphology. In Figure 2.23, the original ECG signals comprised five ECG beats, however after the median ECG reduction algorithm was utilised to reduce the ECG signal using a window size of 8, the second and third beats were eliminated. In addition, some of the first, fourth, and fifth beats missed some P, Q, S, T points and retained only the R points, as depicted in Figure 2.24.

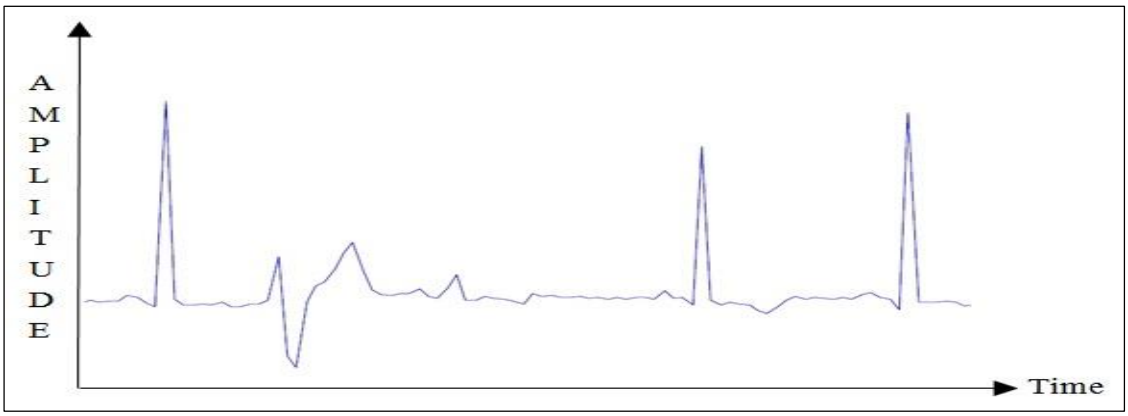

Figure 2.24. Segment of PVC ECG for record no. N007 readings from Shimmer3 ECG dataset with reduced samples and a window of size 8 illustrates some ECG peaks and troughs are missed after reduction process

The median ECG reduction algorithm provied very good signal quality when it was applied to Normal, PAC, and PVC rhythms with a window size set from 2 to 5. In contrast, the median ECG reduction algorithm changed the ECG signal morphology when the window size set higher than 5 and missed P or T or both (P, T) waves when their amplitutes were too low such as in Atrial Fibrilliation rhythm. For instance, in Figure 2.25, the raw ECG signal composed of five ECG beats is shown when the median ECG reduction algorithm was applied to reduce the ECG signal with a window size of 5. Again the morphology of the reduced ECG signals were changed. It misrepresented the first three beats due to the P, Q, R, S, and T waves not being recognised. The morphology of the fourth beat

was changed but the Q, R, S, T waves can be detected. Only the fifth beat was maintained as depicted in Figure 2.26 that led automated detection algorithms to fail in detecting diagnostic features.

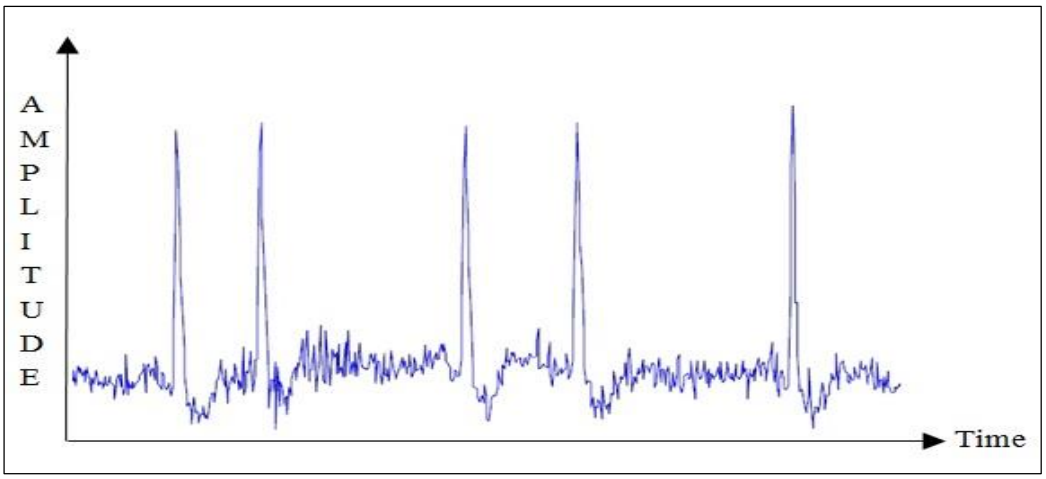

Figure 2.25.Segment of ECG for record no. 200 with raw AF samples reading from MIT-BIH Arrhythmia database

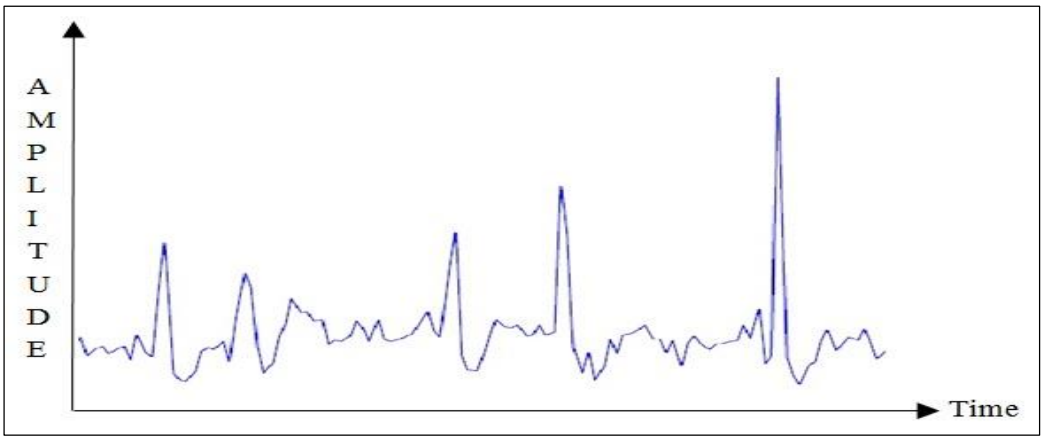

Figure 2.26. Segment of ECG for record no. 200 readings from MIT-BIH Arrhythmia database with reduced AF samples and a window of size 5 illustrates many ECG peaks and troughs were missed after reduction process

Noise and data transmission losses are likely to impact more heavily on wearable ECG sensors because of the interference from other mobile devices in addition to the traditional ECG noise. This is described in the next section.

2.4.2 ECG noise reduction results

Typically, an ECG signal is affected by two main types of noise, electromyogram (EMG) and baseline wander (BW) (Moody, Muldrow, & Mark, 1984). EMG noise is generated because of muscular activity. It is mostly at a high frequency period from 5 to 500Hz. BW noise is generated because of the motion of electrodes or respiration. It is predominantly at low frequency periods under 0.5 Hz. ECG filtering improves diagnostic features recognition for both cardiologists and computerised analysis (Hashemi, Rahimpour, & Merati, 2015). Numerous publications indicated that adaptive filtering influenced the computation of morphological features of ECG signals (Gregg et al., 2008; Łęski & Henzel, 2005; Valvbrde et al., 1998). Censi et al. (2009) investigated how filtering methods

effect ECG signals. They concluded that high-pass filtering methods may reduce peaks and troughs substantially, which leads to inaccurate results. We discovered that all proposed ECG reduction methods can be reduced to a type of ECG noise as explained below.

The mean ECG reduction algorithm removed high frequency noise and maintained diagnostic features based on a window size up to 4 (optimal case) as illustrated in Figure 2.28. When the window size was increased up to 5, the mean ECG reduction algorithm still removed high frequency noise but only when ECG signals had high P and T amplitudes.

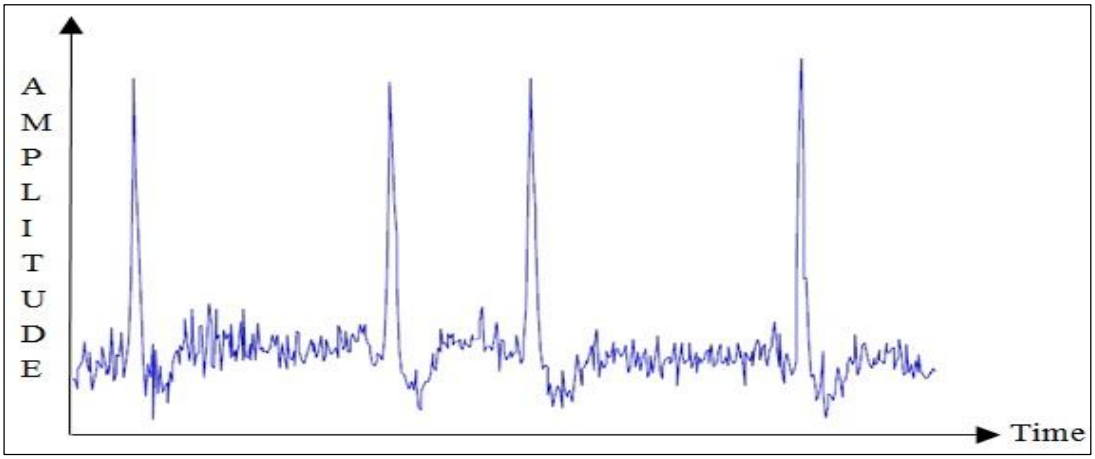

Figure 2.27. Segment of raw ECG for record no. 200 readings from MIT-BIH Arrhythmia database

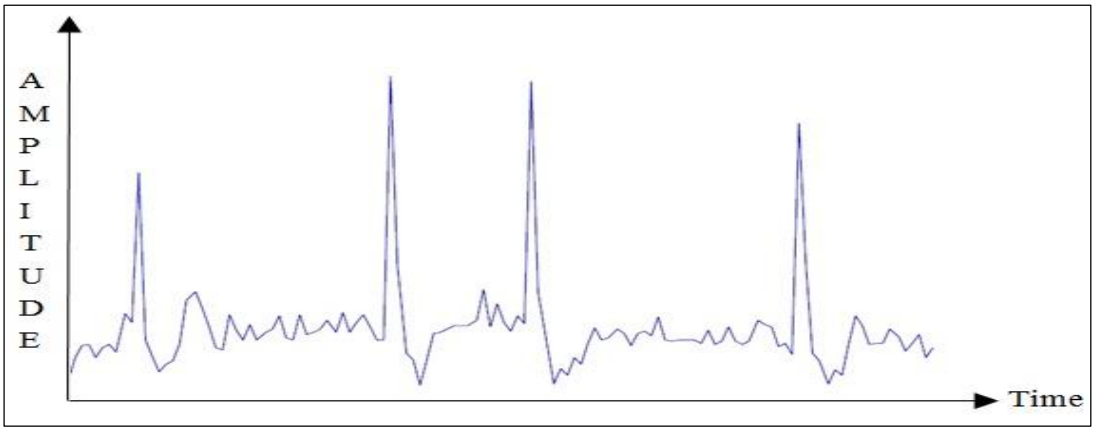

Figure 2.28. Segment of reduced ECG for record no. 200 readings from MIT-BIH Arrhythmia database with a window size of 4 illustrates many ECG peaks and troughs are saved after reduction process

The median ECG reduction algorithm removed high frequency noise and reserved diagnostic features based on a window size up to 4 (optimal case) as shown in Figure 2.30. Also, it removed outliers in any sliding window. When the window size was increased to 5, the median ECG reduction algorithm still removed high frequency and low frequency noise but only when ECG signals had high P and T amplitudes. The time complexity of the median algorithm is O(nlogn) while the time complexity of the mean algorithm is O(n). Therefore, the median ECG reduction algorithm is more computational

expensive than the mean ECG reduction algorithm. However, the mean ECG reduction algorithm was ideal for high frequency noise.

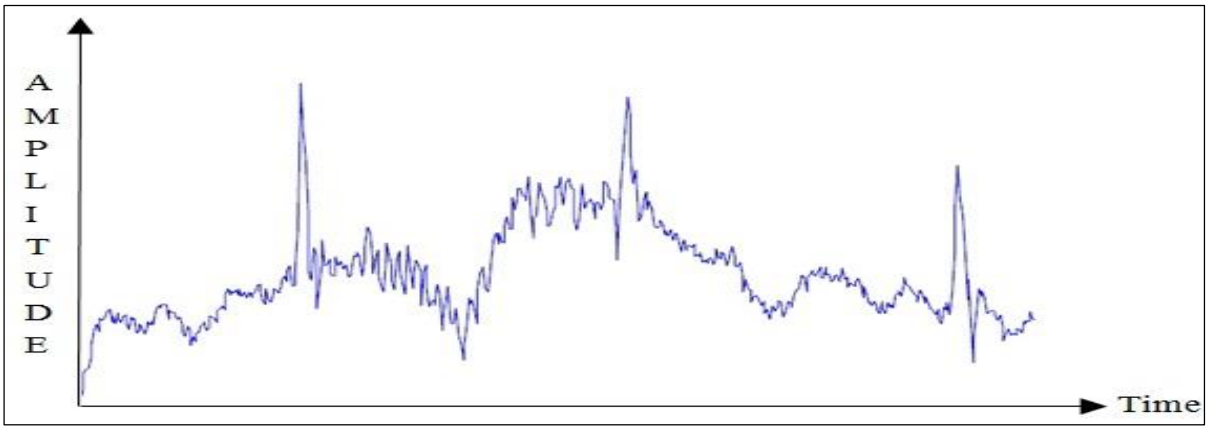

Figure 2.29. Segment of raw ECG for record no. N008 readings from Shimmer3 ECG database

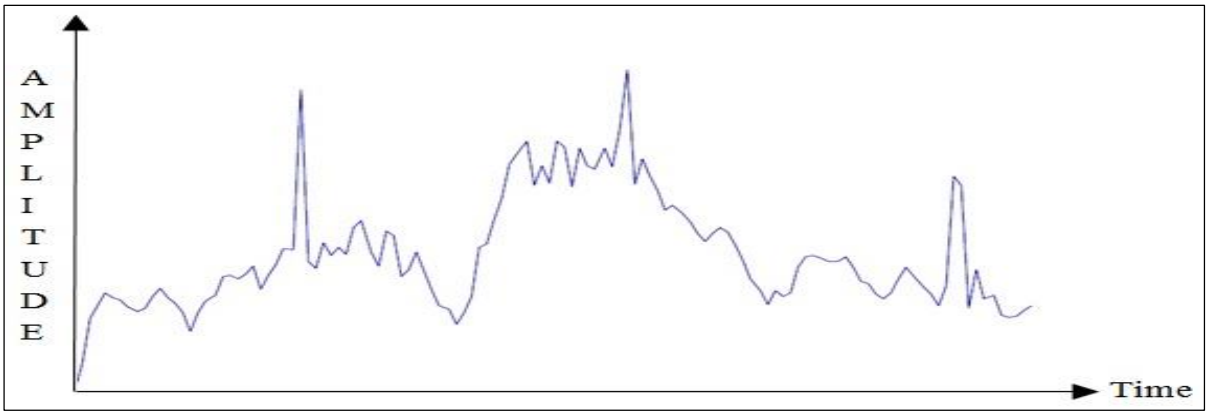

Figure 2.30. Segment of reduced ECG for record no. N008 readings from Shimmer3 ECG database with a window size of 4 illustrates many ECG peaks and troughs are saved after reduction process

The proposed ECG reduction algorithm eliminated high frequency noise and maintained diagnostic features based on a window size of 5 (optimal case) as illustrated in Figure 2.31. Also, it still removed high frequency noise when ECG signals had low P and T amplitudes. The proposed ECG reduction algorithm is similar to the computational efficiency of the mean ECG reduction algorithm. Therefore, it is suitable for real-time ECG filtering.

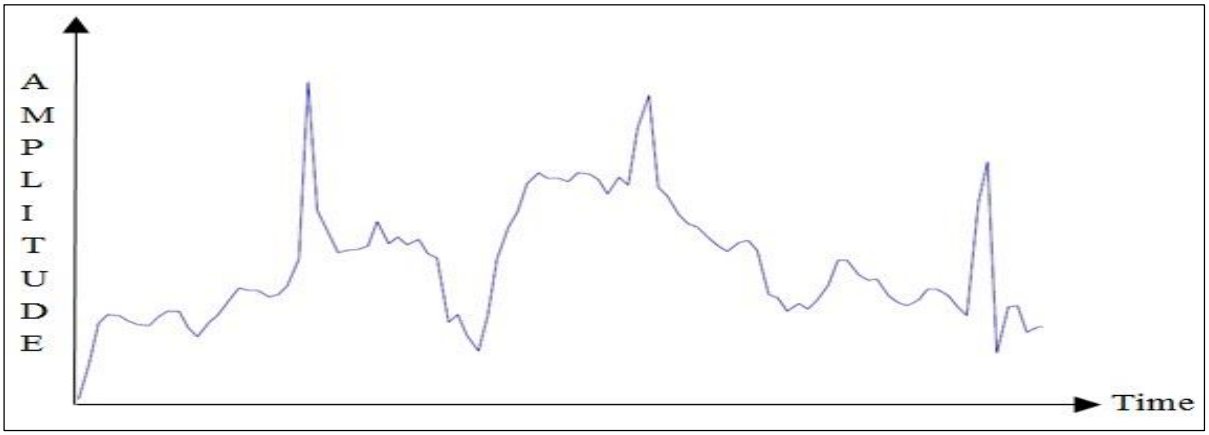

Figure 2.31. Segment of reduced ECG for record no. N008 readings from Shimmer ECG database with a window of size 5 illustrates many ECG peaks and troughs are saved after reduction process

As mentioned, reduction of ECG signals does not require retaining all data points; rather, only some points of the ECG data are essential (P, Q, R, S, and T), as well as relevant intervals. Some data is lost with the proposed ECG reduction algorithms in that all points in the window are discarded except for the minimum or maximum, mean or median. Whether these points are critical for the generation of important ECG indicators is discussed in the next section. The computerised results illustrated that ECG features generated from the reduced data were approximately similar to those generated from the raw data.

2.5 Generation of Features from Reduced ECG Data

Many methods employ P,QRS,T information to measure the distortion between raw and compressed or reduced ECG signal. For example, Zigel et al. (2000) introduced an algorithm to assess the distortion of an ECG signal. This algorithm is based on measures of P, QRS, and T diagnostic features and include the PR interval, ST segment and RR interval of the raw ECG signal and the compressed ECG signal. Zigel et al. (2000) reported that the feedback from cardiologists was more positive than with traditional distortion measures. Also, the link between diagnostic distortion and the PRD metric was categorized as: if the PRD from 0 to 2 % then signal quality is very good, if the PRD from 2 to 9 % then signal quality is very good or good and if the PRD from >= 9 % then signal quality is not possible to determine.

For the evaluation of the proposed ECG reduction methods, we used P, QRS, and T diagnostic features to measure the quality of the reduced signal. Further, we calculated PRD and CR parameters that are most commonly used to quantify the reduction effectiveness and accuracy while analysing the diagnostic quality of the reduced ECG data. CR and PRD are given as below:

$$CR=(X/Y) \tag{2.7}$$

$$PRD=||X-Y||^2/||X||^2 \times 100 \tag{2.8}$$

Where X is the plain signal and Y is the reduced signal.
We computed the P,QRS,T dignostice features for the raw data as follows:

$$A=|i-N| \times 1/frequency \tag{2.9}$$

Where A represents any interval or segment such as PR interval.

Where i refers to start intervel and N referes to end interval.

We reconstructed the dignostic features from the reduced data using Equation 2.10 below:

$$\bar{A} = |(i \times WS) - (N \times WS)| \times 1/frequency \quad (2.10)$$

Where $\bar{A}$ represents any interval or segment such as ST segment and *WS* represents window size. The next section illustrates how the optimal window size was selected.

2.5.1 Window size

Most important ECG features that clinicians and many computerized algorithms apply to diagnose cardiovascular diseases were generated from the reduced ECG signal. Raw ECG signals were examined with window sizes of 2, 3, 4, 5, 6, 7, 8, 9 and 10 samples. We utilised the WFDB software that is available publicly to extract ECG features (diagnostic features) from raw and reduced ECG signals (Silva & Moody, 2014). The window size was started from 2 then increased gradually. The width of window size depended on the detection of essential features (diagnostic features) of the ECG signal (P, Q, R, S, and T). The window size was increased in width if the P, Q, R, S, and T were correctly identified.

Table 2.1. Window size versus Max_Min ECG reduction algorithm accuracy/effectiveness

Window size	CR	PRD% PR interval	PRD% PR segment	PRD% QRS complex	PRD% ST segment	PRD% ST interval	PRD% QT interval	PRD% RR interval
2 samples	2:1	99.9	99.9	99.9	99.9	99.9	99.9	99.9
3 samples	3:1	99.9	99.9	99.9	99.9	99.9	99.9	99.9
4 samples	4:1	99.9	99.7	99.9	99.3	99.9	99.9	99.9
5 samples	5:1	99.2	99.6	99.3	99.1	99.2	99.5	99.4
6 samples	6:1	85.4	69.5	93.9	72.7	78.9	93.5	99.2
7 samples	7:1	71.3	N/A	92.8	N/A	N/A	83.6	98.8
8 samples	8:1	N/A	N/A	92.1	N/A	N/A	74.9	98.8
9 samples	9:1	N/A	N/A	91.4	N/A	N/A	55.9	98.6
10 samples	10:1	N/A	N/A	90	N/A	N/A	55.2	98.3

Note: N/A represents failure to detect an interval

Table 2.1 describes the link between window size, diagnostic features distortion and detection accuracy. When the window size is set to 2, 3 or 5, the quality of the reduced signal is high and the diagnostic features can be detected. When the window size increases to 6, the quality of the reduced signal is good and diagnostic features can be still detected, but the accuracy of the reduced signal decreases when the window size increases above 7. The P and T waves cannot be detected because of the reduced signal distortion resulting in a failure to detect ST and PR intervals. R waves can be

detected correctly with all window sizes from 2 to 10. A window size of 5 has been determined empirically to produce the optimal trade-off between compression ratio, accuracy and computational resources. The window size can be varied to achieve different trade-offs depending on the context.

Table 2.2. Window size versus mean reduction algorithm accuracy/effectiveness

Window size	CR	PRD% PR interval	PRD% PR segment	PRD% QRS complex	PRD% ST segment	PRD% ST interval	PRD% QT interval	PRD% RR interval
2 samples	2:1	99.2	99.1	99.3	99.5	99.2	99.9	99.9
3 samples	3:1	98.9	99.3	99.2	99.7	99.5	99.8	99.9
4 samples	4:1	84.1	91.4	87.1	88.3	88.4	91.7	90.9
5 samples	5:1	73.5	74.4	85.6	86.4	86.4	87.2	87.5
6 samples	6:1	63.6	50.7	73.8	68.4	74.3	74.3	85.7
7 samples	7:1	N/A	N/A	70.1	N/A	N/A	79.8	82.4
8 samples	8:1	N/A	N/A	60.9	N/A	N/A	63.1	73.5
9 samples	9:1	N/A	N/A	46.4	N/A	N/A	43.7	63.2
10 samples	10:1	N/A	N/A	30.8	N/A	N/A	38.5	60.8

It can be observed from Table 2.2, when the window size is set to 2, 3 or 4, the quality of the reduced signal is high and the diagnostic features can be accurately detected. When the window size increases to 5, the quality of the reduced signal is good and the diagnostic features can be still detected. The quality of the reduced signal decreases when the window size increases above 6. The P and T waves cannot be detected because of the reduced signal distortion, resulting in the failure to detect ST and PR intervals.

Table 2.3. Window size versus median reduction algorithm accuracy/effectiveness

Window size	CR	PRD% PR interval	PRD% PR segment	PRD% QRS complex	PRD% ST segment	PRD% ST interval	PRD% QT interval	PRD% RR interval
2 samples	2:1	99.7	99.8	99.7	99.9	99.9	99.9	99.9
3 samples	3:1	98.4	99.5	99.5	99.7	99.5	99.9	99.9
4 samples	4:1	90.3	90.3	90.1	90.5	90.2	90.8	90.5
5 samples	5:1	73.7	74.1	85.3	86.6	86.9	86.9	87.9
6 samples	6:1	63.9	51.9	72.9	68.7	75.1	75.8	86.2
7 samples	7:1	N/A	N/A	71.6	N/A	N/A	80.8	82.8
8 samples	8:1	N/A	N/A	62.1	N/A	N/A	63.6	73.3
9 samples	9:1	N/A	N/A	48.3	N/A	N/A	43.7	63.5
10 samples	10:1	N/A	N/A	32.6	N/A	N/A	39.9	61.2

Table 2.3 indicates that the window size has an almost similar effect on diagnostic features distortion and detection accuracy for both median and mean ECG reduction algorithms

We conclude that based on proposed ECG reduction (Max_Min) algorithm most intervals including the QT interval can be accurately detected from reduced ECG signal with a window size of 5. The RR intervals data detected from the reduced signals have about 99% similarity to the RR data detected

from the raw ECG signal up to a window size of 10. Thus, time-domain, frequency-domain, and nonlinear heart rate variability (HRV) analysis results are almost identical to the original ECG signal results. In addition, we found that based on the median ECG reduction algorithm most intervals including the QT and RR intervals are accurately detected from the reduced ECG signal with a window size of 4. The QT and RR intervals data detected from the reduced signals have about a 99 % similarity to the QT and RR data detected from the raw ECG signal up to a window size of 4. According to the mean ECG reduction algorithm, it can be concluded that most intervals including the RR and QT intervals are accurately detected from the reduced ECG signal with a window size of 4. The RR and QT intervals data detected from the reduced signals have about a 98 % similarity to the RR and QT data detected from the raw ECG signal up to a window size of 4.

Table 2.4. Comparison of proposed ECG data reduction algorithms (mean, median, Max_Min)

Algorithm	**Optimal Window Size**	**Signal Quility**	**Arrhythmia type**	**Sampling Rate**	**CR**	**PRD %**
Mean	2 to 4	Very good	PVC,PAC,Normal,LBBB, RBBB	Any	4	2
Median	2 to 4	Very good	PVC,PAC,Normal,LBBB, RBBB	Any	4	3
Max_Min	2 to 5	Very good	All	Any	5	1

The Max_Min ECG reduction algorithm provided high signal quality and a compression ratio of 5 when implemented with a window size of 5, so we selected this algorithm to compare with existing ECG reduction algorithms.

Table 2.5 illustrates that the proposed ECG reduction algorithm achieves a very low PRD % at a compression ratio of 5 when executed with a window size of 5. This compares favourably with many other algorithms.

Table 2.5. Comparison of ECG data reduction algorithms

Methods	**CR**	**Sampling Rate Hz , (No. of Bits)**	**PRD%**
TP	2	200, 12	5.3
AZTEC	10	500,12	28
CORTES	4.8	200,12	7
FAN/SAPA	3	250,-	4
SLOPE	4.8	250,-	7
Fang et al.	2.5	256,-	-
Proposed method	5	Any	1

The PRD was very low because every point selected was one of the raw ECG points. The compression ratio and accuracy are comparable with the algorithm mentioned in Table 2.5.

The high compression ratio and simple instructions that the proposed ECG reduction method provided have significantly contributed to reduce the power consumption for wearable ECG sensor are described in Section 2.7.2.

2.5.2 Energy consumption for wearable ECG sensor

Power consumption for wearable sensors represents the main challenge of real-time monitoring systems (Craven et al., 2015; Islam et al., 2014). Therefore, an algorithm that can easily be implemented on wearable sensors, provide high compression ratio and maintain signal quality is crucial for reducing energy consumption.

In this study, we used Shimmer3 ECG wearable sensor as a reference to measure energy consumption in milli Joules. The Shimmer3 motherboard consists of a low-power Texas Instrument 16-bit MSP430F5437A microcontroller, 2.7 Volts, a low-power CC2420 IEEE 802.15.4 compliant radio, and has a Bluetooth module. In addition, Shimmer3 has a 450 mAh lithum-ion rechargeable battery that can work up to 16 hours when the sampling rate is 200 Hz. The MSP430 microcontroller runs at 8 MHz and has 16 KB of RAM, 256 KB of Flash memory. Also, it has a fast hardware multiplier, but does not have a floating-point unit (Shimmer, 2015). The energy consumption has been evaluated for the runtime reduction methods by implementing each method on the Shimmer3 ECG board. We coded ECG reduction/compression algorithms on Shimmer3 sensor by using Code Compose Studio (CCS) version 7.1 that is available publicly at (Texas Instruments, 2015b). The execution time for each reduction/compression algorithm was calculated based on an ECG segment size of 1000 samples readings from Shimmer3 ECG database using Equations 2.11 and 2.12. Due to routine interruptions that occur during processing, overall execution time was affected. The reduction/compression processes were repeated 200 times and the average execution time calculated to accurately measure runtime as illustrated in Table 2.6.

$$Power = Volts \times Amp \tag{2.11}$$

$$Energy\ consumption = Power \times Runtime \tag{2.12}$$

Table 2.6. Comparison of ECG data reduction algorithm for energy consumption

Methods	Average run time for 200 runs (ms)	Energy consumption (mJoule)
TP	98	1.47
AZTEC	174	2.61
CORTES	270	4
FAN/SAPA	123	1.84
SLOPE	286	4.30
Fang et al.	253	3.8
Proposed method	102	1.52

The runtime and energy consumption are comparable with the algorithms listed in Table 2.6 and are particularly good, given that the algorithm executes in real-time and increases battery life using high CR, minimal CPU, storage requirements and power consumption as described in the next section.

2.5.3 Energy consumption based on real test data streaming

The executing of simple algorithms within wearable sensors consumes low power but the transmission process drains significant power because the sensor's radio generally accounts for most of the overall power consumption (Craven et al., 2015; Da Poian et al., 2016). For example, the Texas Instruments Inc. state that the CC2420 radio consumes 230nJ of power to transmit a bit of data, except start up and redundancy packed constitutes (Texas Instruments, 2015a).

As previously mentioned, only two methods measured Shimmer power consumption. However, these methods provided inaccurate results because they were based on standard ECG data, not on a real-time monitoring system with ECG data streaming. In contrast, the proposed method was executed based on a real monitoring system with real ECG data generated from a Shimmer3 ECG sensor as follows. Shimmer3 ECG sensor battery life was measured based on different sampling rates 256 Hz without any reduction/compression method to measure the actual battery life. The battery was fully charged and real ECG signals were collected from a volunteer with Normal ECG rhythm via Bluetooth to a laptop device based on Consensys v1.1.0 software that is freely available (Shimmer, 2015). The Consensys v1.1.0 software manages the Shimmer3 ECG sensor and provides many facilities such as Manage device, Live data and Manage data. The Manage data provides information about data size and recording time. The Live data has many options such as connection with the sensor via Bluetooth, record ECG data, setting and display the battery level. From the manage device, researchers can upload their own algorithms on a Shimmer3 sensor node. After that, each reduction/compression method was implemented and uploaded on the Shimmer3 node to calculate the battery life as reported in Table 2.7.

Table 2.7. Battery life based on real test for real-time ECG reduction/compression methods at sampling rate 256 Hz

Method	Battery-life (h)
Standard	13
Tp	18.52
AZTEC	38.47
CORTES	20.17
FAN/SAPA	17.50
SLOPE	18.20
Fang et al.	11.10
Max_Min (N=5)	29.52
Max_Min (N=10)	45.15

Table 2.7 demonstrates that the proposed algorithm increases Shimmer3 battery-life significantly with a window size of 5 or 10. It can be concluded that the Shimmer3 with a window size of 5 can be used as a Holter because it can work more than 24 hours continuously.

Most ECG compression/reduction methods have only been evaluated with statistical measures. The proposed ECG reduction algorithms have been evaluated based on statistical measures, as illustrated above, and with clinical tests, as outlined in Section 2.8 as follow.

2.6 Clinical Analysis

To validate the proposed methods clinical analysis was also performed by an expert cardiologist. We sent large ECG segments via Email that approximately covered all arrhythmia types obtained from Physionet databases (Physionet, 2015) and Shimmer3 ECG dataset to a senior cardiologist (independent/blind cardiologist). The expert cardiologist was not familiar with the research and was asked to assess the ECG segments.

The ECG segments were illustrated in Figure 2.32.

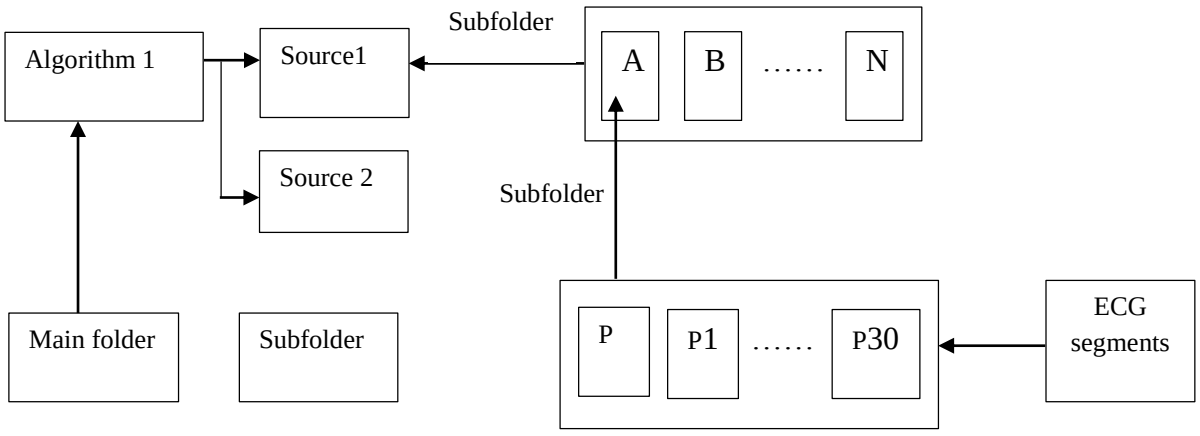

Figure 2.32. ECG data folders that sent to the cardiologist

Algorithm 1 refers to mean ECG reduction algorithm (Folder name).
Source 1 refers to name of File 1 that has ECG segments obtained from Physionet databases.
Source 2 refers to name of File 2 that has ECG segments obtained from Shimmer3 ECG databases.
(A) refers to an arrhythmia segment (ECG picture) such as Normal rhythm that has all ECG segments (raw and reduced segments) inside File 1 or File 2, etc.
P refers to raw ECG (raw ECG picture).
P1 refers to the reduced ECG segments based on mean ECG algorithm with a window size of 2.
P2 refers to the reduced ECG segments based on mean ECG algorithm with a window size of 3, etc.

The cardiologist classified the ECG segments as 'good', 'difficult', and 'fake' then sent the following message:

"The ECG segments that you sent are classified into three groups known as 'good', 'difficult' and 'fake'. 'Good' refers to similar to what I can see on the monitor that is currently used and the clinical condition was easy to diagnose. 'Difficult' are traces that raise uncertainty about the diagnosis. Hence, the diagnosis was not able to be made according to these ECG signals. 'Fake' looks like computerised ECG and unlikely to be generated from a patient monitoring system."

Following the subjective classification the results were sent to three cardiologists in Ibn Alnafees group in order to generalise the expert cardiologist's classification (good, difficult, and fake). The three cardiologists confirmed the expert cardiologist's classification results except for the 'fake' results, some of which were classified as real ECG as illustrated below.

Due to the ECG segments that were sent to the expert/independent cardiologist based on the three proposed ECG reduction methods were very large only some of these ECG segments are described below with the cardiologist's results.

2.6.1 Mean ECG reduction results

We selected some ECG segments that show different type of arrhythmias from Physionet databases.

Figure 2.33 illustrates the normal, raw ECG for record no. 103 was classified as 'good' by the cardiologist.

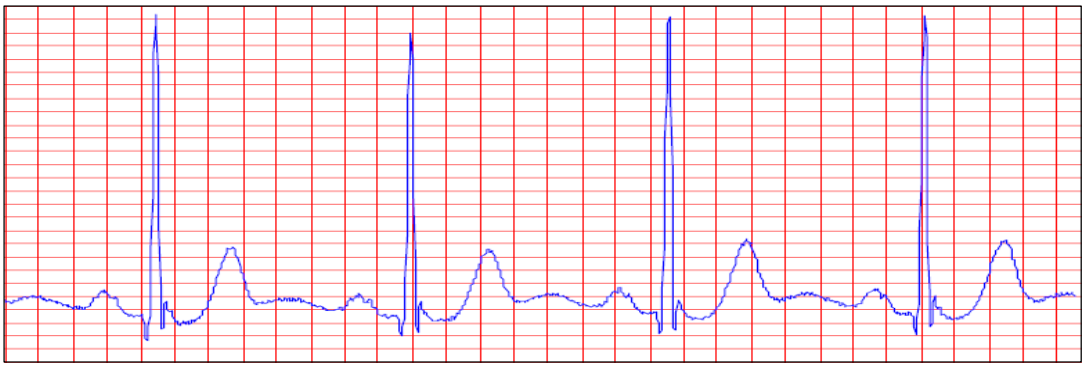

Figure 2.33. Segment of raw Normal ECG for record no. 103 classified as Good readings from MIT-BIH Arrhythmia database

The cardiologist was able to classify the reduced ECG segments based on the mean ECG reduction algorithm with a window size starting from 2 to 11 as depicted in Figure 2.34.

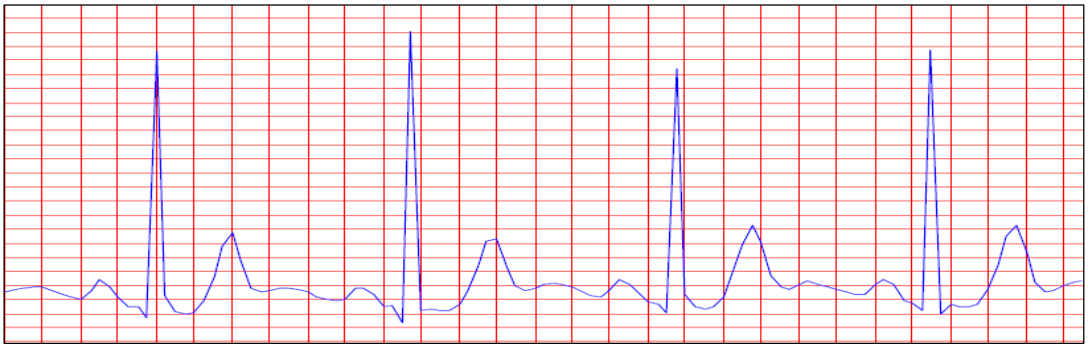

Figure 2.34. Segment of reduced ECG for record no. 103 classified as Good with a window size of 11

Extra complex rhythm is presented in the figures below.

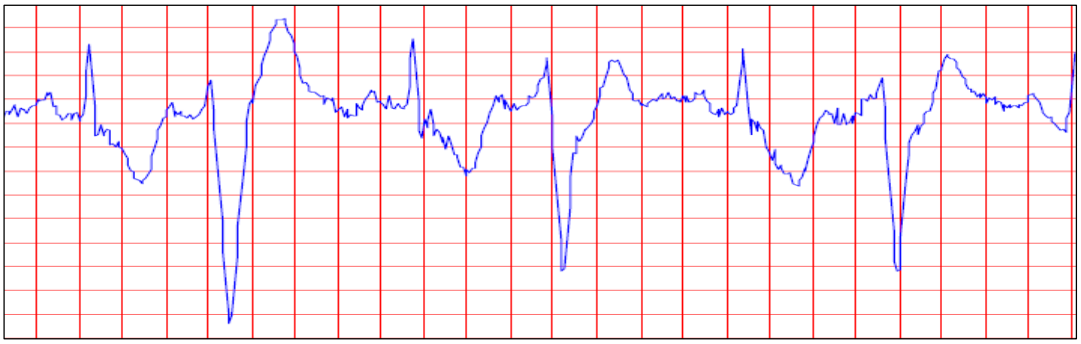

Figure 2.35. Segment of raw SV ECG for record no. 804 classified as ‘good’

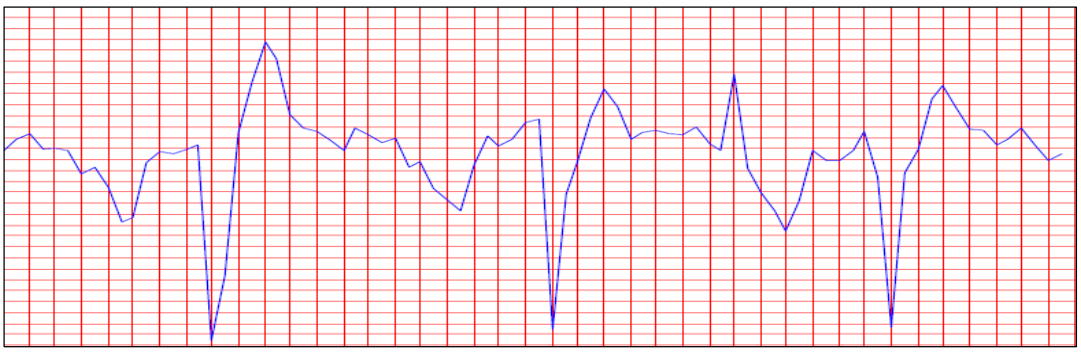

Figure 2.36. Segment of reduced SV ECG for record no. 804 classified as ‘fake’ with a window size of 5

2.6.2 Median ECG reduction results

Median ECG reduction results were almost the same as the mean ECG reduction results from the cardiologist's viewpoint. Some ECG segments that illustrate various type of arrhythmias obtained from the Shimmer3 ECG dataset are shown below in order to illustrate the cardiologist's results.

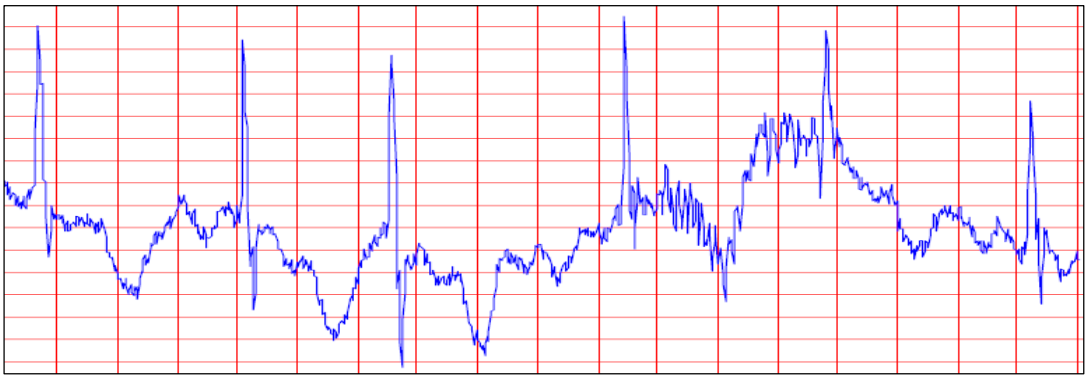

Figure 2.37. Segment of raw AF with Artifact ECG for record no. N001 classified as 'difficult'

The cardiologist classified the reduced ECG segment for record no. N001 as 'difficult' with a window size of 2,3,4,5. When the window was increased to 6, the cardiologist classified the reduced segment as 'fake' as represented in Figure 2.38.

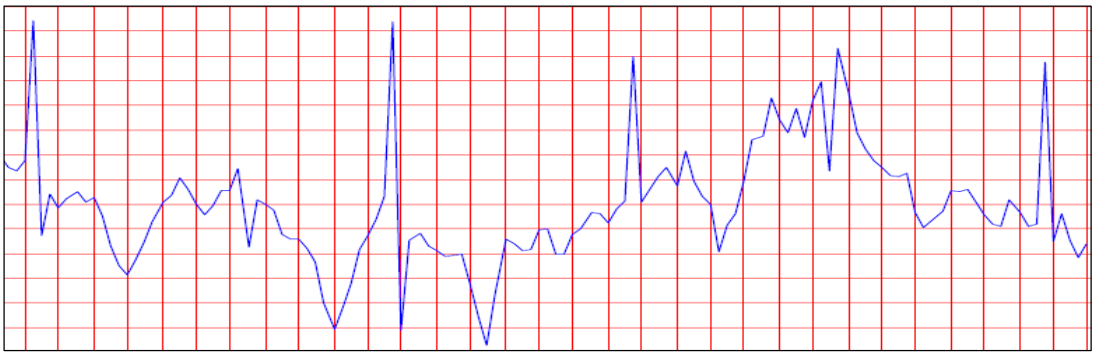

Figure 2.38. Segment of reduced AF with Artifact ECG for record no. N001 classified as 'fake' with a window size of 6

2.6.3 Max_Min ECG reduction results

The cardiologist was able to recognise arrhythmias based on Max_Min ECG reduction algorithm even with a large window such as size of 15. We selected some ECG segments that reflect different type of arrhythmias readings from Shimmer3 ECG dataset and Physionet databases.

Figure 2.39. Segment of raw PVC ECG for record no. 119 classified as *'good'* reading from MIT-BIH Arrhythmia database.

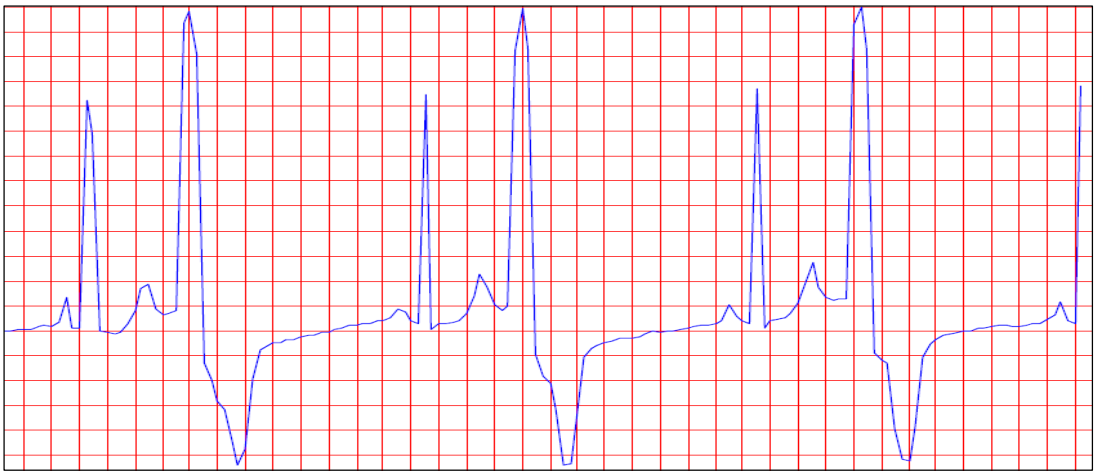

Figure 2.40. Segment of reduced PVC ECG for record no. 119 classified as 'good' with a window size of 15

The overall results that were obtained from the blind/independent cardiologist for the proposed ECG reduction algorithms are summarised in the tables below.

Table 2.8. The cardiologist overall results based on Max_Min ECG reduction algorithm obtained from Physionet databases and Shimmer3 ECG dataset

Arrhythmia type	**Window Size**	**Classification Type**	**Window Size**	**Classification Type**	**Window Size**	**Classification Type**
Normal	0,2,…15	Good	16,17,…19	Fake	----------	---------
AF	0,2,3,… ,6	Good	7,8,….20	Fake	----------	---------
Noisy AF	0,2,3,4	Difficult	5,6,7,8	Good	9,10,…..20	Fake
AFIB	0,2, ,…..15	Good	16,17,….20	Fake	----------	----------
PVC	0,2,…..19	Good	20,21,….30	Fake	----------	----------
APC	0,2,…..15	Good	16,17,…20	Fake	----------	----------
SV	0, 2,3,4	Good	5,6,7,……13	Fake	----------	----------
VFL	0,2,…,8	Good	9,10,……20	Fake	----------	----------
VT	0,2,…. 9	Good	10,12,……20	Fake	----------	----------

Note: zero means raw ECG segment.

Table 2.8 describes the link between window size, diagnosis and arrhythmias type. When the rhythms have high amplitudes such as Normal and PVC rhythms, the cardiologists detect the rhythms as *good* with window size set from 0 to 15 or 19. When the ECG rhythms have low amplitudes such as AF rhythm, the cardiologists classify the rhythm as *difficult* with a window size set from 0 to 4 because of the noise effect. AF rhythm was detected correctly with window sizes from 5 to 8, due to Max_Min algorithm, which reduced the noise and illustrated the rhythm type clearly to the cardiologists. Indeed, a window size of 5 has been identified clinically to provide the ideal trade-off between compression ratio and classification accuracy.

Table 2.9. The cardiologist's overall results based on mean ECG reduction algorithm obtained from Physionet databases and Shimmer3 ECG database

Arrhythmia type	Window Size	Classification Type	Window Size	Classification Type	Window Size	Classification Type
Normal	0,2, ,…11	Good	12,13,…17	Fake	----------	----------
AF	0,2,3	Good	4,5,6	Difficult	7,8,….20	Fake
Noisy AF	0,2,….5	Difficult	6,7,8,….20	Fake	----------	----------
AFIB	0,2, …..10	Good	11,17,….20	Fake	----------	----------
PVC	0,2,……6	Good	7,8, ,….30	Fake	----------	----------
APC	0,2,….7	Good	8,9,…14	Fake	----------	----------
SV	0,2,3,4	Good	5,6,……13	Fake	----------	----------
VFL	0,2,…..,7	Good	8,9,……20	Fake	----------	----------
VT	0,2,…. 10	Good	11,12,……20	Fake	----------	----------

Table 2.10. The cardiologist's overall results based on median ECG reduction algorithm obtained from Physionet databases and Shimmer3 ECG dataset

Arrhythmia type	Window Size	Classification Type	Window Size	Classification Type	Window Size	Classification Type
Normal	0,2,3, …11	Good	12,13,…17	Fake	----------	----------
AF	0,2,3	Good	4,5,6	Difficult	7,8,….20	Fake
AFIB	0,2,3,……6	Good	7,8,….20	Fake	----------	----------
Noisy AF	0,2,3,….5	Difficult	6,7,8,….20	Fake	----------	----------
PVC	0,2,3,…11	Good	12,13, ,….30	Fake	----------	----------
APC	0,2,3, …10	Good	11,12,…14	Fake	----------	----------
SV	0,2,3,4	Good	5,6,……13	Fake	----------	----------
VFL	0,2,…..7	Good	8,9,……20	Fake	----------	----------
VT	0,2,…. 10	Good	11,12,……20	Fake	----------	----------

From Table 2.9 and Table 2.10, it can be observed that the mean and median algorithms change the morphology of the ECG signals, particularly those that have low amplitudes, which causes inaccuracy in classification by the cardiologist.

2.7 Discussion

The transmission, storage and analysis of ECG data in real-time is essential for remote patient monitoring with wearable ECG contexts. However, this remains a challenge to achieve within the power, the storage and processing capacity of wearable sensors. ECG reduction algorithms have an important role to play in reducing the processing requirements for wearable sensors. However, many existing ECG reduction and compression algorithms are computationally expensive to execute in wearable sensors and have not been designed for real-time computation and incremental data arrival. They have not been built for wearable sensor environments.

In this investigation, we tested the effect of statistical Max_Min, mean and median algorithms with different sizes of sliding windows on reduced ECG signal quality based on subjective and objective contents. Also, we measured the energy consumption for ECG sensor.

the mean and median ECG reduction algorithms remove high frequency noise and maintain diagnostic features based on window size up to 4 (optimal case). When window size increases to 5, the mean and median ECG reduction algorithms still remove high frequency noise but only when ECG signals have high P and T amplitudes. Indeed, the median ECG reduction algorithm is more computational expensive than mean ECG reduction algorithm. Thus, the mean ECG reduction algorithm is optimal for high frequency noise. Although the mean and median reduction algorithms achieve good reduction results and accuracy, they can only be applied to some ECG types such as Normal, PVC, and PAC ECG signals because they change morphological diagnostic features.

The Max_Min ECG reduction algorithm removes high frequency noise and maintains diagnostic features based on a window size of 5 (optimal). Also, it still removes high frequency noise when ECG signals have low P and T amplitudes. It is approximately similar in computational efficiency of mean ECG reduction algorithm. Therefore, it is suitable for real-time ECG reduction and filtering. In addition, it provides very good signal quility for all ECG signal types.

Window size plays an important role in ECG signal quality. The Max_Min ECG reduction algorithm retains most intervals accurately from reduced ECG signals with a window size of 5. The RR intervals data detected from the reduced signals have about 99 % similarity to the RR data detected from the raw ECG signal up to a window size of 10. Thus a window size of 10 is possible for investigations using only HRV analysis because reduced RR data results are almost identical to the original RR data results, which leads to a significantly increased sensor battery life. Mean and median ECG reduction

algorithms maintain most intervals from a reduced ECG signal with a window size of 4. Those intervals have about 97 % similarity to the original intervals with a window size up to 4.

Mean and median ECG reduction algorithms change the morphology of ECG signals because they estimate a sample from a window size of 2, 3, 4,…N. If those samples are close to each other as represented in Figure 2.5 (their standard deviation is low) then both algorithms provide good reduction or signal quality whereas if those samples have high standard deviation then both algorithms change ECG signals morphology significantly even with a small size window such as 2 or 3 because they estimate samples far from peaks or troughs. Usually an ECG signal generates samples with low standard deviation (close to each other or repeated) in a small window size. Therefore, the mean and median algorithms can be used to reduce ECG with some type of arrhythmias. In contrast, the Max_Min ECG reduction algorithm maintains the morphology of ECG signals and is guaranteed to select the original peaks and trough as illustrated in Figure 2.5. Also, it enhances the morphology of ECG signals if noise is present. For example, as reported in Table 2.8, the cardiologist classified a raw ECG signal as *difficult,* and after applying the Max_Min algorithm with a window size of 5, the cardiologists classified the reduced ECG signal as *good*.

From a medical point of view, all proposed ECG reduction algorithms can reduce an ECG signal and maintain the diagnostic features but with different window sizes. For instance, mean and median ECG reduction algorithms are good with a window size starting from 2 to 5 if the ECG signals have high P and T amplitudes. When P or T amplitude is low, mean and median ECG reduction algorithms miss P or T waves if the window size is greater than 4. Therefore, they are not recommended for ECG signals that have low P or T amplitudes. The Max_Min ECG reduction algorithm is good for all ECG signals that have low or high P and T amplitudes with a window size ranging between 2 and 5.

Computational test and medical testing recommend the use of Max_Min ECG reduction algorithm to reduce all ECG signal types. Therefore, we selected it for comparison with the real-time ECG reduction algorithms that can be executed on Shimmer3 wearable ECG sensor in term of CR and energy consumption.

Existing methods that executed within Shimmer3 ECG node were not evaluated with an actual real-time system. They employed ECG data obtained from Physionet databases. Hence, the data acquisition stage and runtime calculation of the algorithms may not be reliable. Accordingly, the energy consumption results were inaccurate. Furthermore, there was a waiting time (1 or 2 seconds) for reading ECGs because the sensor had a small memory capacity. All those issues led to inaccurate

measurement of energy consumption in prior literature. In fact, they suffer from wearable sensor resources limitation. Moreover, they measure the energy consumption based on few seconds.

Rechargeable batteries provide different power when they are fully charged, half charged, and low charged. So, a very small segment of time such as 2 seconds or 1 min does not reflect the real time for a battery life. To accurately measure battery life, a complete analysis should be implemented for all battery stages; full charged, half charged, and low charged.

We implemented a complete real-time system based on Shimmer3 ECG sensor to read, reduce, and transmit ECG data to a base station via Bluetooth such as a laptop or a mobile device. This allowed us to accurately measured energy consumption and battery life.

2.8 Conclusion

The recording of ECG data generates a large amount of data which increases with different sampling rates and time. Nowadays, wearable sensor devices are being used in healthcare applications to process large ECG data. These devices are battery-driven and have low processor and memory capacities. In this work, we proposed three ECG reduction algorithms and presented a novel, naïve yet, relatively simple but highly effective algorithm (Max_Min ECG reduction algorithm), which reduces the size of ECG signals in real-time. It was implemented within the constraints of ECG wearable sensor. Our reduced ECG signals reflect the raw ECG signals. In addition, our investigation found a link between the window size that used to reduce ECG signal and the quality of the reduced ECG signal. We infer that most intervals including the QT interval must be accurately recognised from reduced ECG data with a window size of 5. The RR intervals data recognised from the reduced data have 98 % similarity to the RR data recognised from the original ECG data with a window size start from 2 to 10. The proposed technique outperformed other existing real-time reduction and compression ECG data techniques with compression ratio of 5 and with low energy consumption. Most current approaches were evaluated based on computerised analysis, whereas the proposed method was evaluated based on both computerised and clinical analysis. Unlike existing algorithms that provide a fixed CR, the proposed algorithm can be varied. However, when the window size increased P and T samples were missed leading to failure to detect ST and PR intervals.

Moreover, in this chapter, we described a computationally naïve, yet effective, algorithm that achieves high ECG reduction rates while maintaining key diagnostic features including PR, QRS, ST, QT and RR intervals. While reduction does not enable ECG waves to be reproduced, the ability to transmit key indicators (diagnostic features) using minimal computational resources, is particularly

useful in mobile health contexts involving power constrained sensors and devices. Results of the proposed reduction algorithm indicate that the proposed algorithm outperforms other ECG reduction algorithms at a reduction/compression ratio (CR) of 5. If power or processing capacity is low, the algorithm can conceivably switch to a compression ratio of up to 10 while still maintaining an error rate below 10 %.

Moreover, an expert cardiologist evaluated the three proposed reduction algorithms based on real ECG data collected from many patients who wore Shimmer3 ECG sensor and Physionet databases. The cardiologist was able to diagnose all arrhythmia types that were obtained from Max_Min ECG reduction algorithm with window size of 5. For some types of arrhythmia, the cardiologist could diagnose the reduced ECG data with window size start from 5 to 15. Indeed, Max_Min ECG reduction algorithm achieves higher compression ratio than existing real-time ECG reduction methods that can implement on wearable ECG sensor. Also, it extends battery life more than existing real-time ECG reduction methods.
In addition, it provides very good ECG signal quality not only based on computerised tests but also on clinical tests.

The recommendation advanced in this study is that the Max_Min ECG reduction algorithm is particularly well suited for the reduction of ECG data captured from wearable sensors on mobile patients in real-time and applied on programmable ECG sensors. Heart rate variability measures including the standard deviation of inter-beat variations (SDNN) require at least five minutes of ECG recordings to accurately measure HRV. The following chapter explains how to find HRV measures in relatively short time frames with a high degree of accuracy.

CHAPTER 3

3 Heart Rate Variability Forecasting

The previous chapter introduced a novel ECG reduction method that provides high compresion ratio and can also execute in real time with wearable sensors. The ECG sensor implements the proposed ECG reduction algorithm and transmits the reduced ECG data to a nearby, battery operated device usually a Smartphone. As mentioned in Chapter 1, HRV estimations can be calculated from an ECG signal over five minutes. The time from normal ECG peak of the beat (the R peak) to the next normal R peak is called the RR interval (Kranjec et al., 2014) and depicted in Figure 1.2. This chapter presents a new real time approach that uses three minutes ECG traces to reliably forecast HRV measures for recordings of five minutes duration using count data. The second research question regarding predicting HRV indicators minutes into the future within the constraints of remote patient monitoring is answered in this chapter.

Three different approaches to forecast HRV measurements are discussed. The Count data model represents the core novel contribution to forecast HRV measurements whereas the machine learning approach is used for comparison.

The datasets used for prediction is described in Chapter 2. Two datasets MIT-BIH Arrhythmia and Shimmer3 ECG are used for the experiments. The prediction results on the MIT-BIH Arrhythmia dataset were published in a peer reviewed journal (Allami, Stranieri, Balasubramanian, & Jelinek, 2017). In addition, the proposed methods were tested in a real platform based on a Shimmer3 ECG sensor.

This chapter begins with a background on HRV indicators, challenges faced by current ultra-short time frame HRV measurement methods, related works, and then describes the three HRV forecasting techniques.

3.1 Background and Challenges

HRV is typically measured using time-domain, frequency-domain and nonlinear measurements. The root mean square of successive differences (RMSSD) and the standard deviation of normal to normal intervals (SDNN) are common time-domain methods (Task Force, 1996). SDNN represents the over-all (both long-term (24 hours) and short-term (5 minutes) variation within the RR interval series (Task

Force, 1996). SDNN has proven to be important clinically as it allows risk identification of adverse cardiac events (Ahonen et al., 2016; Antônio et al., 2014; Huikuri & Stein, 2013; Kleiger et al., 1987; Loguidice, Schutt, Horton, Minei, & Keeley, 2016; Malliani et al., 1994; Sánchez-Barajas, Figueroa-Vega, del Rocío Ibarra-Reynoso, Moreno-Frías, & Malacara, 2015; Vaage-Nilsen et al., 2001; Wang et al., 2013). The standard deviation of the average RR cycles assessed over non-overlapping five-minute segments (SDANN) for 24 hours is another time domain measure that is particularly stable (Task Force, 1996). Measures of HRV are affected by heart rate and other local variations so readings of at least five minutes have been recommended (Task Force, 1996). However, the potential clinical benefit inherent in raising alarms early have led to many investigations attempting to find HRV measures in ultra-short time frames (Smith, Owen, & Reynolds, 2013b).

Numerous investigations that analyse short-term HRV indices using very short time frames of 10–30 seconds and, 1 to 3 minutes ECG traces have found that the RMSSD is a reliable measure and correlates to RMSSD results over longer ECG traces. However, this is not the case for SDNN or SDANN, which are sensitive to length of recording (Ahonen et al., 2016; Chang & Lin, 2005; Esco & Flatt, 2015; Nussinovitch et al., 2011; Smith et al., 2013a; Thong, Li, McNames, Aboy, & Goldstein, 2003). Therefore, all current studies depending on HRV still use a duration of five minutes as a standard measure, for instance, those proposed by (Beetham, 2015; Sánchez-Barajas et al., 2015; Wang et al., 2013). Recently, one of those studies indicated that time domain measurements calculated from ultra-short time series, especially SDNN, are inaccurate. Hence, for this work five minute recordings were used (Holper et al., 2016).

There has been no publication outlining a reliable way to model long-term RR interval data from short ECG recordings that provide accurate long term SDNN or SDANN results. This study presents an algorithm that uses count data from three-minute ECG traces to reliably forecast HRV measures for recordings of a 5-minute duration.

Predicting the five-minute HRV with three minutes of RR data is important in life-threatening arrhythmia such as those advocated by (Brisinda et al., 2014) as it can forecast AF arrhythmia in three minutes instead of five minutes. Moreover, it is useful in settings where a patient's safety or distress is paramount as well as shortening consultation times. Screening programmes that use HRV, such as those introduced by (Kotecha et al., 2012) can be less stressful to patients and be more cost effective if three-minute rather than five-minute readings are required. Risk assessments based on HRV in emergency settings such as those advocated by (Heldeweg et al., 2016) can then also be performed more rapidly for enhanced patient safety. Low HRV extracted from two-minute traces has been shown

to be associated with sudden cardiac death (Maheshwari et al., 2016) and many other conditions. However, a review of HRV studies of short traces (seconds to three minutes) revealed large variations from recommended norms (Nunan, Sandercock, & Brodie, 2010), which precludes the use of short traces in clinical settings. The motivation underpinning the current study is to discover a mechanism to transform short ECG traces to accurately forecast the five-minute HRV measures so that the accepted norms derived from the five-minute HRV can be applied.

In recent years, real-time HRV patient monitoring systems have emerged, using a wireless protocol to stream data from sensors to a nearby, battery operated device (e.g. Smart phone) that re-transmits the data to a remotely located server (Balasubramanian & Stranieri, 2014). Algorithms that process the data to raise alarms ideally, execute on devices close to the sensor to avoid delays due to connectivity problems or computational resource constraints (Szczepański & Saeed, 2014). Devices for wearable sensors are predominately portable and hence, battery powered. The execution of complex algorithms and transmission of data from these devices consume considerable power and therefore require computationally simple and data efficient algorithms that calculate HRV measures.

The algorithm presented here achieves high accuracy for the RMSSD, SDNN, DSNN/RMSSD, Mean, and SDANN forecasts with minimal computational resources because it increments the frequency counts of RR intervals as ECG data streams in, and uses these counts to update HRV measures.

Although frequency power domain measures of HRV have been found to be powerful, they are computationally expensive (Tarvainen et al., 2014). Also, state-of the-art investigations indicated that some frequency domain indices provided inaccurate measurements, particularly LF/HF and thus the time domain indicator DSNN/RMSSD was introduced as a surrogate indicator (Billman, 2013; Doret, Spilka, Chudáček, Gonçalves, & Abry, 2015; Saboul, Pialoux, & Hautier, 2014). Therefore, frequency domain measures have not been explored in this work. Related work is outlined in the next section. Following that, the methods section contains description of the algorithms before experimental results and discussion.

3.2 Related Work

Measures of HRV are affected by respiration frequency, heart rate and other local variations so readings of five minutes have been recommended especially for time and frequency domain measures (Task Force, 1996). This is to have a long enough trace for meaningful analysis and avoid non-stationarity effects. Non-stationary data can be defined as data where the variance, mean, and

autocorrelation change over time. Time and frequency domain measures within this time period are robust and provide useful immediate or long-term clinical information. The potentially clinical benefits inherent in raising alarms quickly following onset of arrhythmia have led to many investigations attempting to find robust HRV measures in short and ultra-short timeframes. For example, Smith et al., 2013a identified over 70 HRV measures that have been used for short (30 beats) HRV analysis. Their study demonstrated that short-term HRV assessment has the potential to be a good non-invasive diagnostic tool. However, HRV measures utilised for short-term HRV analysis require personalised validation before they can be applied (Smith et al., 2013b).

Esco and Flatt (2015) evaluated the agreement of the RMSSD index with other HRV features under ultra-short term recording conditions with athletes under resting and post-exercise conditions and concluded that 60 seconds may be an acceptable recording time for RMSSD but may not accurately represent other five-minute HRV measures.

Thong et al. (2003) combined two time domain and one frequency domain HRV measure from ten-second traces as a surrogate for a five minute HRV recording. They reported ten-second recordings were not an accurate reflection of a 5-minnute recording although the RMSSD was promising and the high frequency (HF) power required further investigation. Taking a longer timeframe, Chang and Lin (2005) compared three minutes to five minutes recordings and the HRV time and frequency domain measures obtained. The time-domain results indicated that RMSSD and pNN50 analyses were approximately similar at the third and fifth minute but SDNN results were significantly different. In frequency domain, Chang and Lin (2005) found that LF/HF power also varied significantly between the three and five minute recording. Both studies employed data from the MIT-BIH Arrhythmia Database (Mark & Moody, 1997) for their investigations.

Nussinovitch et al. (2011) evaluated the reliability of ultra-short term HRV parameters. Their method calculated HRV indices for 10 seconds and 1 minute recordings and then compared the results to five-minute measurements of HRV. Similarly to other work, they concluded that RMSSD seems reliable for analysing HRV from 10 second or 1 minute ECG recordings but this is not the case for SDNN. Frequency domain parameters require longer recording time depending on the frequency range of interest. A more recent study proposed by (Ahonen et al., 2016) has also confirmed the results of these previous studies. An Android-based patient monitoring system that uses wearable heart sensors to identify three types of cardiovascular diseases in real-time was presented by (Pierleoni, Pernini, Belli, & Palma, 2014). They used SDNN, RMSSD and pNN50 to detect stress states following five-

minute ECG recordings but did not report energy consumption or attempt to determine HRV from shorter recordings.

None of the studies that investigated the correlation of five-minute HRV using ECG traces shorter than five minutes considered the computational cost of calculating HRV measures. As described above, computational costs must be taken into account to prolong battery life when deploying HRV forecasts in a remote patient monitoring system with wearable sensors and mobile devices.

3.3 Method Description

In this chapter, prediction of five-minute SDNN and mean heart rate from a three-minute ECG recording is reported. Results indicated a high degree of accuracy. The approach uses count data combined with two statistical methods called Poisson distribution and binomial distribution. This requires minimal computational resources and is well suited to remote patient monitoring with wearable sensors that have limited power, storage and processing capacity. Furthermore, a machine learning method known as Recurrent Neural Network was employed for comparisons with the statistical methods.

3.3.1 Count data

The count data model has emerged as a powerful statistical tool in many fields including machine learning, pattern recognition, data mining, and bioinformatics (Bakhtiari & Bouguila, 2014) but has not been applied to ECG derived RR time series for risk prediction of arrhythmia. Count data is statistical data that represents frequency counts of the number of distinct data occurrences over a specified interval (Cameron & Trivedi, 2013).

Many researchers have applied the count data model for estimation and prediction over intervals. For example, regression analysis of panel count data has been used to estimate the observation times (Zhao, Tong, & Sun, 2013). Jung and Tremayne (2011) discussed recent interest in time series count data. This is data where the counts of a phenomenon over time are analysed. Techniques include static regression models and their extensions and more complex dynamic models. Furthermore, several knowledge discovery and machine learning techniques have been suggested for count data modelling and classification. For instance, Bakhtiari and Bouguila (2014) developed the Dirichlet model by enhancing the Bayes estimation method that can be used for count data classification and learning. Recently, a count data model enhanced accuracy prediction and reduced the number of trials for investigation in multiple environments such as genotype with environment interaction (Montesinos-López et al., 2017). In addition, Marchal, Cumming, and McIntire (2017) suggested a predictive

model based on Poisson distribution to predict fire in forests based on information obtained from maps of fire weather and land cover. Moreover, in the medical field, count data from urine and plasma tests of children might contribute to identifying risk of acute kidney injury following cardiac surgery (Wang et al., 2016).

Table 3.1 depicts RR data over a period of time. Record No. N024 reflects a normal (N) rhythm from the Shimmer3 ECG dataset and record No. 232 represents an atrial premature contraction (APC) rhythm from the MIT-BIH Arrhythmia database.

Table 3.1. Count RR data for normal beats (record no. N024) and APC beats (record no. 232) heart trace

Record No. 232				**Record No. N024**	
RR data	**Count RR data**	**RR data**	**Count RR data**	**RR data**	**Count RR data**
0.73	53	0.76	2	0.70	77
0.71	49	1.67	2	0.71	58
0.72	42	1.13	2	0.69	57
0.68	27	1.38	2	0.68	51
0.67	25	1.88	2	0.73	32
0.70	23	1.83	2	0.72	27
0.74	23	1.99	2	0.67	23
0.66	13	1.80	2	0.75	18
0.69	11	1.71	2	0.66	17
0.75	8	1.81	2	0.74	16
1.9	7	1.93	2	0.65	13
0.65	5	2.77	1	0.76	10
1.92	4	2.40	1	0.77	5
1.85	4	1.12	1	0.78	4
1.96	4	1.68	1	0.80	3
1.89	4	2.53	1	0.81	3
1.65	4	2.07	1	0.83	2
1.87	3	1.63	1	0.86	2
1.86	3	1.72	1	0.63	1
1.82	3	2.63	1	0.88	1
1.66	2	1.48	1	0.85	1
1.97	2	1.77	1	0.90	1
1.76	2	1.78	1	0.91	1
1.43	2	1.35	1	0.84	1
1.74	2	0.64	1	0.64	1
0.73	53	2.66	1	0.60	1

To predict count RR data, counts RR data was combined with a Poisson-generated function and a binomial-generated function that commonly apply to the count data model as explained in the next section.

3.3.1.1 Poisson distribution

The Poisson distribution is a single parameter discrete probability distribution that takes positive integer numbers. It is appropriate for applications that include the counts of events that occur randomly in a given interval of time, such as distance, area or other dimensions (Winkelmann, 2013). Equation 3.1 describes the Poisson distribution where *X* is the number of events in any given interval, and λ is the mean number of events per interval, then the probability of observing x events in a given interval is given by Equation 3.1:

$$P(X=x) = e^{-\lambda}\frac{\lambda^x}{x!} \qquad x=1,2,3,4,\ldots\ldots\infty \tag{3.1}$$

X in Equation 3.1 refers to the number of RR data occurrences for 3 minutes and λ refers to the mean of RR intervals over specific period. In this study, the raw frequency counts from three minutes were filtered through a Poisson distribution in order to predict the five minutes frequency counts. The Poisson filter is applied through estimating the parameters of the distribution from the data, calculating the probability distribution and multiplying the probability distribution by the number of observations. Indeed, the Poisson probability plays a critical role in the prediction of the RR frequency counts for a five-minute period from the counts from the first three minutes as illustrated in Table 3.4.

The binomial distribution was also used and compared to the results applying the Poisson distribution. Usually the binomial distribution is similar to the Poisson distribution, which depends on the mean function, while the binomial distribution relies on the probability density function. Consequently, it is worthwhile to test count RR data forecasting based on the binomial distribution as described in the subsequent section.

3.3.1.2 Binomial distribution

In statistics, the binomial distribution is defined as discrete probabilities of each of the possible values that appear in a known sample (Winkelmann, 2013). Also, the binomial algorithm has been applied to compute the count number of events that would occur in a specific context.
Equation 3.2 below represents the probability distribution of a binomial random variable Y.

$$P(Y) = X!\,/Y!\times(X-Y)\times q^{Y}(1-q)^{Y-X} \tag{3.2}$$

Where:

Y is the number of events in any given sample size.
X represents the sample size.
q refers to the probability over a known context.

Y refers to the number of RR data occurrences for 3 minutes and q refers to the probability of RR data over a specific period.

The same steps were used to forecast RR data, based on a binomial algorithm.

3.4 RR Data Forecasting Technique

As the standard mean and SDNN equations failed to calculate the mean and SDNN parameters from the Poisson model, the standard mean and SDNN equations were modified in order to calculate the parameters efficiently from the Poisson model, as illustrated as follows.

The traditional equation for the mean RR is given as:

$$\mu = \frac{\sum_{i=1}^{n} x_i}{n} \tag{3.3}$$

While the modified mean count RR is given as:

$$\mu c = \frac{\sum_{i=1}^{n} (RRdata_i \times CountRRdata_i)}{n} \tag{3.4}$$

The traditional equation for SDNN is:

$$SDNN = \sqrt{\frac{\sum_{i=1}^{n} (x_i - \mu)^2}{n-1}} \tag{3.5}$$

Whereas the modified SDNN equation with count RR data is:

$$SDNNc = \sqrt{\frac{\sum_{i=1}^{n} ((RRdata_i \times CountRRdata_i) - \mu)^2}{n-1}} \tag{3.6}$$

Where *RRdata* and *CountRRdata* are represented in Table 3.1 above.

The forecasting technique is implemented in three steps as illustrated in Figure 3.1. First, a real-time QRS detection algorithm (Pan & Tompkins, 1985) was applied to extract RR counts for three minutes. In the second step, the Poisson probability was applied to estimate the count of RR data at a point in

time two minutes later. In the third step, the two equations (3.4, and 3.6) were applied to calculate SDNN and mean based on counted RR.

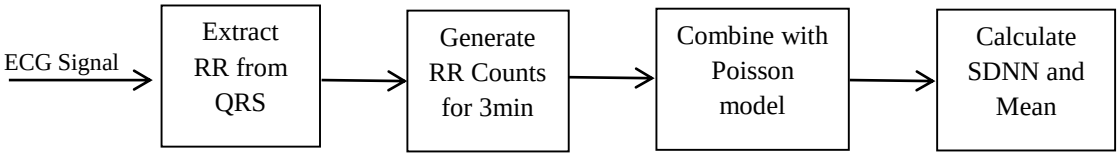

Figure 3.1. Block diagram of the proposed forecasting system

The following algorithm was used to predict the five minutes SDNN and mean RR from three minutes RR data:

Algorithm 3.1: Forecasting algorithm coding schema

Input: Three minutes of ECG data

Output: Predicted SDNN and mean RR

Step 1: While ECG ≠ N Do
Step 2: Apply real-time Pan and Tompkins QRS detection algorithm to extract RR data for three minutes
Step 3: Generate the Count RR data (RR data histogram)
Step 4: Apply the Poisson probability to the RR counts in the RR data histogram to estimate the RR counts after another two minutes
Step 5: Combine the three-minute counted RR data histogram to the predicted two-minute counted RR data histogram to form the predicted five-minutes RR data histogram
Step 6: Use equations (3.4 and 3.6) to calculate mean and SDNN
Step 7: End while

The same steps were used to forecast RR data based on binomial algorithm. In addition, a recurrent neural network was employed to compare the statistical methods as illustrated in Section 3.5.

3.4.1 Forecasting algorithm outputs

The counts for a single record No. 234 are provided in Table 3.2 to illustrate the output of the algorithms. For this patient, 75 beats occurred 0.64 seconds from each other in three minutes and 113 beats occurred with the same interval over five minutes. The Poisson algorithm predicted that 111 beats of 0.64 seconds duration would occur in the five minutes whereas the binomial algorithm predicted that 96 beats of 0.64 seconds duration would occur in the five minutes. Overall, for that patient, the table illustrates that the predicted counts from three minutes of data are close to the five

minutes counts that are actually observed. A new interval, 0.69, appeared once in the actual five minute count that was not present in the three minutes data and therefore not predicted. 0.66 second interval occurred 32 times in the 3 minutes and was predicted to occur 57 times using Poisson algorithm and 52 times using binomial algorithm over 5 minutes however, it occurred 67 times.

Table 3.2. Sample frequencies for record No. 234 reading from MIT-BIH Arrhythmia database based on Poisson and binomial algorithms

Three min RR data		**Forecasting count RR data**		**Five min RR data (Actual RR data)**	
RR data	**Count RR data**	**Poisson**	**Binomial**	**RR data**	**Count RR data**
0.64	75	111	96	0.64	113
0.66	32	57	52	0.66	67
0.65	69	107	90	0.65	112
0.68	7	14	12	0.68	11
0.63	65	97	86	0.63	98
0.67	14	27	28	0.67	25
0.62	15	28	30	0.62	29
0.61	2	4	4	0.61	4
				0.69	1

3.5 Forecasting based on Machine Learning

The forecasts generated using the algorithms above were compared with the forecasts obtained from the Elman recurrent neural network. The Elman recurrent neural network (Elman, 1990) is widely used in time series prediction fields because it has a nonlinear prediction capability, faster convergence, and more accurate mapping ability (Wang & Wang, 2016). Details of the Elman recurrent neural network can be found in (Samarasinghe, 2016). The same three-minute RR data was submitted to the Elman recurrent neural network for comparison. The Elman network from MATLAB was used to learn from the three minutes training data to predict a point in time two minutes later. The network was trained by a continual readjustment process to the weight and the threshold values, in order to reduce the network error to a pre-set minimum of 1% or to stop at a pre-set number of

cycles. Then for the forecasting, held out samples or test data was presented to the trained network to obtain the test results. Results of the count data/Poisson algorithm, binomial algorithm, and Elman neural network are presented in the results section below.

3.6 Results

The evaluation of the proposed forecasting methods was measured by calculation forecasting error. The forecast error is $E_j = X_j - \widehat{X}_j$, which is on the same scale as the data, where X_j denotes the j^{th} observation and $\hat{X}_j$ denotes a forecast of X_j. Accuracy measures that are based on E_j are therefore scale-dependent and cannot be used to make comparisons between series that are on different scales. The most commonly used scale-dependent measures are based on the root mean squared error (RMSE) (Hyndman & Athanasopoulos, 2014).

$$RMSE = \sqrt{\frac{\sum_{j=1}^{n} (E_j)^2}{n}} \tag{3.7}$$

Table 3.4 illustrates that SDNN for the 48 records calculated from the 3 minutes is quite close to the SDNN calculated using the Count-Poisson method from the five-minute actual data. The results were then compared using two tailed paired t-test which was conducted to see if the SDNN results using 3 minutes were significantly different than the actual SDNN.

The level of significance was set at $\alpha = 0.05$. The p-values obtained for the paired t-tests using various methods were noted in the Table 3.3. The t-test comparing the three minutes SDNN with actual five minutes SDNN ($p < 0.05$) confirm previous studies that reported significant differences. In contrast, there was no significant difference between the predicted and actual five minutes SDNN ($p > 0.05$).

Table 3.4 also indicates that the SDNN is similar for the same data using the binomial algorithm ($p>0.05$) and Elman method ($p>0.05$). However, the results of the overall root mean square error (RMSE) between actual and predicted SDNN and mean values for the Poisson model was 3% and 2%, respectively, whereas the results of the overall RMSE between actual and predicted SDNN and mean values applying the binomial algorithm was 6% and 4% respectively. The result of the overall RMSE between actual and predicted SDNN and mean values for the Elman network was 8% and 6%, respectively. The results indicated that the Poisson model achieved a higher prediction accuracy (97%) than the binomial method (94%), and the Elman network (92%). Therefore, the accurate predictions of SDNN from the three-minute recordings compared to the longer recording periods of

the MIT-BIH data decreased the computation time from 24 hours to 14.40 hours, which leads to decreased energy consumption for battery-operated devices.

Table 3.3. P-value results for comparing actual, Poisson, binomial and Elman methods

Method	**P-value**
Actual	0.036
Poisson	0.869
Binomial	0.828
Elman	0.636

The p-value for the 3 minutes was less than the level of significance. Hence, the SDNN is significantly different than the actual SDNN. The p-values for the Poisson, binomial and Elman indicated that there was no significant difference between the predicted and actual five minutes data.

Due to the fact that the SDNN parameter reflects the accuracy of mean and SDNN/RMSSD parameters, the SDNN of each record in the MIT-BIH Arrhythmia database for the three methods presented here was reported.

Table 3.4 Actual and predicted SDNN for MIT-BIH Arrhythmia database records based on Poisson, binomial and Elman methods

Actual Data			**Poisson**		**Binomial**		**Elman**	
Record No.	**Three min SDNN (ms)**	**Actual SDNN (ms) (5 min)**	**Predicted SDNN(ms)**	**RMSE**	**Predicted SDNN(ms)**	**RMSE**	**Predicted SDNN(ms)**	**RMSE**
100	25.2	38.5	35.2	2.33	31.7	4.81	30.3	5.80
101	48.6	55.2	48.1	5.02	51.2	2.83	40	10.75
102	38.5	76.8	73.4	2.40	67.4	6.65	65.6	7.92
103	34	69	76.5	5.30	66	2.12	65.2	2.69
104	40.9	86	80.2	4.10	82.1	2.76	77.7	5.87
105	72.3	105.2	97.4	5.52	92.9	8.70	85.5	13.93
106	210.9	190.3	190.9	0.42	186.7	2.55	180.7	6.79
107	35.3	72.5	74.9	1.70	73.9	0.99	71	1.06
108	45.3	100.2	90.9	6.58	103.8	2.55	101.6	0.99
109	41.3	74.2	75.1	0.64	68.4	4.10	65.3	6.29
111	29.5	30.8	30.3	0.35	25.1	4.03	20.9	7.00
112	14.5	25.4	25	0.28	31.3	4.17	39.3	9.83
113	73	140.2	135.8	3.11	129.6	7.50	120.6	13.86
114	93.6	84.2	80.6	2.55	78.6	3.96	67.6	11.74
115	62.6	123.5	120.2	2.33	111.5	8.49	109	10.25
116	61	80	80.8	0.57	75.9	2.90	75	3.54
117	62.6	134.8	130.9	2.76	128.2	4.67	80.8	38.18
118	30.5	66.2	64.9	0.92	62.4	2.69	60.2	4.24
119	200.2	249.7	243.5	4.38	261.9	8.63	182.8	47.31
121	43	54	55.3	0.92	40.7	9.40	50.8	2.26
122	50	29	30.1	0.78	28.5	0.35	27.9	0.78

Actual Data			Poisson		Binomial		Elman	
Record No.	**Three min SDNN (ms)**	**Actual SDNN (ms) (5 min)**	**Predicted SDNN(ms)**	**RMSE**	**Predicted SDNN(ms)**	**RMSE**	**Predicted SDNN(ms)**	**RMSE**
123	115.6	167.4	167.8	0.28	89.8	54.87	102	46.24
124	33.4	56.3	56.9	0.42	59.3	2.12	57.4	0.78
200	166.3	123.6	125	0.99	136.5	9.12	128.9	3.75
201	144.7	178.2	170.9	5.16	181.2	2.12	176.2	1.41
202	63	67	66.8	0.14	67.9	0.64	59.9	5.02
203	199	157.3	155	1.63	148.3	6.36	145.7	8.20
205	12	64.2	64	0.14	69.5	3.75	64.8	0.42
207	156	369	352.3	11.81	350.5	13.08	362.1	4.88
208	116.1	148.9	147.3	1.13	143.7	3.68	138.5	7.35
209	33.6	33.9	32.7	0.85	32.8	0.78	33.5	0.28
210	109.4	123.8	122.7	0.78	119.5	3.04	119	3.39
212	39.6	42.5	42	0.35	40.8	1.20	46.2	2.62
213	19.3	44	44.6	0.42	50.2	4.38	50.5	4.60
214	135.6	193.2	189.5	2.62	205.2	8.49	185	5.80
215	60.5	78.5	79.9	0.99	68.8	6.86	81	1.77
217	56.7	89.4	90.3	0.64	79.6	6.93	90.8	0.99
219	144.6	130	129.3	0.49	124.4	3.96	121.2	6.22
220	27.3	70.5	64	4.60	50.7	14.00	60.3	7.21
221	194.5	201.4	190.3	7.85	202.7	0.92	194.8	4.67
222	52.5	80.3	79.2	0.78	106.8	18.74	101.2	14.78
223	75.7	73	70.3	1.91	79	4.24	73	0.00
228	124.8	212.3	204	5.87	210.3	1.41	194.6	12.52
230	52.2	90.5	97.4	4.88	95.6	3.61	101.3	7.64
231	207.6	289	271.4	12.45	273.8	10.75	280.8	5.80
232	205.6	478	460	12.73	465.5	8.84	479	0.71
233	125.6	122.8	110.1	8.98	126.1	2.33	98.8	16.97
234	14.1	14.6	20	3.82	15	0.28	12.4	1.56

Table 3.5. Overall results of RMSE between actual and predicted SDNN and mean values using Poisson, binomial and Elman methods

Methods	**RMSE(SDNN)**	**RMSE(Mean)**	**Accuracy %**
Poisson	3	2	97
Binomial	6	4	94
Elman	8	7	92

From Table 3.5, it can be observed that the Poisson algorithm provided higher accuracy results than the other methods. Therefore, the Poisson algorithm was applied to predict count RR data obtained from Shimmer3 ECG database. Although the Elman method could provide more accurate results if combined with another machine learning method such as the technique proposed by (Jalal, Hosseini, & Karlsson, 2016) where the Elman neural network was combined with a nonlinear auto-regressive-exogenous (NARX) neural network to predict volumes in a call centre. However, it is computationally rather expensive and not recommended for battery-operated devices.

Algorithm 3.1 mentioned in Section 3.4 above has been applied to the Shimmer3 ECG dataset to compute the mean and SDNN. Results indicated that the SDNN for the 52 records assessed from the 3 minute recordings is quite close to the SDNN assessed using the Count-Poisson algorithm from the five minutes raw data. The overall RMSE between actual and predicted SDNN and mean values for the Poisson model were 4% and 2%, respectively.

As stated earlier, the main aim of this chapter is to forecast the HRV in real time. In order to fulfil this goal, an online system was built to test the forecasting method on a real platform as described below.

3.6.1 Forecasting results based on a real world system

Figure 3.2 depicts a general diagram for the real system. The reduction algorithm described in Chapter 2 (Max_Min ECG reduction algorithm) with a window size of 10 was installed into the Shimmer3 ECG sensor to stream reduced ECG data to a smartphone device at a sampling rate of 256 Hz. The window size was set to 10 because the forecasting method depends only on RR data and as illustrated in Chapter 2 the RR data that was generated from a window size of 10 achieved a high level of accuracy (98 %) and increases the sensor battery life. The Shimmer3 ECG sensor stored raw ECG data on its SD RAM and transmitted the reduced ECG data to the smartphone device to compare the RR measurements. On the smartphone device, the Pan-Tompkins algorithm was used to calculated RR data and the Poisson algorithm was applied to predict the five minute results from the 3 minute tracings. These procedures were applied to six volunteers (4 men and 2 women, aged between 24 and 65) that had Normal rhythm over 30 minutes.

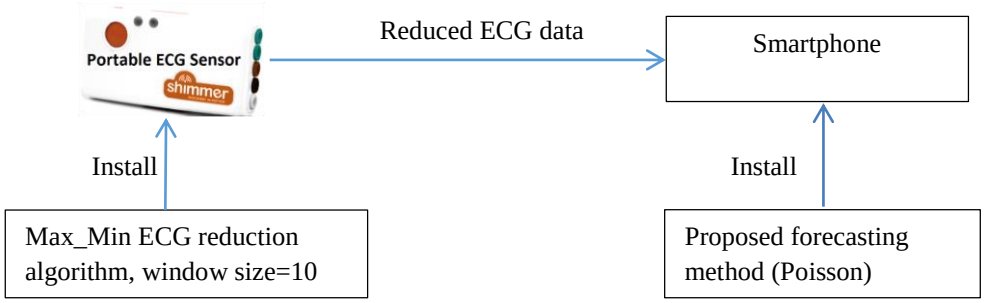

Figure 3.2. General workflow of the proposed online system

The results indicated that the SDNN for the 6 records assessed from the 3 minutes were close to the SDNN assessed from the five minutes original data using the Poisson algorithm. The overall RMSE between actual and predicted SDNN and mean values for the Poisson algorithm were 5% and 3%, respectively.

3.7 Discussion

A forecasting algorithm that can accurately predict the five-minute SDNN parameter from three minutes of data in a computationally simple way has been advanced. The algorithm executes quick enough that it can be applied in real-time as each new data point is obtained using count data, which has not been applied to this type of biosignals before.

This study discovered that RR data is countable over a time as can be seen in Table 3.1 and Table 3.2. Consequently, Poisson and binomial distributions, which are widely used with count data models can be used to forecast count RR data. In count RR data, the Poisson probability approaches the count target faster than the binomial probability and achieves higher prediction accuracy than the binomial model. Although some RR frequency counts occurred infrequently or did not appear during the first three minutes of a five minutes period as represented in Table 3.2, these counts almost had no effect on the prediction. In contrast, RR intervals that appeared frequently play a greater role in the five minutes forecast.

Previous studies found SDNN results differ significantly between 3 and 5 minutes. The current research advances equations that can predict the five-minute SDNN from 3 minutes of RR data in real-time using a counts data model. Results indicated that predicted SDNN results were similar to actual SDNN results with an overall accuracy of 97%. This contributes to obtaining optimal short time recording (5 minutes) for analysing HRV in short term recordings under 5 minutes. The proposed methods apply within the mobile device to determine clinical utility and computational savings.

Forecasting HRV can contribute to the early detection of AF and stress states and raising alarm for patients with heart disease or neurological conditions such as Parkinson's disease and elderly subjects (Pierleoni et al., 2014). Furthermore, many recent investigations indicated that the SDNN/RMSSD parameter provides more accurate result than the LF/HF parameter for measuring cardiac sympathovagal balance, making this a convenient way to determine sympathovagal balance. Consequently, state-of-the-art studies are commonly used the SDNN/RMSSD parameter such as those advocated by (Antônio et al., 2014; Brisinda et al., 2014; Cardoso et al., 2014; Holper et al., 2016; Kang, Kim, Hong, Lee, & Choi, 2016; Paparde, Plakane, Circenis, & Aivars, 2015) but with five minutes of RR data because the SDNN parameter requires five minutes duration to provide accurate results. Therefore, forecasting accurate SDNN contributes to measure all time domain parameters from ultra-short term (3 minutes). Also, it reduces the long-term HRV analysis from 24 hours to 14.40 hours that leads to power savings for both wearable and mobile devices. In addition,

as illustrated above a real-time cardiac monitoring system that use wearable and mobile devices requires simple and fast methods such as time domain methods because transformational methods and intelligent methods are very expensive and consume power.

3.8 Conclusion

Heart rate variability (HRV) measures, including the standard deviation of inter-beat variations (SDNN), require at least five minutes of ECG recordings to accurately measure HRV. In this chapter, counts data derived from a 3 three-minute ECG recording was used to predict, the five-minute SDNN with a high level of accuracy using a simple method. The approach used counts data combined with a Poisson-generated function, which requires minimal computational resources and is well suited to remote patient monitoring with wearable sensors that have limited power, storage and processing capacity. The ease of use and accuracy of the algorithm provides opportunity for accurate assessment of HRV and reduces the time taken to review patients in real-time.

This thesis revealed that RR data is countable during a period of time and the count data model with a Poisson function can predict time domain indicators with a high degree of accuracy. More clinical and computerised investigations based on this finding are necessary. The next chapter will describe how to detect life-threatening arrhythmia based on the count data model together with knowledge-based rules derived from clinical knowledge in short term and also detect life threatening arrhythmia using an artificial neural network (ANN) method in very short term.

CHAPTER 4

4 Detection of Premature Ventricular Contraction

In the previous chapter, a new HRV prediction technique that achieved a high level of forecasting accuracy and can also be implemented on wearable sensors and smartphones in real time was described. Continous monitoring for life-threating arrhythmia based on wearable and smartphone devices is an important application of wearable sensors and real-time analysis. Accordingly, this chapter provides a new PVC arrhythmia detection method that employs three minute RR data to reliably detect PVC beats in a simple and fast way within the constraints of remote patient monitoring. Moreover, it detects PVC beats from Non-PVC beats using an intelligent data mining method in a few seconds. The third thesis question regarding arrhythmia detection within the limitation of battery operated devices is addressed in this chapter.

Two different techniques to detect PVC beats from Non-PVC beats are presented. Counts RR data combined with knowledge-based rules represents the core contribution to detect a life-threating arrhythmia for real time cardiovascular patient monitoring systems whereas the application of a machine learning method is discussed for comparison.

Trials of the PVC detection algorithm were applied to three datasets: MIT-BIH Arrhythmia, St. Petersburg Institute of Cardiological Technics (INCART) (Goldberger et al., 2000) and Shimmer3 ECG databases. The MIT-BIH Arrhythmia database was used for testing and the NCART database was used for measuring the generalisation capability performance of the method. The Shimmer3 ECG dataset was employed to examine the proposed techniques in a clinical setting.

The INCART database contains 75 annotated recordings extracted from 32 Holter records. Each record is 30 minutes long and consists of 12 standard leads, each sampled at 257 Hz. The annotations were produced by an automatic algorithm and then corrected manually, containing over 175,000 annotations. The PVC detection results on the MIT-BIH Arrhythmia database and NCART database were previously published (Allami et al., 2017). This chapter starts with a background and related works on PVC disease and then described the two PVC detection methods. The discussion and conclusion are elucidated prior to the description of experiment results.

4.1 Background and Related Works

Extra excitations can appear in normal or abnormal heart traces known as premature ventricular contractions (PVCs). PVC beats represent the most common ventricular arrhythmia and are found in about 60 % of healthy hearts (Gertsch, 2008). The PVC beat is a pulse that appears earlier than the subsequent coming sinus pulse. Numerous PVC samples have been identified clinically. Samples occur as one PVC follows every sinus pulse (bigeminy), or every three pulses (trigeminy). PVCs possible appear in an abnormal case in pairs as couplets (one sinus beat followed by two PVCs), or triplets, (Qu et al., 2014). PVC beats appear in normal healthy persons, but in diseased hearts the frequency of appearance in the ECG is increased and can be an indicator of morbidity and risk of sudden cardiac death (Massing et al., 2006; Sörnmo & Laguna, 2005). The main causes for PVCs and their complex samples in the heart are still poorly understood (Qu et al., 2014).

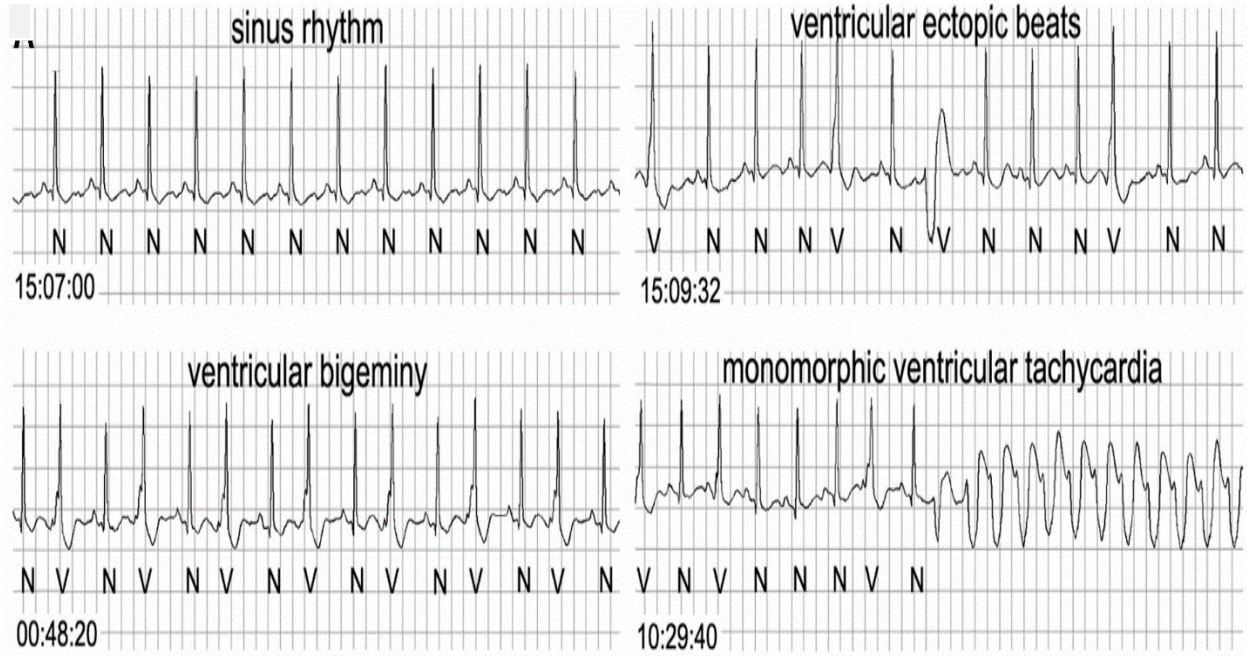

Figure 4.1. PVC patterns (Glass et al., 2011), where the left top section represents normal pattern, the left bottom refers to one PVC following every normal pulse, the right top section illustrates PVC ectopic beats pattern and the right down section depicts monomorphic ventricular tachycardia pattern

PVCs exceeding a certain number per minute is a serious cardiovascular condition that can lead to life-threatening arrhythmias. The instant recognition of life-threatening cardiac arrhythmias is a challenging problem of clinical significance (Li et al., 2014; Liu et al., 2012; Liu et al., 2010). In particular, PVCs have been found to be related to mortality when linked with myocardial infarction (Iwasa, Hwa, Hassankhani, Liu, & Narayan, 2005) and have been shown to be associated with caffeine consumption or stress (Agrafioti & Hatzinakos, 2009).

Although, several studies employed RR data to classify and detect PVC beats (Nabil & Reguig, 2015), approaches that are sufficiently accurate and can execute rapidly for fast real-time PVC detection have proven to be elusive. Knowledge-based rules have classified and detected heart beats based on a sliding window technique (Tsipouras, Fotiadis, & Sideris, 2005) with positive predictive accuracy and sensitivity values of 86.54% and 87.27% respectively. A low complexity algorithm for real-time PVC detection that applied a template matching approach for detection of PVC beats from the MIT-BIH Arrhythmia database (Li et al., 2014) provided robust results of 98.2 % accuracy and 93.1 % sensitivity. Though accurate, the template matching study required the detection of the QRS complex and T waves in real-time for five minutes of training and it was sensitive to the sampling rate. It can only be applied for ECG data sampling at 360 Hz. Similar results were obtained with an Android monitoring system based on wearable heart sensors to classify and detect PVC beats from RR intervals and applying knowledge-based rules (Pierleoni et al., 2014). Cuesta, Lado, Vila, and Alonso (2014) employed a linear discrimination analysis method based on only two RR features that were generated from knowledge-based rules to recognise PVC beats obtained from the MIT-BIH Arrhythmia database with specificity of 82.52% and sensitivity of 90.13%.

The detection method presented in the current study uses frequency counts but requires the detection of only the QRS complex without the T wave, and only for three minutes rather than five, to achieve comparable PVC detection results. Furthermore, the approach advanced here is computationally simpler than template matching and is well suited to execution on power-constrained devices because the additional detection of T wave leads to greater power consumption on mobile devices. Moreover, it can be employed at any sampling rate. Recently many cardiovascular wearable sensor devices such as eMotion Faros (mega, 2016) can detect QRS waves and stream RR data in real-time and so can be deployed directly using the approach advanced here.

Other techniques have been applied to classify PVC beats including nonlinear complexity measures, wavelet transform and sophisticated artificial neural networks (Li et al., 2014). For example, Zhou, Jin, and Dong (2017) combined clinical knowledge-based rules with deep neural networks for PVC detection. Support vector machine (SVM) have been deployed to discern PVC from Non-PVC beats (Bazi, Hichri, Alajlan, & Ammour, 2013). However, these techniques may not always be technically feasible for real-time processing of ECG data from wearable sensors and mobile devices due to high computational resources required and power consumption (Li et al., 2014).

4.2 Method Description

In this study, PVC beats were detected using counts RR data obtained from a three-minute ECG recording with a high level of accuracy. The method utilises counts data with rule-based methods which consume minimal computational resources and is well suited to remote cardiac monitoring with mobile devices restrictions. Moreover, an intelligent method was used, which depends on QRS complex features and morphology, to compare with the statistical methods.

4.2.1 Knowledge-based/Rule-based

A Knowledge-based system represents an important method that is used to build decision support systems for chronic disease monitoring (Minutolo, Esposito, & De Pietro, 2011). For instance, Minutolo, Sannino, Esposito, and De Pietro (2010) designed a rule-based software for monitoring heart diseases based on contextual information. This software received data from wearable ECG sensors with data regarding a patient's physical activities such as walking, running, lying, and standing up then analysed the data for detecting and signalling of critical or abnormal situations. Another research project proposed a rule-based decision support system based on information from HRV data (the expert's selected the SDANN parameter), blood pressure, statistical, and geometric parameters (Minutolo et al., 2010). A multi-purpose real time tele-monitoring system suggested by Sannino, De Falco, and De Pietro (2014) exploited if-then rules to alert health service providers and includes a decision support for critical cases such as fall detection and apnoea monitoring. Furthermore, Exarchos et al. (2007) introduced an algorithm to classify arrhythmic beats. This method extracts a set of rules based on a decision tree produced from training datasets. In addition, fuzzy rule-based methods using RR data have been applied to classify cardiac arrhythmia. The rules were based on human experience and fuzzy logic (Bárdossy et al., 2014).

RR segment analysis has emerged as a powerful tool that contributed to detection of heart arrhythmias, ventricular hypertrophy and other diseases (Ranjeet et al., 2013). The fact that abnormal beats (PVC beats) have a QRS pattern wider than normal beats allows for the identification of these beats relatively easily in addition to RR intervals being significantly different and HRV analysis being possible (Nabil & Reguig, 2015). Many types of arrhythmia, especially bradycardia and tachycardia, cause changes in RR periods (Nguyen et al., 2014). Consequently, an algorithm based on count data and rule-based methods that can automatically detect PVC from Non-PVC rhythms using RR data in short-term recordings is proposed. In addition, the method used in this project maintained detailed information, e.g. SDNN and mean RR data which support algorithm decision making.

A dataset for Normal and PVC rhythms is prepared as an example as shown in Table 4.1. Record No. 112 reflects a normal (N) rhythm and record No. 119 represents a PVC (V) rhythm readings from the MIT-BIH Arrhythmia database for short term recordings.

Table 4.1. Count RR data for PVC beats (Record No. 119) and Non PVC beat (Record No. 112) heart trace

Record No. 119			**Record No. 112**		
RR data	**Annotation**	**Count RR data**	**RR Data**	**Annotation**	**Count RR data**
0.88	N	47	0.70	N	127
0.53	V	33	0.71	N	93
0.91	N	32	0.69	N	91
0.90	N	31	0.68	N	86
0.89	N	30	0.67	N	36
0.54	V	26	0.72	N	29
0.86	N	23	0.73	N	22
0.87	N	22	0.66	N	9
0.93	N	22	0.74	N	6
0.52	V	20			
0.92	N	17			
1.3	N	16			
1.28	N	15			
1.33	N	13			
1.29	N	13			
0.55	V	12			
1.31	N	11			
1.32	N	11			
0.85	N	10			
0.95	N	9			
0.94	N	9			
0.51	V	8			
0.96	N	7			
1.26	N	7			
0.56	V	6			
1.27	N	6			
1.25	N	6			
0.83	N	3			

Record No. 119			Record No. 112		
RR data	**Annotation**	**Count RR data**	**RR Data**	**Annotation**	**Count RR data**
1.35	N	3			
1.23	N	3			
1.34	N	3			
0.84	N	3			
0.59	V	2			
1.24	N	2			
0.57	V	2			
1.22	N	2			
1.36	N	2			
0.63	N	2			
0.58	V	2			
1.4	N	1			
1.38	N	1			
0.98	N	1			
0.65	N	1			
0.97	N	1			
0.72	N	1			
0.50	V	1			

Note: V refers to PVC beat as annotated on the MIT-BIH Arrhythmia database. N refers to Non PVC beats such as N,L,R,a,F, and A, etc. as annotated on the MIT-BIH Arrhythmia database

4.2.2 PVC detection technique based on count data model

PVC beats have a QRS pattern wider than Non-PVC beats, RR intervals will be significantly different which makes the identification of these beats relatively easy (Nabil & Reguig, 2015; Nguyen et al., 2014). Therefore, the RR data that are annotated as PVC beats tend to group together and can be used to discern PVC from Non-PVC beats in a simple and computationally efficient manner for real-time analysis. The PVC detection technique was executed in three steps as demonstrated in Figure 4.2. First, the real-time QRS detection algorithm (Pan & Tompkins, 1985) was applied to extract RR data for three minutes. In the second step, RR counts were generated in the same way as described for the forecasting algorithm. In the third step, knowledge rules were derived (Bauer et al., 2008; Tsipouras et al., 2005) to detect PVC from Non-PVC beats.

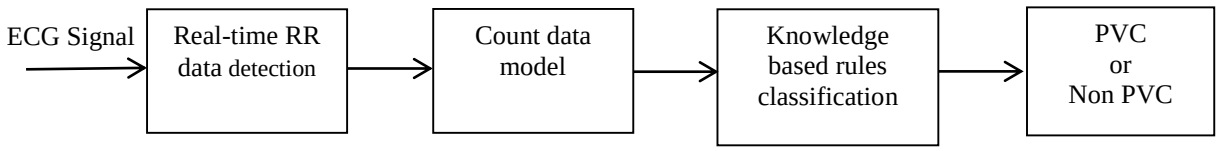

Figure 4.2. Block diagram of the proposed detection system

The algorithm for the detection of PVC and Non-PVC beats is as follows:

Algorithm 4.1: PVC detection algorithm coding schema

Input: Three min of ECG data

Output: Classification of each beat as PVC or Non PVC

Step 1: While ECG ≠ N Do

Step 2 and 3 As per forecasting algorithm (Algorithm 3.1 in Chapter 3)

Step 4: Sort counted data according to the count field in descending order

Step 5: Select the first 6 RR data (i.e. the most frequent RR intervals) and calculate the mean from those (First 6 RR data are empirically identified)

Step 6: For each RR data point, if the RR data < mean and the absolute difference value between (RR data and Mean) > 100 ms
Then the RR data is PVC else the RR data is Non PVC

Step 7: End while

The PVC beats can also be detected based on a few seconds to one minute but using more complex methods and features as explained in the next section.

4.2.3 PVC detection based on ANN for mobile phones

PVC arrhythmias are seriously life-threatening. Identification of PVCs on battery-driven devices requires fast and feasible real-time analysis methods, despite the current limitations in power, processor capability and memory. The same holds for the ability to measure large ECG recordings for one or more days. Existing methods have endeavoured to improve ECG assessment techniques to implement on mobile phones (Hayn, Jammerbund, & Schreier, 2011) as evident in the 2011 PhysioNet/Computing in Cardiology Challenge (Silva, Moody, & Celi, 2011), which has been created to promote the improvement of ECG software that can execute within a mobile phone.

As (Szczepański & Saeed, 2014) note, algorithms execute on mobile devices to automatically classify heart arrhythmias are battery powered. Transmission of data from these devices consumes substantial

power (Gough, 2011). Accordingly, the PVC rhythm was recognised using artificial neural networks, which can work within smartphones for less than 20 seconds as described in the next sections.

4.2.3.1 Arrhythmia recognition for Android-based mobile devices

Many arrhythmia recognition techniques have been developed that execute on phone devices (Baig, Gholam, & Connolly, 2015). In this study, the most recent algorithms that used only RR data for abnormal beat classification was applied using the MIT-BIH Arrhythmia database. For example, AF has been classified based on a smartphone solution. The system used short-term RR data features and provided an accuracy of 97% in classifying AF against healthy controls, with a specificity of 100% and a sensitivity of 93% (Lahdenoja et al., 2017).

Gradl, Kugler, Lohmüller, and Eskofier (2012) introduced a real-time ECG monitoring system using Android-based mobile devices and Shimmer3 ECG sensor to detect abnormal arrhythmia. The system implemented the Pan-Tompkins algorithm for QRS-computation and rules-based proposed by (Krasteva & Jekova, 2007). It resulted in more than 99% overall QRS recognition with 89% sensitivity and 80% specificity for overall abnormal beat discrimination. The authors did not test their system with real ECG data and long-term ECG monitoring on mobile phones and how long it can work with limited battery-driven available devices.

A real-time classification system for arrhythmia detection on Android-based mobile devices has suggested a comparison of the calculation and memory costs for each classification methods using the embedded classification software toolbox (Ring, Jensen, Kugler, & Eskofier, 2012). The comparison study relied on 16 features (statistical, heartbeat, and template-based) that were extracted only from R peak data. Classification methods included AdaBoost M1, C4.5, linear regression, multilayer perceptron, naive Bayes, nearest neighbor, PART and support vector machine (SVM). The C4.5 classifier was not complex and resulted in high detection accuracy (91%). Therefore, (Leutheuser et al., 2014) recommended the implementation of C4.5 classifier on Android-based mobile devices.

A back propagation neural network (BPNN) classifier performed on an Android platform to monitor and classify ECG signal in real-time has also been reported. The BPNN was tolerant of noise when used with higher-order statistics features based on wavelet decomposition. The BPNN algorithm executed based on 30 features that were extracted from R peak data based on the Pan-Tompkins method. Although the BPNN algorithm provided high detection accuracy of 98%, the results were based on only 15 records to recognize 7 different types of arrhythmia. For example, the PVC classification accuracy was 97% (Yen, Chang, & Yu, 2013). All of the above studies did not test on

ECG sensor in real time, and did not report battery life for portable devices. The current study suggests a PVC detection system for real ECG sensor and reports the battery life for portable devices in the next section.

4.2.3.2 Suggested PVC beats detection technique based on ANN for Android smartphones

The use of simple features that can be generated from the real-time method and fed to an ANN plays an important role in the detection of PVC beats within smartphones in a simple and computationally efficient manner for real-time execution. As previously stated, QRS complex shape and RR data are widely used to detect PVC beats. The PVC generally changes the QRS complex shape hence the amplitude of the QRS complex is much smaller or larger than normal QRS complexes (Zhou et al., 2017). Therefore, we used three morphological features and seven time-domain/statistical features that can be directly extracted in real-time from the Pan and Tompkins algorithm.

ANNs are commonly used in classification and pattern recognition applications. The ANNs are capable of learning the desired mapping between the input and output signals of the system without knowing the exact mathematical model of the system and are therefore excellent estimators in nonlinear systems. The feed-forward NN provides high accuracy in ECG data classification and recognition (Elhaj et al., 2016). Therefore, we opted for the cascade forward neural network (CFNN) classifier, which was utilised in system identification, nonlinear control, pattern recognition and classification.

The PVC detection technique is implemented offline on a PC device as illustrated in Figure 4.3. First, the ECG reduction algorithm with a window size equal to 5 was executed to reduce and maintain the ECG signal in real-time. The window size was 5 as the proposed PVC detection algorithm requires to identify all Q, R, and S waves with a high degree of accuracy and as illustrated in Chapter 2, the size-5 window maintained all ECG waves. In the second step, Pan-Tompkins algorithm is applied to detect QRS complex in real-time. In the third step, computationally simple features (statistical and heartbeat features) are generated from 20 seconds that were determined empirically and were calculated for training and classification with the ANN. Finally, the CFNN classifier is applied to detect PVC or Non-PVC beats.

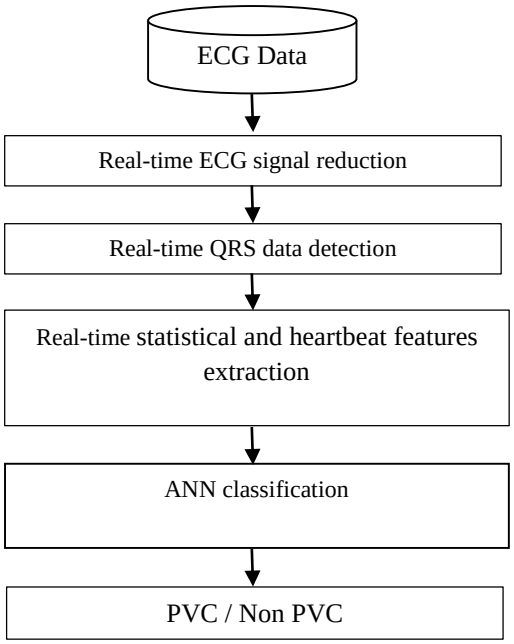

Figure 4.3. Block diagram of the proposed classification system

4.2.3.3 Features extraction

Feature groups play a pivotal role in detection performance and consist of a number of HRV features that optimise classification. Statistical results and heartbeat features are applied directly to the series of successive RR cycle items, so they are suited for real-time applications (Tarvainen et al., 2014). We generated 10 features for each ECG segment that were found very useful for classification (Asl, Setarehdan, & Mohebbi, 2008; Leutheuser et al., 2014; Oresko et al., 2010; Tsipouras & Fotiadis, 2004; Yen et al., 2013). These features consisted of seven statistical features (HRV) and three morphological features (QRS width, QR amplitude, RS amplitude). The statistical features included standard deviation and mean of RR data. Another widely used index is the percentage of differences between adjacent RR intervals that are greater than 50ms or 10ms (pNN50 and pNN10). The description of the time-domain features is summarised in Table 4.2.

Table 4.2. Statistical features

Feature	**Description**
MeanRR	Average of all RR intervals (μ)
SDRR	Standard deviation of all RR intervals
rMSSD	Square root of the mean of the squares of differences between adjacent RR intervals.
pRR50	Percentage of differences between adjacent RR intervals that are greater than 50 ms.
pNN10	Percentage of differences between adjacent RR intervals that are greater than 10 ms.
Ratio	$Ratio = \frac{(maxRR - minRR)}{\mu\ RR}$
SDSD	Standard deviation of differences between successive RR intervals.

4.2.3.4 Performance

For each signal, 10 statistical and heartbeat features were calculated using the MIT-BIH Arrhythmia database. These features were extracted for 20 seconds of ECG data and submitted into a separate vector. Each vector is tagged with one of the two possible labels PVC or Non PVC. For example, a vector for 20 seconds period is labelled as Non PVC provided it consists of 95% Non PVC RR data. Otherwise, the vector is labelled as PVC. These features are normalised to values between 0 and 1 using min-max normalisation by Equation 4.1 and fed into the CFNN classifier for classification. The CFNN classifier trains with the back propagation learning rule for feed-forward networks, but it includes a weight connection from the input to each layer and from each layer to successive layers leading to the output. The main advantage of CFNN is that each layer of the neurons is related to all previous layer of neurons that reduces the training time. Also, it can achieve good results based on a small number of features and data (Bonanno et al., 2014; Littmann & Ritter, 1993). The entire database was 4320 patterns. Ten-fold cross-validation was used to estimate the generalisation.

$$Fn = \frac{N - Nmin}{Nmax - Nmin} \tag{4.1}$$

Where, *Fn* represents the normalised value of the feature, N represents the feature value, *Nmax* refers to the maximum value of the feature and *Nmin* refers to the minimum value of the feature in the corpus.

The PVC detection technique constructed from MIT-BIH Arrhythmia database was tested against Shimmer3 ECG dataset (4680 patterns)

The algorithm for the detection of PVC and Non-PVC beats based on CFNN classifier is as follows:

Algorithm 4.1: PVC diagnosis algorithm coding schema based on ANN

Input: Statistical and Heartbeat features

Output: PVC diagnosis (Yes/No)

Step 1: While ECG ≠ N Do

Step 2: Apply algorithm1 (Set window size, n=5)

Step 3: Use Pan-Tompkins algorithm to detect QRS complex

Step 4: Extract Statistical and Heartbeat features

Step 5: Test pattern (PVC or Non PVC beats) using CFNN classifier

Step 6: End while

The training and testing steps were implemented on a PC device and overall results are reported in Section 4.3.

4.3 Results

4.3.1 PVC detection results based on count data method

The performance of the suggested PVC and Non PVC detection algorithm was measured by sensitivity (*Se*), by the positive predictive (*+P*) value and accuracy (*Ac*) for each of 10, non-overlapping, three-minute segments from a 30 minute recording as described below.

$$Se=TP/(TP+FN) \times 100 \quad (4.2)$$

$$+P=TP/(TP+FP) \times 100 \quad (4.3)$$

$$Ac=(TN+TP)/(TP+FP+TN+FN) \times 100 \quad (4.4)$$

True positive (*TP*) refers to PVC beats correctly recognised, false negative (*FN*) refers to missed PVC beats, false positives (*FP*) refers to non PVC beats recognised as PVC's and true negative (*TN*) refers to correctly recognised non PVC beats.

Overall testing and 10-fold cross validation results of the proposed algorithm are illustrated in Table 4.4. The PVC detection results were compared with four published methods where a part or the full MIT-BIH Arrhythmia database were used (Cuesta et al., 2014; Li et al., 2014; Pierleoni et al., 2014; Tsipouras et al., 2005).

Table 4.3. PVC detection performance for each MIT-BIH Arrhythmia database record

Rec. No.	+P %	Se %	Ac %	Rec. No.	+P %	Se %	Ac %
100	99.5	100	99.9	201	97.8	97.2	96.9
101	98.3	92.1	97.2	202	100	100	100
102	100	100	100	203	50.8	45.7	88.4
103	100	100	100	205	100	100	100
104	97.7	77.4	69.8	207	60.6	11.3	30.4
105	99.2	96.4	95.7	208	100	97.5	96.9
106	99.7	98.8	98.7	209	99.6	98.5	99.6
107	98.2	65.3	70.2	210	100	100	100

Rec. No.	+P %	Se %	Ac %	Rec. No.	+P %	Se %	Ac %
108	99.7	65.4	65.8	212	99.5	99.5	99.8
109	98.8	99.6	99.2	213	100	98.3	98.7
111	99.6	86.5	88.6	214	97.7	99.3	98.7
112	100	100	100	215	98.8	98.3	99.1
113	100	100	100	217	99.9	99.4	99.8
114	100	98.7	99.3	219	98.4	97.9	98.6
115	100	100	100	220	100	100	100
116	99.4	99.3	99.7	221	98.7	96.3	99.2
117	99.8	99.6	100	222	100	100	100
118	100	100	100	223	98.7	96.9	98.9
119	99.2	100	99.9	228	86.7	98.6	98.3
121	100	99.5	99.6	230	99.5	99.8	99.6
122	100	100	100	231	100	100	100
123	100	99.3	99.3	232	99.3	99.1	99.4
124	100	98	99	233	93.6	99.5	99.8
200	74.6	90.4	98.3	234	95.3	100	99.4

Table 4.3 demonstrates the performance of the proposed algorithm for each record. For example, from record No. 100, it is evident that there were no PVC's missed, but there was one false alarm in the 30-minute classifications.

Table 4.4. Overall performance in the testing databases of MIT-BIH Arrhythmia , INCART and Shimmer3 ECG

Database	+P %	Se %	Ac %
MIT-BIH Arrhythmia	96.6	93.7	95.4
INCART	92.7	87.5	94.2
Shimmer3 ECG	92	97	96.3

Table 4.5. Comparison between the suggested method and published real-time methods

Study	+P %	Se %	Ac %
Tsipouras et al.	86.5	87.2	94.9
Li et al.	81.4	93.1	98.2
Cuesta et al.	82.52	90.13	92
Pierleoni et al.	86	87	94
Our method	96.6	93.7	95.4

Table 4.5 illustrates the PVC method presented here provided better accuracy, sensitivity, and positive predictive value to detect PVCs. The algorithm in (Li et al., 2014) recognised PVCs beat-by-beat so it may better meet the real-time analysis requirements. However, it is sensitive to the sampling rate and requires more complex computations. Also, the count data model proposed here can recognise PVCs in real-time based only on RR data that leads to low computational processing time. The previous methods require less data than the proposed method. However, as mentioned before, PVC beats can appear in normal healthy persons but, in diseased hearts, the frequency of PVC appearance in the ECG is increased and can be an indicator of increased risk of morbidity and mortality. Therefore, in a real-time cardiac monitoring system perhaps less data generates more false alarms than more data as not each PVC beat is dangerous, whereas the frequency of appearance over a period of time represents an indicator of risk and needs raising an alarm.

This chapter aims to discuss and show how to detect PVC beats in real time. In order to fulfil the goal of this chapter, an online system has been built to test the detection algorithm in a real-time platform as explained below.

4.3.2 Online PVC detection results based on count data method

Figure 4.4 depicts a general diagram for our real system. The reduction algorithm described in Chapter 2 (Max_Min ECG reduction algorithm) with a window size of 10 was installed in the Shimmer3 ECG sensor to stream reduced ECG data to a smartphone device at sampling rate 256 Hz. The window size set to 10 because the PVC detection method depends only on RR data and as illustrated in Chapter 2 the RR data that was generated from a window size of 10 achieved a high level of accuracy (98%). Hence, the window size of 10 increases the sensor battery life. On the smartphone device, the Pan-Tompkins algorithm was used to process RR data in a simple and fast way that consumed less CPU, RAM, and power as illustrated in the Section 4.3.4. The proposed PVC algorithm was applied to detect PVC beats.

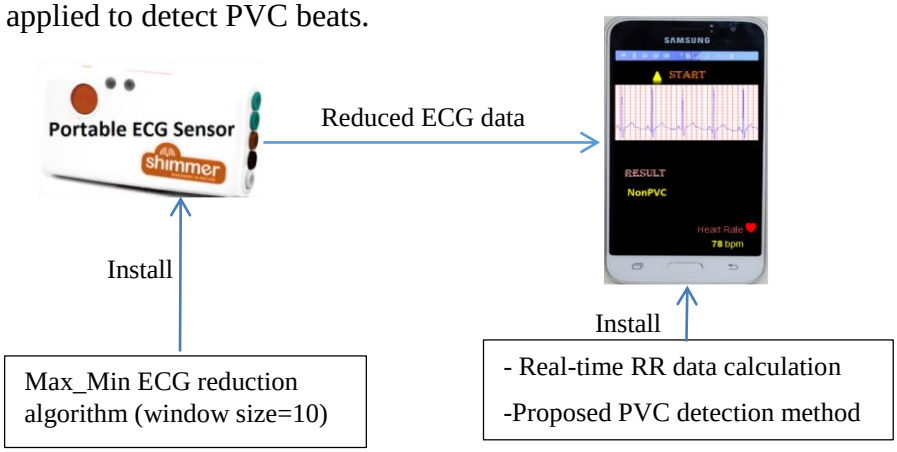

Figure 4.4. General workflow of the proposed PVC detection in real system

The experiment with the Shimmer3 involved recording ECG signals from six volunteers at Ibn Alnafees Hospital (4 men and 2 women aged between 24 and 65) with a normal rhythm over 30 minutes. The overall results illustrated that the non-PVC rhythm for the 6 records assessed for 3 minutes over 30 minutes provided 99%, 98%, and 97% sensitivity, positive predictive and accuracy respectively.

In this chapter, PVC beats were also detected using the complex method of CFNN based on 20 second for comparison with the proposed statistical method in real world system (Shimmer3). Overall results of the intelligent method for sensitivity, positive predictive and accuracy based on a PC device and CFNN were 97.2 %, 98.3% and 97.8%, respectively. The trained data saved and uploaded to the Samsung J1 mobile phone for the classifier in the testing step of the real-time classifier on the mobile phone is described below.

4.3.3 Online system design framework

The real-time cardiac arrhythmia detection system is executed online on the Shimmer3 ECG sensor and Samsung J1 mobile device as depicted in Figure 4.5. First, the ECG reduction algorithm with a window size of five was executed on the Shimmer3 node to reduce and stream the ECG signal in real-time to the mobile phone. Due to the heartbeat features required to detect Q, R, and S waves the window size was set to five in order to maintain all ECG waves (Q, R, and S) as illustrated in Chapter 2. In the second step, within the mobile phone, we applied the Pan-Tompkins algorithm for QRS detection. In the third step, statistical and heartbeat features were calculated for testing using CFNN. Finally, the feed forward back propagation (CFNN) algorithm was applied to detect PVC or Non PVC beats. The PVC detection method within the Samsung J1 phone was implemented using Java software.

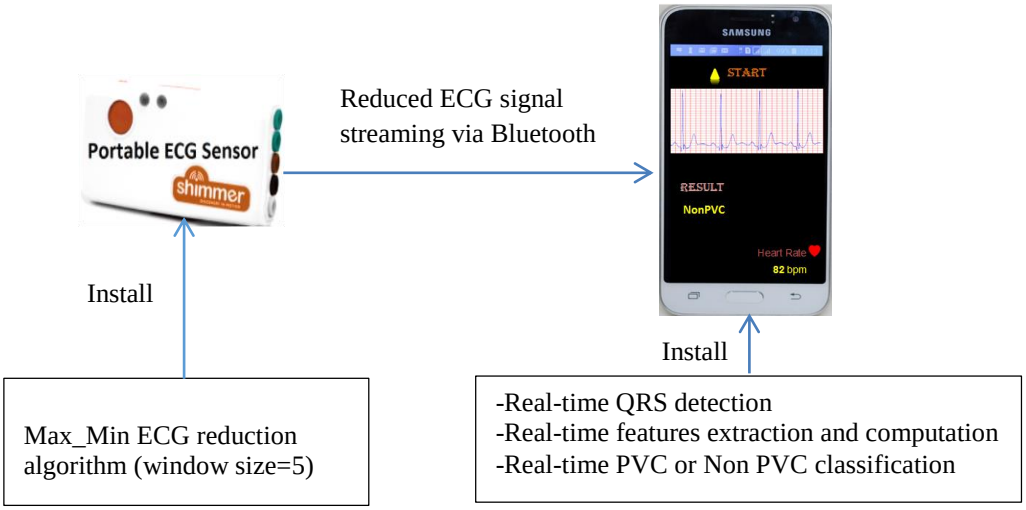

Figure 4.5. General workflow for the proposed online PVC detection system

The online system was applied to the same six volunteers over 30 minutes. The overall results revealed that the Non PVC rhythm for the 6 records monitored over 30 minutes provided 98.3%, 97.6% and 98.9 % sensitivity, a positive predictive value and accuracy respectively. A portable monitoring system is based on battery operated devices. Therefore, low power consumption methods are crucial. The power consumption analysis for the proposed methods is reported next.

4.3.4 Power consumption

In this study, the Samsung Galaxy J1 was used as a reference to measure energy consumption in Joules. The Samsung Galaxy J1 motherboard consists of a quad-core Cortex-A7 CPU clocked at up to 1.2 GHz with about 5 Watts power, 1GB Ram, OS Android 6.0, and has a Bluetooth module. In addition, the Samsung Galaxy J1 has a 1500 mAh rechargeable battery. The energy consumption has been estimated for the runtime PVC method by execution ten heartbeats of operations implemented by the micro-controller unit. The energy consumption is comparable with the algorithms listed in Table 4.6 and is particularly good given that the algorithm executes in real-time reduced energy consumption using, minimal CPU requirements, less time and power consumption.

$$Energy\ consumption = Power \times Runtime \tag{4.5}$$

Table 4.6. Comparison between the suggested methods and more complex methods for energy consumption

Method	**Runtime (Sec)**	**Energy consumption (Joules)**
QRS detection	0.56	2.8
T wave detection	0.080	0.4
Our statistical PVC detection	0.36	1.8
Our machine learning PVC detection	2.1	10.5

In the online PVC detection based on ANN, we tested the Shimmer3 battery-life when it had 10% of charge and 20% of charge with ECG signal sampling at 256 Hz and a window size of 5. When the sensor battery had 10% charge the remaining function of the phone continued for about 1.15 hours. When the window size was increased from 5 to 10, the battery-life extended to about 2.10 hours. When the sensor battery had only 20% of charge remaining the phone continued to record for about 2.35 hours and this increased to 3.2 hours when the window size was increased from 5 to 10. Therefore, it can be concluded that the Max_Min ECG reduction algorithm is more flexible than the existing ECG compression/reduction algorithms which have a fixed CR whereas the CR of the

Max_Min algorithm can be varied and can lead to an extended battery-life and provide an option to manage battery-life.

Furthermore, PVC detection within the smartphone was implemented based on a complex method (ANN) with less time and a low complex method (count data/statistical method) with more time. Therefore, we measured the battery life for the smartphone based on both methods. The complex method consumed more computational resources and power and recognised non-PVC beats for about 2.30 hours whereas the count data algorithm detected non-PVC beats for about 7 hours. Clearly, the statistical PVC detection technique consumes less power than the machine learning method and is more suitable for a continuous real-time cardiac monitoring system based on ECG sensors and smartphones. It reduced the power consumption for both mobile devices: the ECG sensor and smartphone.

4.4 Discussion

The portable cardiac monitoring system based on mobile devices requires algorithms that consume less power consumption and computational resources. A PVC detection technique that can accurately detect PVC beats from non-PVC beats over three minutes of data in a computationally simple way has been advanced. The method is implemented so swiftly that it can be applied in real-time as each new data sample is transmitted. Detection of frequent PVC beats can contribute to raising accurate alarms for patients with risk of serious arrhythmia. In comparison with previous published real-time techniques and machine learning method, the approach presented is computationally simple and can execute in real-time with high accuracy, sensitivity, and a positive predictive value compared with other methods. The method in (Li et al., 2014) requires the detection of QRS and T waves in real-time. This consumes more processing time and power than the statistical approach advanced here which requires only the QRS and uses counts of RR data. In addition, T wave identification is more complex, thereby leading to greater error and power use. This is especially important for mobile devices. Furthermore, sensors streaming RR data are emerging. With our algorithm, the RR data can be processed directly further reducing processing time and resources whereas other techniques such as ANN cannot directly predict RR data because they are designed as block boxes.

The proposed detection algorithm is more precise in alarm raising situations because it collects enough data to detect the frequency of PVC beats. Also, it can provide statistical information (RMSSD, Mean, and SDNN SDNN/RMSSD) which helps in raising an accurate alarm. The high performance that were found with the real trials are due to the classification between PVC and normal rhythms. Also, the number of volunteers is small. More investigation is required to study the optimal

data or period to raising an accurate alarm for real-time PVC monitoring system. In fact, the high performance that were found with the real trials are due to the classification between PVC and normal rhythms. Also, the number of volunteers is small.

4.5 Conclusion

In this study, PVC beats were detected using counts data derived from a three-minute ECG recording using statistical/less complex method and from a few seconds using intelligent/sophisticated approach with a high level of accuracy. The statistical method required minimal computational resources and was well suited for the remote patient monitoring with wearable sensors that have limited power, storage and processing capacity. The time consumed and accuracy of the statistical algorithm provide opportunity for an accurate assessment of serious PVC beats in real time.

Arrhythmias are widely different and may be normal, symptomatic, life threatening or, in some cases, fatal. Hence, automatic arrhythmias classification is critical for cardiology. The next chapter will demonstrate how to automatically classify and detect various cardiac arrhythmias using machine learning methods for reliable and robust analysis of ECG signals captured from wearable sensor and standard devices.

CHAPTER 5

5 Arrhythmias Detection and Classification

In the current chapter investigation of the portable cardiovascular monitoring system with the overarching aim to detect and classify many types of arrhythmias with and without the presence of noise will be discussed. Noisy recordings including diverse ectopics are a common occurrence in ECG traces. These are dealt with primarily by filters included in the recording and analysing software. However, in real-time recording systems filtering options are reduced, especially when count data is used.

Arrhythmias are widely different and may be normal, symptomatic, life threatening or, in some cases, fatal. Thus, automatic arrhythmia classification based on ECG features (diagnostic features) is critical in clinical cardiology. This chapter explains various mechanisms for automatic arrhythmia detection and classification and provides a new wrapper based hybrid technique compared to the most commonly used hybrid methods in the presence of noise. Four different combined structures including genetic algorithm (GA) with artificial neural network (ANN), principal component analysis (PCA) with ANN, GA-SVM (support vector machine), and PCA-SVM are formed by engaging two filtering techniques which are widely used with ECG signal, namely Haar wavelet and Butterworth FIR to render the obscure complexities in the noisy ECG signal. Furthermore, a new arrhythmia classification technique is introduced by combining t-distributed stochastic neighbour embedding (t-SNE) with self organizing maps (SOM). Finally, the chapter details how the proposed technique can improve classification performance.

The datasets used for arrhythmia detection and classification were described in Chapter 2. Two datasets MIT-BIH Arrhythmia and Shimmer3 ECG were used for the experiments described in this chapter. The detection and classification results from the MIT-BIH Arrhythmia dataset were published in a peer reviewed conference (Allami et al., 2016b). In addition, the proposed methods based on the Shimmer3 ECG dataset were examined to validate our results based on a real cardiac monitoring platform.

This chapter starts with a background on the characteristics of arrhythmias, related works, and then it describes the five methods for arrhythmia detection and classification.

5.1 Background and Motivation

Cardiac arrhythmia is the fluctuation of the systematic rhythmic movement of the heart, associated with abnormal electrical heart function. Cardiac arrhythmia can be grouped under two main factors of cardiovascular disease: ventricular and atrial arrhythmias. In both cases, arrhythmias are substantially dangerous and can be life-threatening if not diagnosed properly within a few seconds to a few minutes of their occurrence. The presence of noise impedes cardiologists in detecting arrhythmias. In addition, visual analysis of long term ECG traces consumes time and may cause misdiagnosis or produce inaccurate diagnosis of the heart rhythm (Goldberger et al., 2017). Hence, automated detection and classification of arrhythmias is important for prompt, accurate diagnosis and treatment to reduce morbidity and mortality (Ceylan & Özbay, 2007; Luz, Schwartz, Cámara-Chávez, & Menotti, 2016). There are various characteristics of the ECG signal including interval, amplitude and shape that represent distinct arrhythmia types (Gacek & Pedrycz, 2011) and which makes it possible to distinguish and classify the different types of arrhythmia. In this thesis, the main focus is on classifying the Normal sinus rhythm (N) which represents a normal beat and the erratic heartbeats/arrhythmias for both atrial and ventricular arrhythmias and consider nine types of arrhythmia, including premature atrial contractions (PAC), aberrated atrial premature beats (AA), atrial escape beats (AE), nodal or junctional premature beats (NP), supraventricular escape beats (SVE), premature ventricular contraction (PVC), fusion of ventricular and normal beats (FS), R on T premature ventricular contraction (RPV) and bundle branch block (BBB). The PVC beats were explained in detail in Chapter 4 and the 8 types of arrhythmias are summarised below.

Junctional premature beat is a ventricular contraction generated from the atrioventricular (AV) node. It has a normal QRS complex morphology, the P wave may disappear or be abnormal with a PR interval of less than 120 ms and normal T shape.

Usually, PACs are a common type of arrhythmias that occur due to premature heartbeats emerging in the atrium. A PAC rhythm has an abnormal P wave shape. The QRS complex and T waves however retain their normal shapes. An atrial escape beat presents as an irregular P wave morphology. Nevertheless, depolarisation extends to the ventricles down the atrioventricular junction and the bundle branches. Accordingly, an atrial escape beat produces a normal QRS complex aberrated atrial premature beats are formed by conduction of the supraventricular impulse to the ventricles in a different way from the typical conduction it is characterised by a wide QRS complex. Supraventricular escape beats produce ECG signals with narrow complex rhythms. They may be irregular or regular. They also may provide a normal heart rate, slow or fast heart rate

depending on the underlying arrhythmia mechanism and presence of atrioventricular node block. While evaluating the rhythm, it is important to evaluate whether the P-wave is present and determine if the morphology and duration match the normal P-wave. Fusion beats appear when a ventricular beat joins with a supraventricular impulse to produce a hybrid complex. The fusion beats are of intermediate width and their morphology is similar to the ventricular and supraventricular complexes. The R on T is the superimposition of an ectopic beat on the T wave of a preceding beat and may result in ventricular fibrillation or ventricular tachycardia. Bundle branch block (BBB) is divided into left bundle branch and right bundle branch block. It is a delay or obstruction along the electrical impulse pathways of the heart manifesting in a prolonged QRS interval usually greater than 120ms.

5.2 Related Work

In the last few decades, numerous investigations introduced new techniques to extract ECG from time-domain, frequency-domain and morphological features to build classifiers from different architectures with various levels of complexity and schemes. Each has advantages and limitations. Most existing arrhythmia classification methods used the MIT-BIH Arrhythmia database to develop the classification system of the diverse types of arrhythmias that are recommended by the Association for the Advancement of Medical Instrumentation (AAMI) standard. Five types of ectopic beats are defined including supra-ventricular ectopic beats (S), ventricular ectopic beats (V), fusion beats (F) and unclassifiable and paced beats (U) (ANSI-AAMI, 1998). Many data mining algorithms have been used to classify ECG signals such as that of (Raghav & Mishra, 2008) who applied a local fractal dimension technique to classify heart arrhythmias that provided promising results. Classification has also been implemented using artificial neural network (ANN) classifiers to classify and detect arrhythmias (Jiang & Kong, 2007; Martis et al., 2013; Nadal & Bossan, 1993; Özbay & Tezel, 2010; Yu & Chou, 2008). Numerous studies used support vector machine (SVM) method to classify ECG beats (Acır, 2006; Asl et al., 2008; Melgani & Bazi, 2008; Song, Lee, Cho, Lee, & Yoo, 2005; Zidelmal, Amirou, Ould-Abdeslam, & Merckle, 2013). Self-organizing maps (SOM) mechanism was also applied by many studies for ECG signals classification (He, Hou, Zhen, & Peng, 2006; Lagerholm, Peterson, Braccini, Edenbrandt, & Sornmo, 2000; Orjuela-Cañón et al., 2013; Wenyu, Gang, Ling, & Qilian, 2003). He et al. (2006) recognized four types of arrhythmias using leaning vector quantization (LVQ), back propagation neural network (BPNN) and SOM. The SOM classifier resulted in enhanced accuracy 95% compared with the LVQ with 91% and BPNN with 92%. Other investigations applied different well-known approaches such as k-means clustering (Kiranyaz, Ince, Pulkkinen, & Gabbouj, 2011), Bayesian (Sayadi, Shamsollahi, & Clifford, 2010), Fuzzy logic (Özbay, Ceylan, & Karlik, 2006) and K-nearest neighbor (k-NN) (Arif & Akram, 2010) to classify and detect arrhythmias. Nowadays, deep learning techniques have been used to classify ECG beats.

For instance, Al Rahhal et al. (2016) proposed a deep neural network classifier to classify five types of arrhythmias. The restriction of deep learning NN is that it requires a large amount of ECG signals for training. A comprehensive review for detection and classification of arrhythmias can be found in (Ince, Zabihi, Kiranyaz, & Gabbouj, 2017; Maglaveras et al., 1998)

In the past two decades, many researchers have combined different feature selection approaches with heart beat classifier methods to select most effective features and improve detection and classification performance. Current reduction/optimisation methods to solve the feature reduction problem in ECG classification are described below. Genetic algorithm (GA) combined with a *k*-means algorithm to classify ECG signals into normal and arrhythmia is one option. The GA-*k*-means technique provided an accuracy of 95.97 % (Zhang, Liu, Wei, Wei, & Liu, 2014). In addition, GA integrated with ANN (multi-layer perceptron MLP) to classify many types of arrhythmias resulted in an overall accuracy of 94% (Maliarsky, Avigal, & Herman, 2014). Further, GA combined with many ANN classifiers to detect normal and BBB has also been investigated. The best GA-ANN approach reported a sensitivity, specificity and accuracy of 96%, 98% and 98% respectively (Kora & Krishna, 2016a). Wang, Chiang, Yang, and Hsu (2011) classified different arrhythmias using principal component analysis (PCA) and linear discriminant analysis (LDA) techniques for dimensionality reduction and applied a probabilistic neural network (PNN). PCA-PNN hybrid resulted in improved sensitivity, specificity and accuracy (97.17%, 99% and 99.61% respectively) compared to the LDA-PNN method (89.94%, 98.27% and 98.26% respectively). A more recent study proposed a new method to detect five types of arrhythmias based on a combination of nonlinear and linear feature selection methods compared with the linear methods that require low computational complexity (Elhaj et al., 2016). The method combined discrete wavelet transformation (DWT) results with (PCA). The DWT technique was used to transform ECG signals and the PCA was applied to extract the features. Further, the nonlinear higher order spectra (HOS) cumulants technique and independent component analysis (ICA) for nonlinear dimensionality reduction were employed for analysing of nonlinear ECG data. The selected features that were generated from the DWT-PCA and HOS-ICA were submitted to the SVM and an NN classifiers for automated detection of normal and abnormal ECG data. The DWT-PCA-SVM technique reported an overall accuracy of 94.97%. The DWT-PCA-NN technique reported an overall accuracy of 97.34%. The HOS-ICA-SVM technique reported an overall accuracy of 99.13 %. The HOS-ICA-NN technique provided an overall accuracy of 97.76 %. Classification results based on linear-nonlinear approaches of the (DWT-PCA) + (HOS-ICA) with SVM provided a sensitivity, specificity and accuracy of 98.91%, 97.85% and 98.91% respectively) compared to the (DWT-PCA) + (HOS-ICA) with NN achieved sensitivity, specificity and accuracy (98.90%, 98.90% and 98.90% respectively).

A new combined approach has been advocated by (Afkhami, Azarnia, & Tinati, 2016) to classify many types of arrhythmias based on a Gaussian mixture modelling (GMM) for feature selection with an expectation maximisation (EM) classifier. The GMM-EM reported an overall sensitivity, specificity and accuracy of 96.15%, 94.85% and 99% respectively. A Hermite function has been integrated with SOM technique to classify four types of heart beats and provided a high degree of accuracy at 98.5% (Lagerholm et al., 2000). In addition, Wenyu et al. (2003) combined the PCA feature extraction method with a SOM classifier to reveal the relationship between ECG beat clusters and clinical categories. Other studies combined different well-known techniques such as fuzzy c-means clustering (FCM) with PCA-NN and FCM-WT-NN (Ceylan & Özbay, 2007), ICA-PNN (Yu & Chou, 2008), FCM-PNN (Haseena, Mathew, & Paul, 2011), Cartesian genetic programming (CGP) with neural network (NN) (Ahmad, Khan, & Mahmud, 2013) and firefly and particle swarm optimization (FFPSO) technique with a Levenberg Marquardt neural network (LMNN) (Kora & Krishna, 2016b). More details about arrhythmia classification using hybrid techniques have been published (Luz et al., 2016; Martis, Acharya, & Adeli, 2014a)

These existing methods were tested on noise-free or carefully chosen, often clean ECG signals, which produced accurate classification results (Elhaj et al., 2016). However, these methods may not provide the same high accuracy in the presence of a noisy ECG (Martis et al., 2014a). In addition, there has been no publication outlining a reliable way to classify and detect the accuracy of various type of arrhythmias based on noisy environments such as a wireless cardiac monitoring system. Noise and data transmission losses are likely to have a strong impact on wearable ECG sensors because of interference from other portable devices.

5.3 Methodology

It is clear from related works that there is a need for a computationally efficient technique for detection and classification of various type of arrhythmias that can provide high classification accuracy, high sensitivity as well as high specificity (almost no misses) based on noisy platforms. In this research, a novel wrapper based hybrid model is proposed for the classification of arrhythmias which uses stochastic neighbour embedding (t-SNE) in combination with self organizing maps (SOM) to improve classification performance.

In this chapter, the approach adopted for fulfilling the main goal of the chapter has been laid out. An empirical technique has been applied and a series of classification experiments have been designed to assess the efficacy of t-SNE-SOM classification. Experiments have also been designed to compare the performance with the state-of-the-art hybrid approaches. A step by step procedure with all the

parameters and software programs harnessed for the experiments has also been presented in this chapter. The evaluation metrics adopted for comparing the performances have also been described in detail.

All the classification experiments were implemented using MATLAB 2016a Software. The machine used for all experiments was Intel Corei7 CPU PC with Windows 10 (64 bit) operating system.

5.4 Method Description

An empirical/experimental methodology has been applied in this chapter to evaluate the effectiveness of the t-SNE feature selection for arrhythmias classification based on noisy and clean ECG signals. Essentially, classification of ten categories of arrhythmias was investigated. The classification performance of the t-SNE feature selection was assessed using a quantitative technique to compare the t-SNE method with current state-of-the-art feature selection methods applied for arrhythmia classification. Statistical analysis including sensitivity, specificity and accuracy were used. For instance, consider the confusion matrix for normal and arrhythmia classification as represented in Table 5.1.

Table 5.1. Confusion matrix for normal and arrhythmia classification

Actual class	**Predicted class**	
	Normal	Arrhythmia
Normal	*TP* (True Positive)	*FN* (False Negative)
Arrhythmia	*FP* (False Positive)	*TN* (True Negative)

Sensitivity is a very significant factor to consider when it comes to the detection of a certain disease from a clinical perspective. The high degree of sensitivity denotes lower value of *FP* results. In addition, Sensitivity, the 'true positive rate' and was represented in Equation 4.2 in Chapter 4. An evaluation with a high level of sensitivity tends to represent all possible positive conditions without missing any. Specificity and accuracy are also important measures. Specificity assesses the proportion of negatives that are correctly detected. It is also called the 'true negative rate' and is represented in Equation 5.1 below. The higher degree of specificity suggests a lower number of false negatives. Hence, a high level of specificity is better for ruling out a disease condition. 'Accuracy' represents the total number of correct predictions of all predictions made and is described in Chapter 4 in Equation 4.4.

$$Specificity = TN/TN + FP \tag{5.1}$$

5.5 General System Design

The overriding aim of this chapter was to report on the classification of arrhythmias. A novel feature selection approach t-SNE was proposed for the classification. This approach is described in detail in Section 5.5.3. Figure 5.1 depicts a schematic overview of the technique utilised to use the wrapper based hybrid approach for the detection of arrhythmias. Each phase is described in the following subsections.

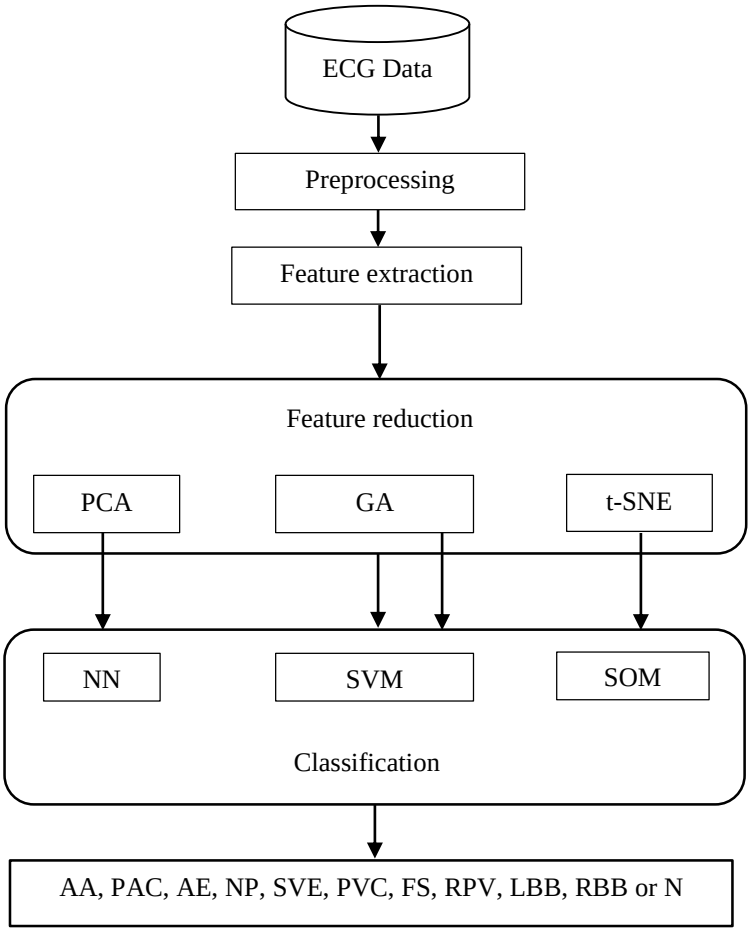

Figure 5.1. General schematic of experimental procedure

5.5.1 Pre-processing

A typical ECG tracing of the cardiac cycle consists of a P wave, QRS complex, and T wave (Gacek & Pedrycz, 2011), as represented in Chapter 1, Figure 1.2. The performance of an ECG analysis system depends heavily upon the accurate and reliable detection of the QRS complex, as well as the T and P waves (Yochum, Renaud, & Jacquir, 2016). ECG signals are usually contaminated with noise including artifacts, power-line interference, baseline wander, and EMG noise (Afonso, Tompkins, Nguyen, Michler, & Luo, 1996). The elimination of noise from ECG signals is an essential task in arrhythmia classification because it contributes to accurate and reliable detection of the P-QRS-T waves that directly impact forecasts and classifications. We adopted two of the most widely used

filters for noise reduction: wavelet transforms (WT) and finite impulse response (FIR) (Lynn, 1971). In the last decade, numerous approaches based on wavelet transforms have been applied to eliminate noise, since they maintain ECG signal characteristics and thus avoiding missing diagnostic features. Also, they are computationally less complex than other methods (Singh & Tiwari, 2006). In our design, the Haar wavelet and Butterworth FIR filters were used to denoise the ECG signals. The Haar transform works well by providing a relatively sparse wavelet representation for signals that are approximately piecewise constant. The FIR filter attenuates recognized frequency bands including the noise generated from an electrical network (50 or 60 Hz), as it allows quick and easy application of the reject band filter. The primary obstacle with the FIR filter is that the frequency of the noise in the ECG signal is not always recognised (Luz et al., 2016). However, different frequency band filters can be applied to the signal in order to address the problem.

5.5.2 Feature extraction

The feature extraction phase plays an important role to provide reliable results in classification of the heartbeat. Any data generated from an ECG signal can be harnessed to identify its type and may considered as a feature. ECG features can be extracted in different ways including time-domain or frequency domain, ECG morphology and cardiac rhythm (Luz et al., 2016).

The original amplitude of the time-domain ECG data was used as a feature vector to represent the ECG data after noise removal and baseline drift suppression. Then the QRS complex was detected using real-time Pan-Tompkins algorithm, the ECG data in a window of 550ms was selected as an ECG signal. In order to ensure the window covers most of the ECG properties, the length of the ECG signal before and after the R peak in each ECG beat were set at 140ms and 410ms respectively. For each signal, 19 features including PQ interval, RR interval and PT interval were identified. Additional features that were included were QR, QS and RS as well as a difference value in these features such as L(S) -L(Q).

After feature extraction, the normalisation of the ECGs has an important role to play in improving classification performance. A typical classifier executes better when the input features are scaled/normalised within a standard range (Aksoy & Haralick, 2001). There are several methods to do this type of normalization/scaling.

In this study, the Minmax normalisation method was used to normalise ECG features to values between 0 and 1 as described in Equation 4.1 in Chapter 4. Usually, the Minmax method transform data to a fixed range between 0-1. This way minimal standard deviations can be obtained, which reduce the impact of outliers. Normalisation/scaling the features can make training of the classifier

faster by suppressing the possibility of getting stuck in a local minimum. All ECG features were identified for each beat and submitted to separate vectors as either AA, APC, AE, NP, SVE, PVC, FS, RPV, LB, RB or N (Normal). The next phase involved feature reduction.

5.5.3 Feature selection/reduction

The process for determining the optimal subset of features from all the features is called feature selection/reduction. The feature selection process provides three main advantages for classification; reducing training time, improving accuracy and reducing overfitting and hence superior generalisation (Adnan & Islam, 2016; Rahman & Islam, 2014).

Feature selection methods transform the extracted features from ECG signals from their original N dimension space to a new M dimension space, where M<N and preserve most useful information. The main aim of the feature selection methods is to select the most representative subset features to enhance the classification process. Some features that were extracted from ECG data may be irrelevant or redundant. Irrelevant features can result in overfitting and the redundant features require more training time, which leads to a less generalised classification model (Adnan & Islam, 2016).

The aim of this experiment is to discover if a subset of features, which can discern different arrhythmia classes, and to identify the most significant features in order to decrease the training time, testing time and enhance classification performance.

Many feature selection/reduction approaches have been used to identify the most significant features. Two most commonly used feature selection/reduction methods (PCA and GA) were employed for the experiments in addition to the proposed method t-SNE. The PCA method has been commonly used in statistical data analysis and feature selection (Castells, Laguna, Sörnmo, Bollmann, & Roig, 2007). The motivation of PCA is to select significant features from high dimensions by transforming a set of variables in S^L space, which are uncorrelated with each other and each of is a linear combination of the raw values, into another set in S^M space maintaining the largest amount of variance in the data where basically M is less than L.

PCA is implemented by projecting the variables into the feature space to compute the correlation between those features. The PCA calculates the principal components as a percentage of the full variability in the dataset. The first principal component produces the vector of the maximum variability; uncorrelated. The second principal component produces the vector for the subsequent direction orthogonal to the first principal component and so on. PCA divides the covariant structure

of the dependent variables into orthogonal components by computing the eigenvectors and eigenvalues of the covariance matrix. Measuring the covariance matrix of the data including sorting of eigenvectors in decreasing order of eigenvalues, eigenvalue decomposition and projection of the data into the new basis defined by the principal components. It takes the inner product of the raw data and the sorted eigenvectors (Castells et al., 2007; Martis et al., 2013).
The main procedures of the PCA are listed below.

Step 1: Find covariance matrix using Equation 5.2

$$CM=(A-\bar{A}) \times (A-\bar{A})^{T} \quad (5.2)$$

where A is the matrix in a subset of K x 4200, K is the total number of patterns and $\bar{A}$ refers to the mean vector of A.

Step 2: Find the matrix of eigenvectors eV and diagonal matrix of eigenvalues eD using Equation 5.3

$$eV^{-1} \times CM \times eV=eD \quad (5.3)$$

Step 3: Eigenvectors in eV are sorted in descending order of eigenvalues in eD and the data on these eigenvector directions are projected by taking the inner product between the data matrix and the sorted eigenvector matrix using Equation 5.4.

$$Projected\ data\ (P) = \{eV^{T} \times (A-\bar{A})^{T}\}^{T} \quad (5.4)$$

where eV represents 4200 x 4200 dimension and each row refers to an eigenvector. Six features were selected from six columns of the projected data.

The PCA technique was implemented for each subset and six principal components were extracted using 99 % of the total variability. In general, twelve features, 6 from each subset, were submitted to the SVM and ANN classifiers for the automated detection of normal and abnormal ECG data.

The GA is an optimisation technique that replicates natural survival of the fittest where feature subsets with the best performance are included in the generation of new feature subsets. The next generation of subsets preserve favourable characteristics while unfavourable characteristics are omitted, leading to species progressive evolution (Mitchell, 1998). GA iterates and evolves a population by forming a new population at every step through selection, recombination, mutation and finally applying a fitness function (Beg, Islam, & Estivill-Castro, 2016; Mitchell, 1998). The selection process directly selects subsets of features to form a current population. Each subset (chromosome) is evaluated using a fitness function. Within each subset, a crossover operation or recombination creates a new feature

subset. Mutation applied to each feature subset to produce modified subsets. The fitness function then measures the quality of the solution expressed as the percentage of individuals correctly classified. The classification system is described in Figure 5.2 below that emphasizes the GA optimization.

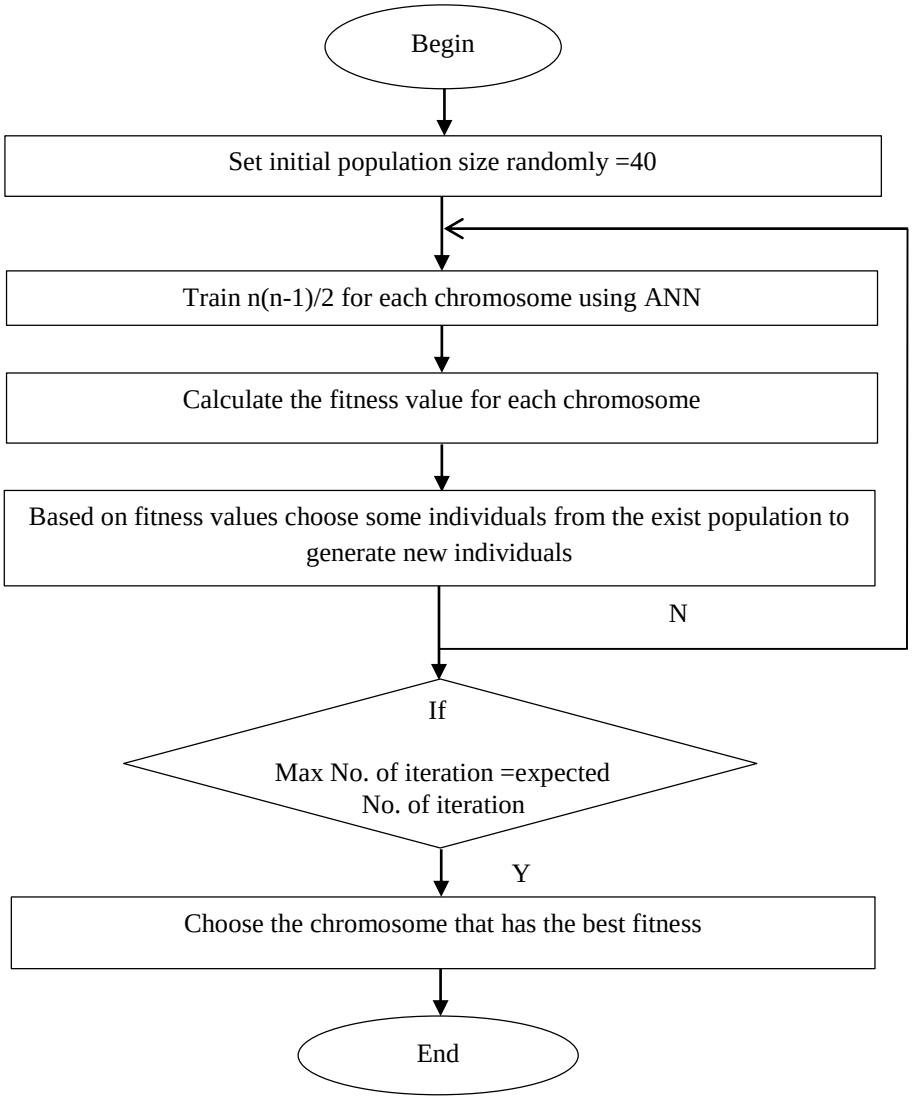

Figure 5.2. GA training process.

A vector of 19 features with each component being either one or zero was used for the encoding. A value of one means the corresponding feature is selected and a value of zero means the corresponding feature is ignored. The original population comprised 40 chromosomes that were randomly selected. The Swapping and Roulette Wheel selection techniques were utilized for crossover and mutation procedures. The Swap procedure randomly changed the location of two samples. The probability parameter of mutation was set to 0.1.

Recently, a new dimensional reduction method called t-distribution stochastic neighbour embedded (t-SNE) has been introduced by Maaten and Hinton (2008). The t-SNE visualises high dimensional

data by providing each data sample a position in a two or three dimensional map (Maaten & Hinton, 2008). This approach is a modification of the stochastic neighbour embedding (SNE) method that was proposed by (Hinton & Roweis, 2003). It is much easier to optimise than the SNE and provides significant enhancement in feature reduction by compressing the tendency to crowd samples together in the centre of the structure. Most of the existing nonlinear dimensionality reduction methods are not able to maintain global and local structures of the data in a single map. The t-SNE achieves more accurate results than current algorithms in creating a single map that exposes structure at numerous scales (Maaten & Hinton, 2008).

The t-SNE converts a high dimensional dataset into a matrix of pairwise similarities and preserves the local structure of the high dimensional data and also reveals global structure such as the presence of clusters at many scales. It reduces the difference between two distributions: the distribution that estimates pairwise similarities of the input objects and the distribution that estimates pairwise similarities of the corresponding low dimensional samples in the embedding. For example, if the input of high dimensional dataset/ input objects Z = (y_1,y_2,y_3,….,y_N) and a function z(y_i, y_j) that measures the distance between a pair of objects is the Euclidean distance z(y_i, y_j) =||y_i - y_j|| and the aim is to learn a k-dimensional embedding in which each object is represented by a sample; E=(x_1,x_2,x_3,….,x_M) where $x_i \in R^k$. The t-SNE uses the symmetrising two conditional probabilities ($Pro_{i|j}$) that compute the pairwise similarity between objects y_i and y_j as below:

$$Pro_{j|i} = \frac{\exp\left(-z(y_i,y_j)\right)^2/2\sigma_i^2}{\sum_{l\neq i}\exp(-z(y_i,y_l)^2/2\sigma_i^2} \quad , Pro_{i|j} = \frac{Pro_{j|i} + Pro_{i|j}}{2N} \text{ where } Pro_{i|i}=0 \tag{5.5}$$

The bandwidth of the Gaussian kernels (σ_i) in Equation 5.5 set in a way that the perplexity of the conditional distribution Pro_i is equal to the predefined perplexity u. Therefore, the best number of σ_i differs per object in area of the data space with a higher data density and with lower density σ_i tends to be minimal in area of the data space (Hinton & Roweis, 2003).

In the k-dimensional embedding E, the similarities between two samples x_i and x_j such as the low dimensional models of y_i and y_j are computed using a normalised heavy-tailed kernel. The embedding similarity h_{ij} between the two samples x_i and x_j is estimated as a normalised Student-t kernel with a single degree of freedom as represented in Equation 5.6 below.

$$h_{ij} = \frac{\left(1+||x_i - x_j||^2\right)^{-1}}{\sum_{l\neq k}(1+||x_l - x_k||^2)^{-1}} \quad \text{where } h_{ii}=0 \tag{5.6}$$

Dissimilar input objects (X_i and X_j) are modelled and matched far samples (X_i and X_j) in low dimensional using heavy tails of the normalised Student t-distribution. It provided more space to precisely model the small pairwise distances such as the local data map in the low dimensional embedding.

The positions of the embedding samples X_i are identified by minimising the Kullback-Leibler (KL) distance/divergence function between the joint distributions (Pro and H). The KL is a distance formula from the true probability distribution (Pro) to a target probability distribution (H) as illustrated in Equation 5.7 below.

$$C(E) = KL(\text{Pro}||H) = \sum_{i \neq j} Pro_{ij} \log \frac{Pro_{ij}}{h_{ij}} \quad (5.7)$$

The gradient of the KL function between Pro and the Student t-distribution based joint probability distribution H is computed using Equation 5.7 above.

Due to the asymmetry of the KL function, the objective function emphasises modelling high samples of Pro_{ij} (identical objects) by high samples of h_{ij}(nearby samples in the embedding space). The objective function is non-convex in the embedding E. Typically, it is minimized by descending along the gradient as described in Equation 5.8 below.

$$\frac{\delta C}{\delta x_i} = 4 \sum_j (Pro_{ij} - h_{ij})(x_i - x_j)(1 + \left|\left|x_i - x_j\right|\right|^2)^{-1} \quad (5.8)$$

The algorithm of the t-SNE method is described below.

Algorithm 5.1. t-SNE method coding schema

Input: ECG data Y= (Y_1, Y_2, Y_3,…,Y_N)
Output: Reduced ECG features X=(X_1, X_2, X_3, ..., X_M)

Step 1: Set optimisation parameters; number of iterations *S*, learning rate £, momentum α(*s*)
Step 2: Find pairwise similarities $Pro_{j|i}$ using Equation 5.5
Step 3: While (s ≠ S) Do
Step 4: Find low dimensional similarities h_{ij} using Equation 5.6
Step 5: Find gradient $\frac{\delta C}{\delta X}$ using Equation 5.8
Step 6: Set $X^{(s)} = X^{(s-1)} + £ \frac{\delta C}{\delta X} + \alpha(s) (X^{(s-1)} - X^{(s-2)})$
Step 7: s=s+1
Step 8: End while
Step 9: Return to Step 3

5.5.4 Classification

After normalisation of ECG features, the next phase is classification of the arrhythmias based on the hybrid methods. The confusion matrix from the classification is identified and the performance is compared using sensitivity, specificity and accuracy.

Numerous different classifiers have been harnessed for arrhythmia classification tasks (Martis et al., 2014a). Each has limitations and advantages. Three most widely used classifiers; support vector machine (SVM), multilayer perceptron (MLP) and self organizing map (SOM) were applied for the experiments. Basically, the SVM classifiers apply different combinations of subsets of input data to reveal the optimal feature subset to separate out two groups. On the other hand, the MLP classifiers provide good results with uncertainty and noise. Also, they consider all the input features for identifying the output class. Therefore, it skips numerous features but could be valuable to identify if there are any dominant features which are capable to detect a specific arrhythmia among the various arrhythmia categories. The SOM classifier is a generic classifier which can process various categories and has been applied for variety of datasets.

SOM is a non-parametric and flexible machine learning approach utilised for classification and clustering. The SOM techniques are related to the nodes of a regular, generally two dimensional map. A SOM classifier builds the structures such that the closer samples will be related with nodes that are similar in the map, whereas less closer samples will be moved gradually farther away in the map (Kohonen, 2013). A SOM converts high dimensional, nonlinear statistical connections into simple geometric connection in a k-dimensional matrix as represented in Figure 5.3. SOM classifies input data according to how they are grouped in the input domain and learns both the topology and distribution of the input data. The topology of the SOM is composed of two layers: input layer and output layer. The input layer is entirely linked to the output layer of the map samples with weight vectors representing the feature of the samples. The samples in the output layer compete among themselves to find a winner sample. The winner sample adjusts its neighbours and weights by moving neighbours weight vectors to be closer to the input vector. As training proceeds, the sample and its neighbours represent similar groups whereas samples are not close to each other in the structure representing dissimilar groups. The final weight vectors usually relied on the series of the input dataset.

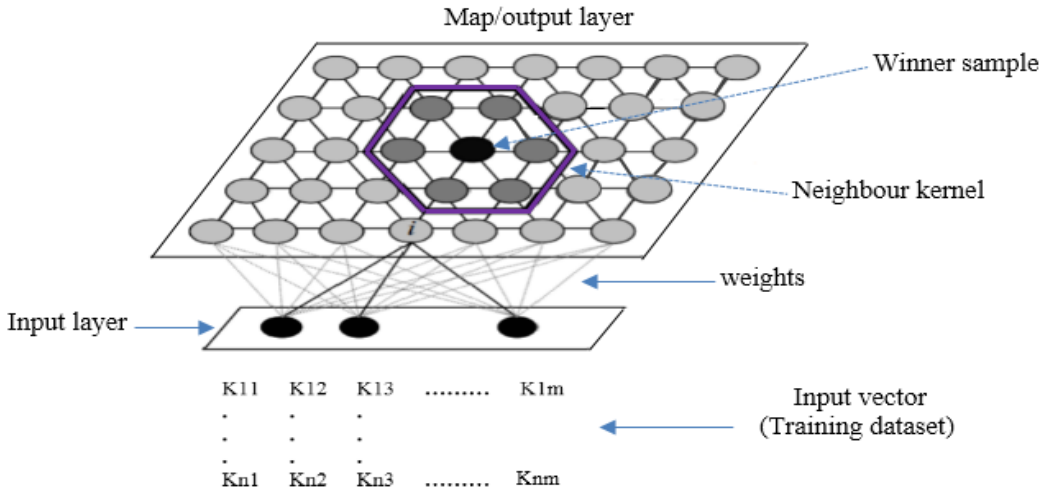

Figure 5.3. Classification by SOM method

When percentage of training data for one category is the same as that of the other category, the training is called balanced learning. Nevertheless, in many datasets, this is not the case. It has been found that ANN methods outperform SVM methods when balanced learning is absent and the implementation of both classifiers become comparable with balanced learning (Ren, 2012). Classifiers such as SVM and MLP require a heavy learning/training stage. On the other hand, SOM methods can naturally process numerous number of classes, avoid overfitting, and most importantly require no training phase. Also, it can organise large and complex datasets. The training time required is zero in this case. However, as SOM must measure the similarity between nearest neighbours for each point during the classification process, more time is required during the classification stage. Therefore, SOM applies a learning technique where a function is estimated locally, and hence the prediction process is slow. Furthermore, it is difficult to identify what input weights to employ (Kohonen, 2001, 2013).

The cascade forward neural network (CFNN) which was used with 10 hidden layers in the current study is trained with back propagation of errors (Bonanno et al., 2014) similar to feed-forward networks but includes a weight connection from the input to each layer and from each layer to successive layers. The ANNs are capable of learning the desired mapping between the inputs and outputs signals of the system without knowing the exact mathematical model of the system and are therefore excellent estimators of nonlinear systems. The network was trained by a continual readjustment process to the weight and the threshold value, in order to reduce the network error to a pre-set minimum of 1% or to stop at a pre-set number of cycles. Then for the forecasting, held out samples or test data was presented to the trained network to obtain the test results according to a standard approach.

GA was used to optimise the input features of the ANN and SVM to obtain smaller and more effective inputs. Data in the GA were represented by n-bit binary vectors. Thus, the search space corresponds to an n-sized Boolean space. For each generation, the evaluation of the data, i.e. input feature subset required for the training of the ANN and SVM and use of the result in an objective function.

The SVM classifier illustrates a generalisation capability when using the maximal margin principle. A margin is the distance between the support vectors of two different groups. The training data from both groups nearby hyperplane is known as support vectors. To extend SVM from two-class to multiclass classification task one of the most commonly used method called one against all (OAA) (Zhang, Dong, Luo, Choi, & Wu, 2014) was employed. Numerous kernel transformation methods are utilised to map the data into high dimensional functions including polynomial, quadratic and radial basis function (RBF)/Gaussian kernel. The RBF/Gaussian kernel is widely used with SVM classification and provides high degree of accuracy (Elhaj et al., 2016). Therefore, we selected the RBF kernel transformation method in SVM classification.

The proposed method based on t-SNE and SOM is illustrated in Algorithm 5.2 below.

Algorithm 5.2. Proposed t-SNE +SOM approach coding schema

Input: ECG Features

Output: AA/PAC/AE/NP/SVE/PVC/FS/RPV/LBB/RBB or N

Step 1: Randomly initialise all weight vectors

Step 2: Select random data from the feature reduced training data from t-SNE and submit it to the SOM classifier

Step 3: Compute the winner node or best matching unit (BMU) in the map

Step 4: Identify the nodes within the neighbour nodes of the winner node (the size of the neighbour nodes and learning rate reduce with each loop)

Step 5: Adapt the weight of the nodes in the winner node neighbour according to the selected data

Step 6: Repeat steps from 2 to 5 for K loops/convergence

In the proposed t-SNE +SOM approach, the matrix size was 8400 patterns. The t-SNE parameters were randomly set up where the momentum was 0.5, the number of iterations was 1000 and the learning rate was 0.01.

Two optimization methods, early exaggeration and early compression, were utilized to optimize the t-SNE cost function and reduce the number of required iterations. The early exaggeration method was used to multiply all thePro_{ij}'s by an *n>1* in the initial stages of the optimization. This caused the h_{ij}'s to be very small to model their corresponding $Pro_{ij}'s$, so that the optimization focused on modelling the large Pro_{ij}'s. The early compression method forced the map data to be close to each other at an early stage of optimization so that it was easy to explore the possible global organization space of the data.

The MATLAB SOM toolbox was used in this stage to apply the training and accuracy classification. The SOM algorithm gradually led to an organized representation of the activation patterns drawn from the input space. We used two identifiable phases of the adaptive process, ordering and convergence. In the ordering phase, the topological ordering of the weight vector was set to 1000 iterations of the SOM algorithm and careful consideration was given to selecting the neighbourhood and learning rate parameters. In the convergence phase, the feature map provided an accurate statistical quantification of the input space. The number of iterations in this phase was at least 500 times the number of neurons in the network and the parameters were selected carefully.

5.6 Experimental Results

The aim of this experiment is to reveal if a subset of features, which can recognise types of arrhythmia classes, exists, and to identify the most significant features in order to reduce the training time and improve classification accuracy. Moreover, it is to find which hybrid approach is more robust to noise and improves classification performance by testing each method using noisy and less noisy ECG signals.

Four different combined approaches including GA-ANN, GA-SVM, PCA-ANN and PCA-SVM were used by engaging two filtering techniques that are widely used with ECG signals, namely the Haar wavelet and Butterworth FIR to render the obscure complexities in the noisy ECG signal. Furthermore, a new arrhythmia classification technique known as t-SNE-SOM was introduced by combining t-distributed stochastic neighbour embedding (t-SNE) with self organizing maps (SOM). These five approaches were used in order to detect which method performs best for the arrhythmias classification task. 10-fold cross-validation technique was used for estimating the generalisation. The overall performance of the classifiers was estimated by computing the mean of the 10-fold cross-validations. Performance was compared using sensitivity, specificity and accuracy. Experimental results for each hybrid approach based on the MIT-BIH Arrhythmia and Shimmer3 datasets are reported below.

5.6.1 Experiment results on MIT-BIH Arrhythmia dataset

As noted before, noise is likely to have a heavier effect on wearable ECG sensors because of the interference from other portable devices. Usually, the MIT-BIH Arrhythmia database is clean, hence, we added Gaussian white noise to the all MIT-BIH Arrhythmia ECG signals as noise source to test the classification performance based on standard MIT-BIH Arrhythmia ECG signals and ECG signals have interference noise.

5.6.1.1 Sensitivity

Sensitivity is an indicator for measuring the number of people with actual arrhythmia conditions to the total test subject data of people with arrhythmia. This reveals how effective the classification algorithm in detecting the type of arrhythmia classes.

Table 5.2. Arrhythmia classification results for sensitivity using GA-ANN

Method	**Sensitivity %**										
GA-ANN	APC	AA	NP	SVE	PVC	RPV	FS	AE	N	LB	RB
Standard MIT-BIH and Haar filter	99.8	100	100	100	100	99.9	100	98.9	100	100	100
With noise and Haar filter	99.6	100	100	100	100	99.3	100	98.2	100	100	100
Standard MIT-BIH and FIR filter	99.7	100	100	100	100	99.8	100	98.9	100	100	100
With noise and FIR filter	99.5	100	100	100	100	99.2	100	98.1	100	100	100
Standard MIT-BIH without filter	99.3	99.6	100	100	99.6	98.8	99.8	98	100	100	100

Table 5.3. Arrhythmia classification results for sensitivity using GA-SVM

Method	**Sensitivity %**										
GA-SVM	APC	AA	NP	SVE	PVC	RPV	FS	AE	N	LB	RB
Standard MIT-BIH and Haar filter	99.6	100	100	100	100	100	99.6	98.4	100	100	100
With noise and Haar filter	99	100	98.8	100	100	100	99.1	97.9	100	100	100
Standard MIT-BIH and FIR filter	99.6	100	100	100	100	100	99.6	98.4	100	100	100
With noise and FIR filter	99	100	98.8	100	100	100	99.3	97.5	100	100	100
Standard MIT-BIH without filter	99.2	99.3	97.9	100	100	100	99	87.5	100	98.4	98.7

Table 5.4. Arrhythmia classification results for sensitivity using PCA-ANN

Method	**Sensitivity %**										
PCA-ANN	APC	AA	NP	SVE	PVC	RPV	FS	AE	N	LB	RB
Standard MIT-BIH and Haar filter	100	99.7	100	100	99.8	100	100	100	100	100	100
With noise and Haar filter	100	98.3	100	100	98.6	100	100	100	100	100	100
Standard MIT-BIH and FIR filter	100	99.7	100	100	99.8	100	100	100	100	100	100
With noise and FIR filter	100	98.2	100	100	98.6	100	100	100	100	100	100
Standard MIT-BIH without filter	100	98	100	100	97.3	99.8	100	100	100	100	100

Table 5.5. Arrhythmia classification results for sensitivity using PCA-SVM

Method	**Sensitivity %**										
PCA-SVM	APC	AA	NP	SVE	PVC	RPV	FS	AE	N	LB	RB
Standard MIT-BIH and Haar filter	99.2	82.3	84.3	100	98.8	98.5	98.2	81.2	100	100	99.9
With noise and Haar filter	99	80.9	84	100	98.2	97.2	96.8	80.3	100	92.9	97.5
Standard MIT-BIH and FIR filter	99.2	82.5	84.3	100	98.3	98.1	97.9	62.5	100	98.6	97.8
With noise and FIR filter	99	80.3	83.5	100	98.4	96.6	96.9	61.4	100	92.5	95.2
Standard MIT-BIH without filter	99	79.8	82.4	100	97.9	96	96.4	56.2	100	91.4	87.2

Table 5.6. Arrhythmia classification results for sensitivity using t-SNE-SOM

Method	**Sensitivity %**										
t-SNE-SOM	APC	AA	NP	SVE	PVC	RPV	FS	AE	N	LB	RB
Standard MIT-BIH and Haar filter	100	100	100	100	99.9	100	100	100	100	100	100
With noise and Haar filter	100	100	100	99.8	99.7	100	100	100	100	100	100
Standard MIT-BIH and FIR filter	100	100	100	100	99.9	100	100	100	100	100	100
With noise and FIR filter	100	100	100	99.8	99.6	100	100	100	100	100	100
Standard MIT-BIH without filter	99.2	100	100	100	99.6	98.8	100	98.9	100	100	100

From the sensitivity results, it can be seen that PCA in combination with SVM performed to a lesser degree in identifying the type of arrhythmias with noise added to the ECG signals or with standard

ECG signals. The same trend was reflected even with filters added to reduce the noise from the signal. Also, many patients with APC, AA, AE, NP condition were left undiagnosed with this feature reduction and classification technique. ANN classifier performed better when combined with the feature reduction methods including GA or PCA over the SVM classifier when combined with GA or PCA. The proposed t-SNE+SOM method classified all the arrhythmia classes at approximately 100%, except few SVE and PVC beats, based on noisy, standard ECG signals with filters and with standard ECG signals without filter. Therefore, it indicated the superiority over the existing methods. GA+SVM was weaker than GA+ANN for differentiating of atrial beats but its results were not of less value and other sensitivity values were in par with GA+ANN.

5.6.1.2 Specificity

The specificity results are provided for all the different classification methods in the tables below. It evaluates which classification technique performs better when compared to each other. The specificity results are importance because it finds the ratio of properly diagnosed healthy people with no condition from a pool of test patients who are healthy. This is essential to the overall structure of the classification scheme as it is properly diagnosed the healthy from the people with diseased heart.

Table 5.7. Arrhythmia classification results for specificity using GA-ANN

Method	**Specificity %**										
GA-ANN	APC	AA	NP	SVE	PVC	RPV	FS	AE	N	LB	RB
Standard MIT-BIH and Haar filter	99.9	100	100	100	100	100	99.8	100	100	100	100
With noise and Haar filter	99.7	100	100	100	100	100	99.5	100	100	100	100
Standard MIT-BIH and FIR filter	99.9	100	100	100	100	100	99.8	100	100	100	100
With noise and FIR filter	99.7	100	100	100	100	100	99.5	100	100	100	100
Standard MIT-BIH without filter	99.1	99.8	100	100	99.4	100	99	99.2	100	100	100

Table 5.8. Arrhythmia classification results for specificity using GA-SVM

Method	**Specificity %**										
GA-SVM	APC	AA	NP	SVE	PVC	RPV	FS	AE	N	LB	RB
Standard MIT-BIH and Haar filter	99.5	98.7	100	100	100	100	100	99.8	100	100	100
With noise and Haar filter	99.2	98.3	100	100	99.8	100	100	99	100	100	100
Standard MIT-BIH and FIR filter	99.5	98.7	100	100	99.9	100	100	100	100	100	100
With noise and FIR filter	99.3	98.3	100	100	99.8	100	100	99	100	100	100
Standard MIT-BIH without filter	99.1	97.8	100	100	99.5	99.4	100	98	100	100	99.5

Table 5.9. Arrhythmia classification results for specificity using PCA-ANN

Method	**Specificity %**										
PCA-ANN	APC	AA	NP	SVE	PVC	RPV	FS	AE	N	LB	RB
Standard MIT-BIH and Haar filter	99.9	100	100	99.2	100	100	100	99.8	100	100	100
With noise and Haar filter	99.7	100	100	99	100	100	100	99.7	100	100	100
Standard MIT-BIH and FIR filter	99.9	100	100	99.2	100	100	100	99.8	100	100	100
With noise and FIR filter	99.7	100	100	99	100	100	100	99.6	100	100	100
Standard MIT-BIH without filter	99.6	99.9	99.9	98.9	99.8	99.9	99.9	99.4	100	99.8	99.9

Table 5.10. Arrhythmia classification results for specificity using PCA-SVM

Method	**Specificity %**										
PCA-SVM	APC	AA	NP	SVE	PVC	RPV	FS	AE	N	LB	RB
Standard MIT-BIH and Haar filter	99.7	99.9	99.8	99.9	99.6	99.8	99.7	99.7	99.9	99.3	99.8
With noise and Haar filter	99.2	98.7	99.3	99.1	99.2	98.5	99.2	98.9	99.2	98.8	99.5
Standard MIT-BIH and FIR filter	99.6	99.8	99.6	99.9	99.6	99.8	99.6	99.8	99.9	99.3	99.8
With noise and FIR filter	99	98.8	99.2	98.9	98.9	98.5	99	98.9	99.1	98.5	99.4
Standard MIT-BIH without filter	98.3	97.8	98.5	98	99.4	97.8	98.9	98.2	99	98.3	99.2

Table 5.11. Arrhythmia classification results for specificity using t-SNE-SOM

Method	**Specificity %**										
t-SNE-SOM	APC	AA	NP	SVE	PVC	RPV	FS	AE	N	LB	RB
Standard MIT-BIH and Haar filter	99.8	100	100	100	100	100	100	100	100	100	100
With noise and Haar filter	99.6	100	100	100	100	100	100	100	100	100	100
Standard MIT-BIH and FIR filter	99.8	100	100	100	100	100	100	100	100	100	100
With noise and FIR filter	99.5	100	100	100	100	100	100	100	100	100	100
Standard MIT-BIH without filter	99.3	100	100	100	100	100	99	99.3	100	100	100

From specificity results, it can be clearly observed that the proposed t-SNE-SOM classifier performed extraordinarily well with the specificity value of about 100 % for every class of arrhythmia, except the APC beats the specificity value was about 99.8 %, with noise added to the signals, without filter and with filters. This clearly states its supremacy in detecting the healthy individuals in the pool of

test patients. PCA-ANN and GA-ANN based classifiers also achieved high degree of performance whereas the performance of PCA and GA reduced when combined with SVM classifier.

5.6.1.3 *Accuracy*

Accuracy measures the feature reduction and classifier performance and detects accuracy of the arrhythmia class that were precisely identified. In fact, it provides the ratio of the heart beats that were correctly or properly detected out of the total number of beats.

Table 5.12. Arrhythmia classification results for accuracy using GA-ANN

Method	**Accuracy %**										
GA-ANN	APC	AA	NP	SVE	PVC	RPV	FS	AE	N	LB	RB
Standard MIT-BIH and Haar filter	99.7	100	100	100	100	99.9	100	99.9	100	100	100
With noise and Haar filter	99.8	100	100	100	100	99.8	99.7	99.2	100	100	100
Standard MIT-BIH and FIR filter	99.7	100	100	100	100	99.9	100	99.9	100	100	100
With noise and FIR filter	99.8	100	100	100	100	99.7	99.7	99.1	100	100	100
Standard MIT-BIH without filter	99.5	100	100	99.8	100	98.8	99.6	99.8	100	100	100

Table 5.13. Arrhythmia classification results for accuracy using GA-SVM

Method	**Accuracy %**										
GA-SVM	APC	AA	NP	SVE	PVC	RPV	FS	AE	N	LB	RB
Standard MIT-BIH and Haar filter	99.8	100	100	100	99.8	100	100	99.5	100	100	100
With noise and Haar filter	99.7	100	100	100	99.3	100	99.7	99.3	100	100	100
Standard MIT-BIH and FIR filter	99.8	100	100	100	99.8	100	100	99.5	100	100	100
With noise and FIR filter	99.6	100	99.4	100	99.3	100	99.6	99.4	100	100	100
Standard MIT-BIH without filter	99.6	97.6	99.3	100	99.2	100	98.9	98.5	100	98.7	97.5

Table 5.14. Arrhythmia classification results for accuracy using PCA-ANN

Method	**Accuracy %**										
PCA-ANN	APC	AA	NP	SVE	PVC	RPV	FS	AE	N	LB	RB
Standard MIT-BIH and Haar filter	99.7	99.8	100	100	99.9	100	100	100	100	100	100
With noise and Haar filter	99.2	99.5	100	100	99.6	100	100	100	100	100	100
Standard MIT-BIH and FIR filter	99.7	99.8	100	100	99.9	100	100	100	100	100	100
With noise and FIR filter	99.2	99.5	100	100	99.6	100	100	100	100	100	100
Standard MIT-BIH without filter	99.2	99.2	100	99.6	99.5	99.7	100	100	100	99.5	99.6

Table 5.15. Arrhythmia classification results for accuracy using PCA-SVM

Method	**Accuracy %**										
PCA-SVM	APC	AA	NP	SVE	PVC	RPV	FS	AE	N	LB	RB
Standard MIT-BIH and Haar filter	99.8	94.1	92	99.9	99.2	99.4	99	90.5	99.9	99.7	99.8
With noise and Haar filter	98.4	92.1	90	98.3	98.6	98.4	98.3	89.5	99.6	99.3	98.4
Standard MIT-BIH and FIR filter	99.7	93.7	92	99.9	99.1	98.9	99	90.1	99.9	99.7	99.7
With noise and FIR filter	98.4	92.1	90	98	98.4	98.4	98.3	81.1	99.6	99	98
Standard MIT-BIH without filter	97.9	92	89.2	97.7	97.3	97.5	98	78	99.2	98.7	97.8

Table 5.16. Arrhythmia classification results for accuracy using t-SNE-SOM

Method	**Accuracy %**										
t-SNE-SOM	APC	AA	NP	SVE	PVC	RPV	FS	AE	N	LB	RB
Standard MIT-BIH and Haar filter	99.9	100	100	99.7	100	100	100	99.8	100	100	100
With noise and Haar filter	99.8	100	100	99.6	100	100	100	99.7	100	100	100
Standard MIT-BIH and FIR filter	99.9	100	100	99.7	100	100	100	99.7	100	100	100
With noise and FIR filter	99.8	100	100	99.5	100	100	100	99.7	100	100	100
Standard MIT-BIH without filter	99.7	99.9	99.9	99.7	99.8	99.9	99.8	99.6	99.9	99.8	99.8

From sensitivity, specificity and accuracy results, it can be observed that overall the methods discussed in this work provided less performance than other combination approaches whether with noise added to the signal or without noise. ANN combined with the feature reduction methods including GA or PCA performed considerably accurate, classifying the arrhythmic heart beats and providing approximately 99% accuracy in most of the arrhythmia classes across all the evaluation methods with noise, without noise and without both FIR and Haar filters. SVM combined with GA achieved reduced performance than GA-ANN method, as it struggled to provide the consistency over all the classes of arrhythmia such as with the sensitivity results. It also fails in the detection of the APC, AA. Our proposed t-SNE+SOM classification method achieved consistent performance throughout the evaluation of parameters and its sensitivity, specificity and accuracy values were approximately 99.8 % for all the classes of arrhythmia when tested with standard ECG signals, noisy ECG signals with filters and even with standard ECG signals without filter. That indicates its superiority over the existing ECG classification and detection techniques. Usually FIR and Haar filters achieve the same results. However, the Haar filter occasionally provided improvement in classification performance than FIR filter. Moreover, it can be concluded that feature

reduction/selection methods improve classification performance, especially our proposed method t-SNE-SOM. Therefore, the selection of significant features plays a vital role in the classification, particularly when the ECG data is noisy.

5.6.2 Experiment results on Shimmer3 dataset

Shimmer3 ECG dataset contains all arrhythmia types that reported in the MIT-BIH Arrhythmia database except bundle branch block (BBB) rhythms, hence, nine types of arrhythmia have been classified using Shimmer3 ECG dataset as represented below. The Harr filter providing superior results over the FIR filter so was selected to remove noise from the Shimmer3 dataset. As the Shimmer3 ECG dataset was collected based on wearable ECG sensor/mobile environment, we did not add noise to the ECG signals.

Overall testing and validation results of the proposed algorithm are illustrated in Table 5.17 and Table 5.18. The proposed arrhythmia classification and detection results were compared with four commonly used approaches using MIT-BIH Arrhythmia and Shimmer3 ECG dataset.

Table 5.17. Overall classification performance using Shimmer3 dataset

Method	Se%	Sp%	Ac%
GA-ANN using Shimmer3 and Haar filter	99.82	99.53	99.20
GA-ANN using Shimmer3 without filter	99.42	99.36	99
GA-SVM using Shimmer3 and Haar filter	98.67	98.44	97.68
GA-SVM using Shimmer3 without filter	97.23	96.37	93.50
PCA-ANN using Shimmer3 and Haar filter	99.50	99.39	99.13
PCA-ANN using Shimmer3 without filter	99.21	99	98.93
PCA-SVM using Shimmer3 and Haar filter	90.56	98.77	90
PCA-SVM using Shimmer3 without filter	84.90	95.99	86.94
t-SNE-SOM using Shimmer3 and Haar filter	99.83	99.62	99.50
t-SNE-SOM using Shimmer3 without filter	99.66	99.55	99.10

It can be observed from Table 5.17, that the ANN classifier achieved a better performance than the SVM classifier when combined with GA or PCA feature reduction methods with filter or without filter. The proposed t-SNE-SOM classifier achieved a higher degree of sensitivity, specificity and accuracy than existing detection and classification approaches for every class of arrhythmia with

noisy or less noisy ECG signals. This clearly shows its superiority in classification of the healthy individuals in the pool of test patients.

Table 5.18. Overall classification performance using MIT-BIH Arrhythmia database

Method	Se%	Sp%	Ac%
GA-ANN using MIT-BIH with noise and Haar filter	99.73	99.92	99.86
GA-ANN using standard MIT-BIH without filter	99.55	99.68	99.77
GA-SVM using MIT-BIH with noise and Haar filter	99.52	99.66	99.81
GA-SVM using standard MIT-BIH without filter	98.18	99.39	99
PCA-ANN using MIT-BIH with noise and Haar filter	99.71	99.85	99.84
PCA-ANN using standard MIT-BIH without filter	99.55	99.72	99.66
PCA-SVM using MIT-BIH with noise and Haar filter	93.34	99	96.44
PCA-SVM using standard MIT-BIH without filter	89.66	98.48	94.84
t-SNE-SOM using MIT-BIH with noise and Haar filter	99.95	99.96	99.91
t-SNE-SOM using standard MIT-BIH without filter	99.68	99.78	99.80

Table 5.17 and Table 5.18 illustrate the arrhythmia classification approach presented here provided high level of accuracy, sensitivity and specificity to detect and classify arrhythmias based on MIT-BIH Arrhythmia and Shimmer3 ECG datasets with the presence of noise or with less noise.

5.7 Discussion

An automated method that can accurately detect and classify cardiac arrhythmias has been advanced. The primary challenge in the automated classification of the ECG data arises from the notable intra-class variations in ECG data. The inter-person variation can cause a bigger challenge due to the inconsistency in classification performance between the class-oriented evaluation and the subject-oriented evaluation. The existence of inter-person variations in ECG is further confirmed by the fact that individual characteristic information carried by ECG data can even be employed for human identification (Elhaj et al., 2016; Luz et al., 2016).

The construction of subject-customised classification models, to observe the inter-person variations are made up of two categories, general models and specific models, which represent the data of the general population and the exact aspects of a subject, respectively. These models are implemented to complement each other, allowing personalized ECG analysis.

Both the statistical and heuristic classification models that are commonly used to evaluate the effect of those models on the results were selected and compared to our novel model. The ECG data from both the MIT-BIH Arrhythmia and the Shimmer3 ECG databases were used to train the classifier models and tested for the evaluation parameters in the detection of cardiac arrhythmias. The feature selection/reduction process and the classifier methods combined to present the results of the classification and the performance of each classifier for the ECG signals with noise removed and with noise introduced in the system. Noise removal provides improvement in classification performance as illustrated in Table 5.17 and Table 5.18. Filters were deployed to remove the noise from the signals and the performance of the classifier was analysed. Also, the raw signal was analysed with the inherent noise in the signal and the performance was evaluated. The efficiency of the classifier with all the parameters with noise, without noise, with filtering, and without filters was carefully studied and the results were evaluated and the findings were presented.

The utility of the GA feature selection/optimization depends on the classifier and dataset. We have found that GA provides a powerful searching capability in high-dimensional feature spaces. The results of the GA combined with classifier methods ANN and SVM supports our discussion. The performance of ANN classifier in general was better when combined with GA or PCA than the SVM classifier under all the testing parameters. However, the classification accuracy suffered a bit with noise introduced and without any filter used in the GA-ANN model. PCA-SVM model provided less performance than other combination approaches whether with noise was added to the signal or without noise. It also fails in the detection of the atrial beats. This is partly because the classifier depends on how the features are scaled. Also, SVM is not efficient with a large number of features compared to the training samples. This is clear when looking at the performance of the PCA-SVM classifier for accuracy and sensitivity results.

The proposed t-SNE-SOM classifier presented in this study, provides a higher level of accuracy, sensitivity, specificity than existing detection and classification approaches for every class of arrhythmia with noisy or less noisy ECG signals. This clearly demonstrates its superiority in the classification of the many types of arrhythmia in the pool of test patients.

5.8 Conclusion

In this work, a novel ECG classification and detection approach were proposed. The t-SNE+SOM hybrid resulted in improved sensitivity, specificity and accuracy compared to the most widely used models in the presence of noise and with less noise. The t-SNE+SOM model provides a better, more accurate identification for presence of arrhythmias from wearable ECG recordings/mobile environment and standard environment leading to more timely diagnosis and treatment outcomes.

The t-SNE improved the diagnostic accuracy by ignoring redundant and noisy features to determine the most significant features. Our results indicate that the SOM has the ability to self-learn, organise the dataset, and detect possible interactions by the predictor variables. For all datasets and classifiers that were evaluated, the t-SNE-SOM approach provided improvements in the classification accuracy, sensitivity and specificity even with noisy data. One of the reasons behind the successful performance of the t-SNE-SOM model is its capability to integrate various optimal solutions given by the t-SNE method to enhance the generality of the final solution. Furthermore, it can be concluded that feature reduction/selection methods improve classification performance, especially our proposed method t-SNE, even the ECG signals have noise without applying de-noising process. Therefore, selection of significant features plays a vital role in the classification, particularly when the ECG data is noisy.

CHAPTER 6

6 Liminations and Future Work

In this thesis, we attempted to address some problems that hinder health care monitoring system harnessing the power of mobile devices such as wearable ECG sensors and smartphones, especially for remote cardiovascular monitoring systems. In this chapter, the results of the various experiments are summarised and related back to the research questions. Also, we summarise the limitations of the current research and the ideas for extending the proposed techniques and various possible applications.

6.1 Work Limitations and Suggested Future Work

The experiments presented in this thesis produced a solution for remote monitoring of cardiovascular patients utilizing the power of portable computational platform, wearable ECG sensors and new analysis techniques. The telecardiology environment demonstrated within this study supports the assertion that remote monitoring can save lives of cardiovascular patient with faster solutions for transmission, power saving, forecasting and diagnosis. Nevertheless, there is a room for enhancement.

Investigation on even simpler, efficient and faster ECG reduction, transmission and power saving for battery-driven devices with innovative lossy ECG data reduction/compression methods is required. The current study provides a compression ratio of 5 (optimal case) and maintains all diagnostic features with very good ECG signal quality. Also, the compression ratio could be increased up to 10 and still achieve good ECG signal quality if RR interval data was used. A study on innovative ECG data reduction/compression method with higher compression ratios that can implemented on wearable ECG sensors is needed.

The proposed methods presented in this thesis were mainly for standard ECG data (MIT-BIH Arrhythmia database and wearable ECG sensor dataset (Shimmer3 ECG dataset). Therefore, an investigation on advanced ECG reduction, forecasting and diagnosis techniques suitable for other ECG devices such as implantable devices needs to be performed.

The forecasting accuracy was assessed against an often limited dataset of ECG signals that provided 97 % of accuracy over 3 minutes. Also, the online forecasting was tested based on only a few volunteers for 30 minutes. The forecasting methods need to be validated on a larger dataset of ECG signals and shorter recording time such as 20 seconds or one minute.

For PVC detection, RR data for three minutes was used to reliably detect PVC beats from non-PVC beats using a simple and fast approach within the constraints of continuous remote patient monitoring. Also, PVC beats were detected from non-PVC beats using an intelligent method in a very short time period of a few seconds. An investigation using RR data to detect PVC beats using shorter recording time is required. Using a Count data model for 30 seconds or one minute to predict PVC beats can be an option. Moreover, the PVC detection method in a real mobile platform (ECG wearable sensor and smartphone devices) based on few volunteers for 30 minutes was implemented and tested. A study implementing our detection techniques but using only a wearable ECG sensor with more volunteers and time with cardiovascular disease and arrhythmias needs to be achieved.

For automated arrhythmia detection and classification, the new hybrid intelligent method was implemented, which resulted in improved sensitivity, specificity and accuracy compared to the most widely used models in the presence of noise, using a PC device. Further research implementing the hybrid methods with a smartphone and measuring power consumption for each method to identify which method is suitable for real-time cardio monitoring system is required. The intelligent methods require complex computational processes and consume more power. A simple and fast method that requires minimal computational resources and which may be implemented with a wearable ECG sensor node needs to be developed. Using QRS complex features and P and T morphology and time-domain statistical approaches such as template matching with knowledge-based rules may be an option.

6.2 Summary

Improvements in wearable sensor devices in recent years make it possible to constantly monitor physiological parameters such as electrocardiograph (ECG) signals for long periods. Remote patient monitoring with wearable sensors has an important role to play in health care, particularly given the prevalence of cardiovascular diseases (CVDs), a prominent cause of death world-wide.

The analysis of ECG features from real time ECG signals generated from wearable sensors provides unique challenges. Sensors and mobile devices that receive and process the signals have limited power, storage and processing capacity. ECG sensors generate large streams of data that easily exhaust storage of mobile devices and need high bandwidth capacity for transmission. Consequently, algorithms that process ECG signals need to operate very quickly, use minimal storage resources and accurately detect abnormalities so that alarms can be raised. This is an emerging field and few algorithms that operate within the constraints of wearable sensor networks have been developed to date.

This research presented four techniques that enable ECG signals to be processed within the limitations of mobile devices. The first technique is a new real time ECG data reduction algorithm that detects and transmits only those key points on an ECG stream that are critical for the generation of accurate ECG features. Reducing the amount of ECG data transmitted without compromising clinical effectiveness markedly represents the first contribution. The second contribution involved using data transmitted to make forecasts of data characteristics in the near future, enabling algorithms that detect anomalies to operate on predicted data. The second technique accurately predicted the five-minute heart rate variability measure using only three minutes of data with an algorithm that executes in real time using minimal computational resources. The third contribution advanced approaches that predicted heart conditions using predictive analytics adapted for low resource computing. A real-time recognition system that has been applied to diagnose life-threatening heart diseases such as Premature Ventricular Contraction is advanced. A classification algorithm to enhance the performance of automated ECG classification with special focus in determining arrhythmic heart beats based on noisy ECG signals was also described.

References

Abenstein, J. P., & Tompkins, W. J. (1982). A new data-reduction algorithm for real-time ECG analysis. *IEEE Transactions on Biomedical Engineering,* (1), 43-48.

Acır, N. (2006). A support vector machine classifier algorithm based on a perturbation method and its application to ECG beat recognition systems. *Expert Systems with Applications, 31*(1), 150-158.

Adnan, M. N., & Islam, M. Z. (2016). Optimizing the number of trees in a decision forest to discover a subforest with high ensemble accuracy using a genetic algorithm. *Knowledge-Based Systems, 110*, 86-97.

Afkhami, R. G., Azarnia, G., & Tinati, M. A. (2016). Cardiac arrhythmia classification using statistical and mixture modeling features of ECG signals. *Pattern Recognition Letters, 70*, 45-51.

Afonso, V., Tompkins, W., Nguyen, T., Michler, K., & Luo, S. (1996). Comparing stress ECG enhancement algorithms. *IEEE Engineering in Medicine and Biology Magazine, 15*(3), 37-44.

Agrafioti, F., & Hatzinakos, D. (2009). ECG biometric analysis in cardiac irregularity conditions. *Signal, Image and Video Processing, 3*(4), 329-343.

Ahmad, A. M., Khan, G. M., & Mahmud, S. A. (2013). Classification of arrhythmia types using cartesian genetic programming evolved artificial neural networks. *Proceedings on the International Conference on Engineering Applications of Neural Networks* (pp. 282-291), Springer.

Ahonen, L., Cowley, B., Torniainen, J., Ukkonen, A., Vihavainen, A., & Puolamäki, K. (2016). Cognitive collaboration found in cardiac physiology: Study in classroom environment. *PLOS ONE 11*(7). doi:10.1371/journal.pone.0159178

Aksoy, S., & Haralick, R. M. (2001). Feature normalization and likelihood-based similarity measures for image retrieval. *Pattern Recognition Letters, 22*(5), 563-582.

Al Rahhal, M. M., Bazi, Y., Al Hichri, H., Alajlan, N., Melgani, F., & Yager, R. R. (2016). Deep learning approach for active classification of electrocardiogram signals. *Information Sciences, 345*, 340-354.

Algra, A., Tijssen, J. G., Roelandt, J. R., Pool, J., & Lubsen, J. (1993). Heart rate variability from 24-hour electrocardiography and the 2-year risk for sudden death. *Circulation, 88*(1), 180-185.

Allami, R., Stranieri, A., Balasubramanian, V., & Jelinek, H. F. (2016a). ECG reduction for wearable sensor. *Proceedings on the 12th International Conference on Signal-Image Technology & Internet-Based Systems (SITIS)* (pp. 520-525). Naples, Italy, IEEE.

Allami, R., Stranieri, A., Balasubramanian, V., & Jelinek, H. F. (2016b). A genetic algorithm-neural network wrapper approach for bundle branch block detection. *Proceedings on the Computing in Cardiology Conference* (pp. 461-464). Vancouver, Canada, IEEE.

Allami, R., Stranieri, A., Balasubramanian, V., & Jelinek, H. F. (2017). A count data model for heart rate variability forecasting and premature ventricular contraction detection. *Signal, Image and Video Processing, 11*, 1427-1435.

ANSI-AAMI. (1998). Testing and reporting performance results of cardiac rhythm and ST segment measurement algorithms. *Association for the Advancement of Medical Instrumentation, Arlington, VA.*

Antônio, A., Cardoso, M., & De Abreu, L. (2014). Fractal dynamics of heart rate variability: A study in healthy subjects. *Journal of Cardiovascular Disease, 2*(3), 137-142.

Arif, M., & Akram, M. U. (2010). Pruned fuzzy K-nearest neighbor classifier for beat classification. *Journal of Biomedical Science and Engineering, 3*(04). doi:10.4236/jbise.2010.34053

Ashkenazy, Y., Lewkowicz, M., Levitan, J., Moelgaard, H., Thomsen, P. B., & Saermark, K. (1998). Discrimination of the healthy and sick cardiac autonomic nervous system by a new wavelet analysis of heartbeat intervals. *Fractals, 6*(03), 197-203.

Asl, B. M., Setarehdan, S. K., & Mohebbi, M. (2008). Support vector machine-based arrhythmia classification using reduced features of heart rate variability signal. *Artificial Intelligence in Medicine, 44*(1), 51-64.

Australian Institute of Health and Welfare. (2015). Surveillance and monitoring of chronic diseases and associated risk factors. Retrieved from http://www.aihw.gov.au/WorkArea/DownloadAsset.aspx?id=6442459405

Baig, M. M., Gholam, h., Hamid, & Connolly, M. J. (2015). Mobile healthcare applications: System design review, critical issues and challenges. *Australasian Physical & Engineering Sciences in Medicine, 38*(1), 23-38.

Bakhtiari, A. S., & Bouguila, N. (2014). A variational Bayes model for count data learning and classification. *Engineering Applications of Artificial Intelligence, 35*, 176-186.

Balasubramanian, V., & Stranieri, A. (2014). Performance evaluation of the dependable properties of a body area wireless sensor network. *Proceedings on the International Conference on Optimization, Reliabilty, and Information Technology (ICROIT)* (pp. 229-234), IEEE.

Baraniuk, R. G. (2007). Compressive sensing [lecture notes]. *IEEE Signal Processing Magazine, 24*(4), 118-121.

Bárdossy, A., Blinowska, A., Kuzmicz, W., Ollitrault, J., Lewandowski, M., Przybylski, A., & Jaworski, Z. (2014). Fuzzy logic-based diagnostic algorithm for implantable cardioverter defibrillators. *Artificial Intelligence in Medicine, 60*(2), 113-121.

Bauer, A., Malik, M., Schmidt, G., Barthel, P., Bonnemeier, H., Cygankiewicz, I., . . . Oto, A. (2008). Heart rate turbulence: Standards of measurement, physiological interpretation, and clinical use: International society for holter and noninvasive electrophysiology consensus. *Journal of the American College of Cardiology, 52*(17), 1353-1365.

Bazi, Y., Hichri, H., Alajlan, N., & Ammour, N. (2013). Premature ventricular contraction arrhythmia detection and classification with Gaussian process and S transform. *Proceedings on the Fifth International Conference on Computational Intelligence, Communication Systems and Networks (CICSYN)* (pp. 36-41), IEEE.

Beetham, K. S. (2015). *Exercise and lifestyle intervention and high intensity interval training in patients with chronic kidney disease.* (PhD Thesis), The University of Queensland, Australia.

Beg, A., Islam, M. Z., & Estivill-Castro, V. (2016). Genetic algorithm with healthy population and multiple streams sharing information for clustering. *Knowledge-Based Systems, 114*, 61-78.

Billman, G. E. (2013). The LF/HF ratio does not accurately measure cardiac sympatho-vagal balance. *Frontiers in Physiology 4*. doi:10.3389/fphys.2013.00026

Bonanno, F., Capizzi, G., Sciuto, G. L., Napoli, C., Pappalardo, G., & Tramontana, E. (2014). A cascade neural network architecture investigating surface plasmon polaritons propagation for thin metals in openmp. *Proceedings on the International Conference on Artificial Intelligence and Soft Computing* (pp. 22-33). Zakopane, Poland, Springer.

Brisinda, D., Venuti, A., Iantorno, E., Efremov, K., & Cataldi, C. (2014). Discriminant analysis of heart rate variability after electrical cardioversion predicts atrial fibrillation recurrence. *International Journal of Clinical Cardiology, 1*(010).

Cameron, A. C., & Trivedi, P. K. (2013). *Regression analysis of count data* (Vol. 53): Cambridge University Press.

Cárdenas-Barrera, J. L., & Lorenzo-Ginori, J. V. (1999). Mean-shape vector quantizer for ECG signal compression. *IEEE Transactions on Biomedical Engineering, 46*(1), 62-70.

Cardoso, M. A., Dos Santos, M. A., Abreu, L. C. d., Fontes, A. M. G., Silva, A. G. d., Ogata, C. M., . . . Cano, A. d. S. (2014). Fractal scaling exponents of heart rate variability association with linear indices and Poincare plot. *Experimental and Clinical Cardiology*, 2444-2456.

Carvalho, J., Rocha, A., dos Santos, I., Itiki, C., Junqueira, L., & Nascimento, F. (2003). Study on the optimal order for the auto-regressive time-frequency analysis of heart rate variability. *Proceedings on the 25th Annual International Conference of Engineering in Medicine and Biology Society* (pp. 2621-2624). Cancun, Mexico, IEEE.

Castells, F., Laguna, P., Sörnmo, L., Bollmann, A., & Roig, J. M. (2007). Principal component analysis in ECG signal processing. *EURASIP Journal on Applied Signal Processing,* (1). doi:10.1155/2007/74580

Censi, F., Calcagnini, G., Triventi, M., Mattei, E., Bartolini, P., Corazza, I., & Boriani, G. (2009). Effect of high-pass filtering on ECG signal on the analysis of patients prone to atrial fibrillation. *Annali Dell'istituto Superiore Di Sanita, 45*(4), 427-431.

Ceylan, R., & Özbay, Y. (2007). Comparison of FCM, PCA and WT techniques for classification ECG arrhythmias using artificial neural network. *Expert Systems with Applications, 33*(2), 286-295.

Chang, G. H., & Lin, K. P. (2005). Comparison of heart rate variability measured by ECG in different signal lengths. *Journal of Medical and Biological Engineering, 25*(2), 67-71.

Chen, W., Hsieh, L., & Yuan, S. (2004). High performance data compression method with pattern matching for biomedical ECG and arterial pulse waveforms. *Computer Methods and Programs in Biomedicine, 74*(1), 11-27.

Chen, X., Yao, R., Yin, G., & Li, J. (2017). Consecutive ultra-short-term heart rate variability to track dynamic changes in autonomic nervous system during and after exercise. *Physiological Measurement, 38*(7). doi:https://doi.org/10.1088/1361-6579/aa52b3

ChuDuc, H., NguyenPhan, K., & NguyenViet, D. (2013). A review of heart rate variability and its applications. *APCBEE Procedia, 7*, 80-85.

Cox, J., Nolle, F., Fozzard, H., & Oliver, G. (1968). AZTEC, a preprocessing program for real-time ECG rhythm analysis. *IEEE Transactions on Biomedical Engineering, 2*(BME-15), 128-129.

Craven, D., McGinley, B., Kilmartin, L., Glavin, M., & Jones, E. (2015). Compressed sensing for bioelectric signals: A review. *IEEE Journal of Biomedical and Health Informatics, 19*(2), 529-540.

Cuesta, P., Lado, M. J., Vila, X. A., & Alonso, R. (2014). Detection of premature ventricular contractions using the RR-interval signal: A simple algorithm for mobile devices. *Technology and Health Care, 22*(4), 651-656.

Da Poian, G., Brandalise, D., Bernardini, R., & Rinaldo, R. (2016). Energy and quality evaluation for compressive sensing of fetal electrocardiogram signals. *Sensors, 17*(1). doi:10.3390/s17010009

Doret, M., Spilka, J., Chudáček, V., Gonçalves, P., & Abry, P. (2015). Fractal analysis and hurst parameter for intrapartum fetal heart rate variability analysis: A versatile alternative to frequency bands and LF/HF ratio. *PlOS ONE, 10*(8). doi:10.1371/journal.pone.0136661

Elgendi, M. (2013). Fast QRS detection with an optimized knowledge-based method: Evaluation on 11 standard ECG databases. *PLOS ONE, 8*(9). doi:10.1371/journal.pone.0073557

Elgendi, M., Eskofier, B., Dokos, S., & Abbott, D. (2014). Revisiting QRS detection methodologies for portable, wearable, battery-operated, and wireless ECG systems. *PLOS ONE, 9*(1). doi:10.1371/journal.pone.0084018

Elhaj, F. A., Salim, N., Harris, A. R., Swee, T. T., & Ahmed, T. (2016). Arrhythmia recognition and classification using combined linear and nonlinear features of ECG signals. *Computer Methods and Programs in Biomedicine, 127*, 52-63.

Elman, J. L. (1990). Finding structure in time. *Cognitive Science, 14*(2), 179-211.

Esco, M., & Flatt, A. (2015). Ultra-short-term heart rate variability indexes at rest and post-exercise in athletes: Evaluating the agreement with accepted recommendations. *Journal of Sports Science and Medicine, 13*, 535-541.

Exarchos, T. P., Tsipouras, M. G., Exarchos, C. P., Papaloukas, C., Fotiadis, D. I., & Michalis, L. K. (2007). A methodology for the automated creation of fuzzy expert systems for ischaemic and arrhythmic beat classification based on a set of rules obtained by a decision tree. *Artificial Intelligence in Medicine, 40*(3), 187-200.

Fang, W., Huang, H., & Tseng, S. (2013). Design of heart rate variability processor for portable 3-lead ECG monitoring system-on-chip. *Expert Systems with Applications, 40*(5), 1491-1504.

Francescon, R., Hooshmand, M., Gadaleta, M., Grisan, E., Yoon, S. K., & Rossi, M. (2015). Toward lightweight biometric signal processing for wearable devices. *Proceedings on the 37th Annual International Conference of the Engineering in Medicine and Biology Society (EMBC)* (pp. 4190-4193). Milan, Italy, IEEE.

Gacek, A., & Pedrycz, W. (2011). *ECG signal processing, classification and interpretation: A comprehensive framework of computational intelligence*: Springer Science & Business Media.

Gertsch, M. (2008). *The ECG manual: An evidence-based approach*: Springer Science & Business Media.

Glass, L., Lerma, C., & Shrier, A. (2011). New methods for the analysis of heartbeat behavior in risk stratification. *Frontiers in Physiology, 2*. doi:10.3389/fphys.2011.00088

Goldberger, A. L., Amaral, L. A., Glass, L., Hausdorff, J. M., Ivanov, P. C., Mark, R. G., . . . Stanley, H. E. (2000). Physiobank, physiotoolkit, and physionet components of a new research resource for complex physiologic signals. *Circulation, 101*(23), 215-220.

Goldberger, A. L., Goldberger, Z. D., & Shvilkin, A. (2017). *Clinical electrocardiography: A simplified approach*: Elsevier Health Sciences.

Gough, C. (2011). *The digitisation of ECG filtering for wireless medical sensor networks*: VDM Verlaq Dr. Muller

Gradl, S., Kugler, P., Lohmüller, C., & Eskofier, B. (2012). Real-time ECG monitoring and arrhythmia detection using Android-based mobile devices. *Proceedings on the Annual International Conference of Engineering in Medicine and Biology Society (EMBC)* (pp. 2452-2455), IEEE.

Gregg, R. E., Zhou, S. H., Lindauer, J. M., Helfenbein, E. D., & Giuliano, K. K. (2008). What is inside the electrocardiograph? *Journal of Electrocardiology, 41*(1), 8-14.

Grosan, C., & Abraham, A. (2011). *Intelligent systems—A modern approach*: Springer, Berlin.

Guzzetti, S., Borroni, E., Garbelli, P. E., Ceriani, E., Della Bella, P., Montano, N., . . . Porta, A. (2005). Symbolic dynamics of heart rate variability. *Circulation, 112*(4), 465-470.

Habib, S. H., Biswas, K. B., Akter, S., Saha, S., & Ali, L. (2010). Cost-effectiveness analysis of medical intervention in patients with early detection of diabetic foot in a tertiary care hospital in Bangladesh. *Journal of Diabetes and its Complications, 24*(4), 259-264.

Hamine, S., Gerth, G., Emily, Faulx, D., Green, B. B., & Ginsburg, A. S. (2015). Impact of mHealth chronic disease management on treatment adherence and patient outcomes: A systematic review. *Journal of Medical Internet Research, 17*(2). doi:10.2196/jmir.3951

Haseena, H. H., Mathew, A. T., & Paul, J. K. (2011). Fuzzy clustered probabilistic and multi layered feed forward neural networks for electrocardiogram arrhythmia classification. *Journal of Medical Systems, 35*(2), 179-188.

Hashemi, A., Rahimpour, M., & Merati, M. R. (2015). Dynamic Gaussian filter for muscle noise reduction in ECG signal. *Proceedings on the 23rd Iranian Conference on Electrical Engineering (ICEE)* (pp. 120-124). Tehran, Iran, IEEE.

Hayn, D., Jammerbund, B., & Schreier, G. (2011). ECG quality assessment for patient empowerment in mHealth applications. *Proceedings on the Computing in Cardiology* (pp. 353-356), IEEE.

He, L., Hou, W., Zhen, X., & Peng, C. (2006). Recognition of ECG patterns using artificial neural network. *Proceedings on the Sixth International Conference on Intelligent Systems Design and Applications* (pp. 477-481), IEEE.

Heart Foundation. (2016). Heart disease in Australia. Retrieved from https://www.heartfoundation.org.au/about-us/what-we-do/heart-disease-in-australia

Heldeweg, M. L. A., Liu, N., Koh, Z. X., Fook-Chong, S., Lye, W. K., Harms, M., & Ong, M. E. H. (2016). A novel cardiovascular risk stratification model incorporating ECG and heart rate variability for patients presenting to the emergency department with chest pain. *Critical Care, 20*(1). doi:https://doi.org/10.1186/s13054-016-1367-5

Hinton, G. E., & Roweis, S. T. (2003). Stochastic neighbor embedding. *Proceedings on the Advances in Neural Information Processing Systems* (pp. 857-864).

Holper, L., Seifritz, E., & Scholkmann, F. (2016). Short-term pulse rate variability is better characterized by functional near-infrared spectroscopy than by photoplethysmography. *Journal of Biomedical Optics, 21*(9). doi:10.1117/1.JBO.21.9.091308

Horspool, R. N., & Windels, W. J. (1994). An LZ approach to ECG compression. *Proceedings on the Computer-Based Medical Systems* (pp. 71-76). Winston-Salem, USA, IEEE.

Huang, B. (2004). *Compression ECG signals with feature extraction, classification, and browsability.* (PhD Thesis), University of Manitoba, Canada.

Huang , Y., Huang, C., & Liu, S. (2014). Hybrid intelligent methods for arrhythmia detection and geriatric depression diagnosis. *Applied Soft Computing, 14*, 38-46.

Huikuri, H. V., & Stein, P. K. (2013). Heart rate variability in risk stratification of cardiac patients. *Progress in Cardiovascular Diseases, 56*(2), 153-159.

Hyndman, R. J., & Athanasopoulos, G. (2014). *Forecasting: Principles and practice*: OTexts.

Ibaida, A. (2014). *Secure steganography, compression and diagnoses of electrocardiograms in wireless body sensor networks.* (PhD Thesis), RMIT University, Australia

Ibaida, A., Al-Shammary, D., & Khalil, I. (2014). Cloud enabled fractal based ECG compression in wireless body sensor networks. *Future Generation Computer Systems, 35*, 91-101.

Ince, T., Zabihi, M., Kiranyaz, S., & Gabbouj, M. (2017). Learned vs. hand-designed features for ECG beat classification: A comprehensive study. In H. Eskola, O. Väisänen, J. ViikJari, & J. Hyttinen (Eds.), *EMBEC & NBC 2017* (pp. 551-554): Springer.

Islam, M. Z., Mamun, Q., & Rahman, M. G. (2014). Data cleansing during data collection from wireless sensor networks. *Proceedings on the 12th Australasian Data Mining Conference (AusDM)* (pp. 195- 203). Brisbane, Australia.

Iwasa, A., Hwa, M., Hassankhani, A., Liu, T., & Narayan, S. M. (2005). Abnormal heart rate turbulence predicts the initiation of ventricular arrhythmias. *Pacing and Clinical Electrophysiology, 28*(11), 1189-1197.

Jalal, M. E., Hosseini, M., & Karlsson, S. (2016). Forecasting incoming call volumes in call centers with recurrent neural networks. *Journal of Business Research, 69*(11), 4811-4814.

Jalaleddine, S. M., Hutchens, C. G., Strattan, R. D., & Coberly, W. A. (1990). ECG data compression techniques-a unified approach. *IEEE Transactions on Biomedical Engineering, 37*(4), 329-343.

Jarrin, D. C., McGrath, J. J., Giovanniello, S., Poirier, P., & Lambert, M. (2012). Measurement fidelity of heart rate variability signal processing: The devil is in the details. *International Journal of Psychophysiology, 86*(1), 88-97.

Jelinek, H. F., Adam, M. T., Krones, R., & Cornforth, D. J. (2017). Diagnostic accuracy of random ECG in primary care for early, asymptomatic cardiac autonomic neuropathy. *Journal of Diabetes Science and Technology, 11*(6), 1165–1173.

Jiang, W., & Kong, S. G. (2007). Block-based neural networks for personalized ECG signal classification. *IEEE Transactions on Neural Networks, 18*(6), 1750-1761.

Johnson, A., & Loewy, A. (1990). *Central regulation of autonomic functions*: Oxford University Press.

Jung, R. C., & Tremayne, A. (2011). Useful models for time series of counts or simply wrong ones? *AStA Advances in Statistical Analysis, 95*(1), 59-91.

Kamen, P., & Tonkin, A. M. (1995). Application of the Poincare plot to heart rate variability: A new measure of functional status in heart failure. *Internal Medicine Journal, 25*(1), 18-26.

Kang, J. H., Kim, J. K., Hong, S. H., Lee, C. H., & Choi, B. Y. (2016). Heart rate variability for quantification of autonomic dysfunction in fibromyalgia. *Annals of Rehabilitation Medicine, 40*(2), 301-309.

Khandoker, A. H., Jelinek, H. F., & Palaniswami, M. (2009). Identifying diabetic patients with cardiac autonomic neuropathy by heart rate complexity analysis. *Biomedical Engineering Online, 8*(1). doi:10.1186/1475-925X-8-3

Khandoker, A. H., Karmakar, C., Brennan, M., Palaniswami, M., & Voss, A. (2013). *Poincaré plot methods for heart rate variability analysis*: Springer.

Kim, J., & Mazumder, P. (2017). Energy-efficient hardware architecture of self-organizing map (SOM) for ECG clustering in 65nm cmos. *IEEE Transactions on Circuits and Systems II: Express Briefs, 64*(9), 1097 - 1101.

Kiranyaz, S., Ince, T., Pulkkinen, J., & Gabbouj, M. (2011). Personalized long-term ECG classification: A systematic approach. *Expert Systems with Applications, 38*(4), 3220-3226.

Kleiger, R. E., Miller, J. P., Bigger, J. T., & Moss, A. J. (1987). Decreased heart rate variability and its association with increased mortality after acute myocardial infarction. *The American Journal of Cardiology, 59*(4), 256-262.

Kohonen, T. (1982). Self-organized formation of topologically correct feature maps. *Biological Cybernetics, 43*(1), 59-69.

Kohonen, T. (2001). *Self-organizing maps* (Third ed. Vol. 30): Springer.

Kohonen, T. (2013). Essentials of the self-organizing map. *Neural Networks, 37*, 52-65.

Kolasa, M., Długosz, R., Talaśka, T., & Pedrycz, W. (2017). Efficient methods of initializing neuron weights in self-organizing networks implemented in hardware. *Applied Mathematics and Computation*. doi:https://doi.org/10.1016/j.amc.2017.01.043

Kora, P., & Krishna, K. S. R. (2016a). Bundle block detection using genetic neural network. In S. C. Satapathy, J. K. Mandal, S. K. Udgata, & V. Bhateja (Eds.), *Information systems design and intelligent applications* (pp. 309-317): Springer.

Kora, P., & Krishna, K. S. R. (2016b). Hybrid firefly and particle swarm optimization algorithm for the detection of bundle branch block. *International Journal of the Cardiovascular Academy, 2*(1), 44-48.

Kortman, C. (1967). Redundancy reduction—A practical method of data compression. *Proceedings of the IEEE, 55*(3), 253-263. doi:10.1109/PROC.1967.5479

Kotecha, D., New, G., Flather, M., Eccleston, D., Pepper, J., & Krum, H. (2012). Five-minute heart rate variability can predict obstructive angiographic coronary disease. *Heart, 98*(5), 395-401.

Kranjec, J., Beguš, S., Geršak, G., & Drnovšek, J. (2014). Non-contact heart rate and heart rate variability measurements: A review. *Biomedical Signal Processing and Control, 13*, 102-112.

Krasteva, V., & Jekova, I. (2007). QRS template matching for recognition of ventricular ectopic beats. *Annals of Biomedical Engineering, 35*(12), 2065-2076.

Kurths, J., Voss, A., Saparin, P., Witt, A., Kleiner, H., & Wessel, N. (1995). Quantitative analysis of heart rate variability. *Chaos: An Interdisciplinary Journal of Nonlinear Science, 5*(1), 88-94.

La Rovere, M. T., Bigger, J. T., Marcus, F. I., Mortara, A., Schwartz, P. J., & Investigators, A. (1998). Baroreflex sensitivity and heart-rate variability in prediction of total cardiac mortality after myocardial infarction. *The Lancet, 351*(9101), 478-484.

Lagerholm, M., Peterson, C., Braccini, G., Edenbrandt, L., & Sornmo, L. (2000). Clustering ECG complexes using Hermite functions and self-organizing maps. *IEEE Transactions on Biomedical Engineering, 47*(7), 838-848.

Lahdenoja, O., Hurnanen, T., Iftikhar, Z., Nieminen, S., Knuutila, T., Saraste, A., . . . Pankaala, M. (2017). Atrial fibrillation detection via accelerometer and gyroscope of a smartphone. *IEEE Journal of Biomedical and Health Informatics*. doi:10.1109/JBHI.2017.2688473

Laplante, P. A., & Ovaska, S. J. (2011). *Real-time systems design and analysis: Tools for the practitioner*: John Wiley and Sons.

Lee, H., & Buckley, K. M. (1999). ECG data compression using cut and align beats approach and 2-D transforms. *IEEE Transactions on Biomedical Engineering, 46*(5), 556-564.

Lee, R., Chen, K., Hsiao, C., & Tseng, C. (2007). A mobile care system with alert mechanism. *IEEE Transactions on Information Technology in Biomedicine, 11*(5), 507-517.

Lee, S. (2016). *Framework and algorithms for wearable medical applications.* (PhD Thesis), University of California, Irvine.

Lee, S., Kim, J., & Lee, M. (2011). A real-time ECG data compression and transmission algorithm for an e-health device. *IEEE Transactions on Biomedical Engineering, 58*(9), 2448-2455.

Lee, T., & Chiu, H. (2010). Frequency-domain heart rate variability analysis performed by digital filters. *Proceedings on the Computing in Cardiology* (pp. 589-592). Belfast, UK, IEEE.

Łęski, J. M., & Henzel, N. (2005). ECG baseline wander and powerline interference reduction using nonlinear filter bank. *Signal Processing, 85*(4), 781-793.

Leutheuser, H., Gradl, S., Kugler, P., Anneken, L., Arnold, M., Achenbach, S., & Eskofier, B. M. (2014). Comparison of real-time classification systems for arrhythmia detection on Android-based mobile devices. *Proceedings on the 36th Annual International Conference of the Engineering in Medicine and Biology Society (EMBC)* (pp. 2690-2693). Chicago, USA, IEEE.

Li, P., Liu, C., Wang, X., Zheng, D., Li, Y., & Liu, C. (2014). A low-complexity data-adaptive approach for premature ventricular contraction recognition. *Signal, Image and Video Processing, 8*(1), 111-120.

Littmann, E., & Ritter, H. (1993). Generalization abilities of cascade network architecture. *Proceedings on the Advances in Neural Information Processing Systems* (pp. 188-195). Baltimore,USA

Liu, C., Li, L., Zhao, L., Zheng, D., Li, P., & Liu, C. (2012). A combination method of improved impulse rejection filter and template matching for identification of anomalous intervals in RR sequences. *Journal of Medical and Biological Engineering, 32*(4), 245-249.

Liu, C., Liu, C., Shao, P., Li, L., Sun, X., Wang, X., & Liu, F. (2010). Comparison of different threshold values r for approximate entropy: Application to investigate the heart rate variability between heart failure and healthy control groups. *Physiological Measurement, 32*(2), 167-180.

Loguidice, M. J., Schutt, R. C., Horton, J. W., Minei, J. P., & Keeley, E. C. (2016). Heart rate variability as a predictor of death in burn patients. *Journal of Burn Care & Research, 37*(3), 227-233.

Lou, D., Chen, X., Zhao, Z., Xuan, Y., Xu, Z., Jin, H., . . . Fang, Z. (2013). A wireless health monitoring system based on Android operating system. *IERI Procedia, 4*, 208-215.

Luz, E. J. d. S., Schwartz, W. R., Cámara-Chávez, G., & Menotti, D. (2016). ECG-based heartbeat classification for arrhythmia detection: A survey. *Computer Methods and Programs in Biomedicine, 127*, 144-164.

Lynch, T. J. (1985). *Data compression: Techniques and applications*: Lifetime Learning Publications.

Lynn, P. (1971). Recursive digital filters for biological signals. *Medical and Biological Engineering and Computing, 9*(1), 37-43.

Maaten, L. v. d., & Hinton, G. (2008). Visualizing data using t-SNE. *Journal of Machine Learning Research, 9*, 2579-2605.

Maglaveras, N., Stamkopoulos, T., Diamantaras, K., Pappas, C., & Strintzis, M. (1998). ECG pattern recognition and classification using non-linear transformations and neural networks: A review. *International Journal of Medical Informatics, 52*(1), 191-208.

Maheshwari, A., Norby, F. L., Soliman, E. Z., Adabag, S., Whitsel, E. A., Alonso, A., & Chen, L. Y. (2016). Low heart rate variability in a 2-minute electrocardiogram recording is associated with an increased risk of sudden cardiac death in the general population: The atherosclerosis risk in communities study. *PLOS ONE 11*(8). doi:10.1371/journal.pone.0161648

Maliarsky, E., Avigal, M., & Herman, M. (2014). A neuro-genetic system for cardiac arrhythmia classification. *Proceedings on the 10th International Workshop on Machine Learning and Data Mining in Pattern Recognition* (pp. 343-360). Petersburg, Russia, Springer.

Malliani, A., Lombardi, F., & Pagani, M. (1994). Power spectrum analysis of heart rate variability: A tool to explore neural regulatory mechanisms. *British Heart Journal, 71*(1).

Mamaghanian, H., Khaled, N., Atienza, D., & Vandergheynst, P. (2011). Compressed sensing for real-time energy-efficient ECG compression on wireless body sensor nodes. *IEEE Transactions on Biomedical Engineering, 58*(9), 2456-2466.

Marchal, J., Cumming, S. G., & McIntire, E. J. (2017). Exploiting Poisson additivity to predict fire frequency from maps of fire weather and land cover in boreal forests of Québec, Canada. *Ecography, 40*(1), 200-209.

Mark, R., & Moody, G. (1997). Mit-bih arrhythmia database 1997. *URL* http://ecg. *mit. edu/dbinfo. html*.

Martis, R. J., Acharya, U. R., & Adeli, H. (2014a). Current methods in electrocardiogram characterization. *Computers in Biology and Medicine, 48*, 133-149.

Martis, R. J., Acharya, U. R., & Min, L. C. (2013). ECG beat classification using PCA, LDA, ICA and discrete wavelet transform. *Biomedical Signal Processing and Control, 8*(5), 437-448.

Martis, R. J., Prasad, H., Chakraborty, C., & Ray, A. K. (2014b). The application of genetic algorithm for unsupervised classification of ECG. *Machine Learning in Healthcare Informatics*, 65-80.

Massing, M. W., Simpson, R. J., Rautaharju, P. M., Schreiner, P. J., Crow, R., & Heiss, G. (2006). Usefulness of ventricular premature complexes to predict coronary heart disease events and mortality (from the atherosclerosis risk in communities cohort). *The American Journal of Cardiology, 98*(12), 1609-1612.

mega. (2016). eMotion Faros devices. Retrieved from http://www.megaemg.com/products/faros/

Melgani, F., & Bazi, Y. (2008). Classification of electrocardiogram signals with support vector machines and particle swarm optimization. *IEEE Transactions on Information Technology in Biomedicine, 12*(5), 667-677.

Miličević, G. (2005). Low to high frequency ratio of heart rate variability spectra fails to describe sympatho-vagal balance in cardiac patients. *Collegium Antropologicum, 29*(1), 295-300.

Minutolo, A., Esposito, M., & De Pietro, G. (2011). A mobile reasoning system for supporting the monitoring of chronic diseases. *Proceedings on the 2nd International Conference on Wireless Mobile Communication and Healthcare* (pp. 225-232). Kos Island, Greece, Springer.

Minutolo, A., Sannino, G., Esposito, M., & De Pietro, G. (2010). A rule-based mHealth system for cardiac monitoring. *Proceedings on the Biomedical Engineering and Sciences* (pp. 144-149). Kuala Lumpur, Malaysia, IEEE.

Mitchell, M. (1998). *An introduction to genetic algorithms*: MIT press.

Montesinos-López, O. A., Montesinos-López, A., Crossa, J., Toledo, F. H., Montesinos-López, J. C., Singh, P., . . . Salinas-Ruiz, J. (2017). A Bayesian Poisson-lognormal model for count data for multiple-trait multiple-environment genomic-enabled prediction. *G3: Genes, Genomes, Genetics, 7*(5), 1595-1606.

Moody, G. B., Muldrow, W., & Mark, R. G. (1984). A noise stress test for arrhythmia detectors. *Computers in Cardiology, 11*(3), 381-384.

Moody, G. B., Soroushian, K., & Mark, R. G. (1987). ECG data compression for tapeless ambulatory monitors. *Computers in Cardiology, 14*, 467-470.

Mueller, W. C. (1977). Arrhythmia detection program for an ambulatory ECG monitor. *Biomedical Sciences Instrumentation, 14*, 81-85.

Mukhopadhyay, S., Mitra, S., & Mitra, M. (2012). An ECG signal compression technique using ASCII character encoding. *Measurement, 45*(6), 1651-1660.

Murray, A., Ewing, D., Campbell, I., Neilson, J., & Clarke, B. (1975). RR interval variations in young male diabetics. *British Heart Journal, 37*(8), 882-885.

Nabil, D., & Reguig, F. B. (2015). Ectopic beats detection and correction methods: A review. *Biomedical Signal Processing and Control, 18*, 228-244.

Nadal, J., & Bossan, M. d. C. (1993). Classification of cardiac arrhythmias based on principal component analysis and feedforward neural networks. *Proceedings on the Computers in Cardiology* (pp. 341-344). London, UK, IEEE.

Nguyen, T., Lou, W., Caelli, T., Venkatesh, S., & Phung, D. (2014). Individualized arrhythmia detection with ECG signals from wearable devices. *Proceedings on the International Conference on Data Science and Advanced Analytics (DSAA)* (pp. 570-576). Shanghai, China, IEEE.

Niskanen, J., Tarvainen, M. P., Ranta-Aho, P. O., & Karjalainen, P. A. (2004). Software for advanced HRV analysis. *Computer Methods and Programs in Biomedicine, 76*(1), 73-81.

Nunan, D., Sandercock, G. R., & Brodie, D. A. (2010). A quantitative systematic review of normal values for short-term heart rate variability in healthy adults. *Pacing and Clinical Electrophysiology, 33*(11), 1407-1417.

Nussinovitch, U., Elishkevitz, K. P., Katz, K., Nussinovitch, M., Segev, S., Volovitz, B., & Nussinovitch, N. (2011). Reliability of ultra-short ECG indices for heart rate variability. *Annals of Noninvasive Electrocardiology, 16*(2), 117-122.

Ong, M. E. H., Padmanabhan, P., Chan, Y. H., Lin, Z., Overton, J., Ward, K. R., & Fei, D. (2008). An observational, prospective study exploring the use of heart rate variability as a predictor of clinical outcomes in pre-hospital ambulance patients. *Resuscitation, 78*(3), 289-297.

Oresko , J. J. (2010). *Portable heart attack warning system by monitoring the ST segment via smartphone electrocardiogram processing.* (Master Thesis), University of Pittsburgh.

Oresko, J. J., Jin, Z., Cheng, J., Huang, S., Sun, Y., Duschl, H., & Cheng, A. C. (2010). A wearable smartphone-based platform for real-time cardiovascular disease detection via electrocardiogram processing. *IEEE Transactions on Information Technology in Biomedicine, 14*(3), 734-740.

Orjuela-Cañón, A., Posada-Quintero, H., Delisle-Rodríguez, D., Cuadra-Sanz, M., de la Vara-Prieto, R. F., & López-Delis, A. (2013). Onset and peak detection over pulse wave using supervised SOM network. *International Journal of Bioscience, Biochemistry and Bioinformatics, 3*(2), 133-137.

Özbay, Y., Ceylan, R., & Karlik, B. (2006). A fuzzy clustering neural network architecture for classification of ECG arrhythmias. *Computers in Biology and Medicine, 36*(4), 376-388.

Özbay, Y., & Tezel, G. (2010). A new method for classification of ECG arrhythmias using neural network with adaptive activation function. *Digital Signal Processing, 20*(4), 1040-1049.

Padhy, S., Sharma, L., & Dandapat, S. (2016). Multilead ECG data compression using SVD in multiresolution domain. *Biomedical Signal Processing and Control, 23*, 10-18.

Pan, J., & Tompkins, W. J. (1985). A real-time QRS detection algorithm. *IEEE Transactions on Biomedical Engineering*(3), 230-236.

Paparde, A., Plakane, L., Circenis, K., & Aivars, J. I. (2015). Effect of acute systemic hypoxia on human cutaneous microcirculation and endothelial, sympathetic and myogenic activity. *Microvascular Research, 102*. doi:https://doi.org/10.1016/j.mvr.2015.07.005

Parkale, Y. V., & Nalbalwar, S. L. (2017). Application of compressed sensing (CS) for ECG signal compression: A review. *Proceedings on the International Conference on Data Engineering and Communication Technology* (pp. 53-65), Springer.

Physionet. (2013). Challenge 2013 dataset. Retrieved from https://www.physionet.org/challenge/2013/

Physionet. (2015). Physio bank ATM. Retrieved from http://www.physionet.org/cgi-bin/atm/ATM

Pierleoni, P., Pernini, L., Belli, A., & Palma, L. (2014). An Android-based heart monitoring system for the elderly and for patients with heart disease. *International journal of telemedicine and applications*. doi:10.1155/2014/625156

Porta, A., Guzzetti, S., Montano, N., Furlan, R., Pagani, M., Malliani, A., & Cerutti, S. (2001). Entropy, entropy rate, and pattern classification as tools to typify complexity in short heart period variability series. *IEEE Transactions on Biomedical Engineering, 48*(11), 1282-1291.

Qu, Z., Hu, G., Garfinkel, A., & Weiss, J. N. (2014). Nonlinear and stochastic dynamics in the heart. *Physics Reports, 543*(2), 61-162.

Raghav, S., & Mishra, A. K. (2008). Fractal feature based ECG arrhythmia classification. *Proceedings on the TENCON 10 Conference* (pp. Hyderabad, India, IEEE.

Rahman, M. A., & Islam, M. Z. (2014). A hybrid clustering technique combining a novel genetic algorithm with K-Means. *Knowledge-Based Systems, 71*, 345-365.

Rai, H. M., Trivedi, A., & Shukla, S. (2013). ECG signal processing for abnormalities detection using multi-resolution wavelet transform and artificial neural network classifier. *Measurement, 46*(9), 3238-3246.

Rajoub, B. A. (2002). An efficient coding algorithm for the compression of ECG signals using the wavelet transform. *IEEE Transactions on Biomedical Engineering, 49*(4), 355-362.

Ranck, J. (2014). The wearable computing market: A global analysis. Retrieved from http://electronichealthreporter.com/wearable-devices-wear-well-be-in-2014/

Ranjeet, K., Kumar, A., & Pandey, R. K. (2011). ECG signal compression using different techniques. In S. Unnikrishnan, S. Surve, & D. Bhoir (Eds.), *Advances in Computing, Communication and Control* (pp. 231-241): Springer.

Ranjeet, K., Kumar, A., & Pandey, R. K. (2013). An efficient compression system for ECG signal using QRS periods and CAB technique based on 2D DWT and Huffman coding. *Proceedings on the International Conference on Control, Automation, Robotics and Embedded Systems (CARE)*. Jabalpur, India, IEEE.

Reddy, B. S., & Murthy, I. (1986). ECG data compression using Fourier descriptors. *IEEE Transactions on Biomedical Engineering,* (4), 428-434.

Reed, M. J., Robertson, C., & Addison, P. (2005). Heart rate variability measurements and the prediction of ventricular arrhythmias. *Qjm, 98*(2), 87-95.

Ren, J. (2012). ANN vs. SVM: Which one performs better in classification of MCCs in mammogram imaging. *Knowledge-Based Systems, 26*, 144-153.

Ring, M., Jensen, U., Kugler, P., & Eskofier, B. (2012). Software-based performance and complexity analysis for the design of embedded classification systems. *Proceedings on the 21st International Conference on Pattern Recognition (ICPR)* (pp. 2266-2269). Tsukuba, Japan, IEEE.

Rodríguez-Liñares, L., Lado, M. J., Vila, X. A., Méndez, A. J., & Cuesta, P. (2014). gHRV: Heart rate variability analysis made easy. *Computer Methods and Programs in Biomedicine, 116*(1), 26-38.

Rodríguez-Liñares, L., Méndez, A. J., Lado, M. J., Olivieri, D. N., Vila, X. A., & Gómez-Conde, I. (2011). An open source tool for heart rate variability spectral analysis. *Computer Methods and Programs in Biomedicine, 103*(1), 39-50.

Rossi, P., Casaleggio, A., Chiappalone, M., Morando, M., Corbucci, G., Reggiani, M., . . . Chierchia, S. (2002). Computationally inexpensive methods for intra-cardiac atrial bipolar electrogram compression. *Europace, 4*(3), 295-302.

Saboul, D., Pialoux, V., & Hautier, C. (2014). The breathing effect of the LF/HF ratio in the heart rate variability measurements of athletes. *European Journal of Sport Science, 14*(sup1), 282-288.

Samarasinghe, S. (2016). *Neural networks for applied sciences and engineering: From fundamentals to complex pattern recognition*: CRC Press.

Sánchez-Barajas, M., Figueroa-Vega, N., del Rocío Ibarra-Reynoso, L., Moreno-Frías, C., & Malacara, J. M. (2015). Influence of heart rate variability and psychosocial factors on carotid stiffness, elasticity and impedance at menopause. *Archives of Medical Research, 46*(2), 118-126.

Sannino, G., De Falco, I., & De Pietro, G. (2014). Multi-purpose mobile monitoring system based on automatic extraction of rule-sets. *Proceedings on the International Conference on Biomedical and Health Informatics (BHI)* (pp. 630-634). Valencia, Spain, IEEE.

Sayadi, O., Shamsollahi, M. B., & Clifford, G. D. (2010). Robust detection of premature ventricular contractions using a wave-based Bayesian framework. *IEEE Transactions on Biomedical Engineering, 57*(2), 353-362.

Scully, C. G., Lee, J., Meyer, J., Gorbach, A. M., Granquist-Fraser, D., Mendelson, Y., & Chon, K. H. (2012). Physiological parameter monitoring from optical recordings with a mobile phone. *IEEE Transactions on Biomedical Engineering, 59*(2), 303-306.

Shimmer. (2015). Shimmer ECG sensor Retrieved from http://www.shimmersensing.com

Shin, S. Y., Park, H. S., & Kwon, W. H. (2007). Packet error rate analysis of IEEE 802.15. 4 under saturated IEEE 802.11 b network interference. *IEICE Transactions on Communications, 90*(10), 2961-2963.

Silva, I., & Moody, G. B. (2014). An open-source toolbox for analysing and processing physionet databases in Matlab and Octave. *Journal of Open Research Software, 2*(1). doi: 10.5334/jors.bi

Silva, I., Moody, G. B., & Celi, L. (2011). Improving the quality of ECGs collected using mobile phones: The physionet/computing in cardiology challenge 2011. *Proceedings on the Computing in Cardiology* (pp. 273-276). Hangzhou, China, IEEE.

Singh, B., Kaur, A., & Singh, J. (2015). A review of ECG data compression techniques. *International Journal of Computer Applications, 116*(11), 39-44.

Singh, B. N., & Tiwari, A. K. (2006). Optimal selection of wavelet basis function applied to ECG signal denoising. *Digital Signal Processing, 16*(3), 275-287.

Sloane, D., & Morgan, S. P. (1996). An introduction to categorical data analysis. *Annual Review of Sociology, 22*(1), 351-375.

Smith, A., Owen, H., & Reynolds, K. J. (2013b). Heart rate variability indices for very short-term (30 beat) analysis. Part 2: Validation. *Journal of Clinical Monitoring and Computing, 27*(5), 577-585.

Smith, A., Owen, H., & Reynolds, K. J. (2013a). Heart rate variability indices for very short-term (30 beat) analysis. Part 1: Survey and toolbox. *Journal of Clinical Monitoring and Computing, 27*(5), 569-576.

Song, M. H., Lee, J., Cho, S. P., Lee, K. J., & Yoo, S. K. (2005). Support vector machine based arrhythmia classification using reduced features. *International Journal of Control Automation and Systems, 3*(4), 571-579.

Sörnmo, L., & Laguna, P. (2005). *Bioelectrical signal processing in cardiac and neurological applications* (Vol. 8): Academic Press.

Sufi, F. (2011). *Efficient and secured wireless monitoring systems for detection of cardiovascular diseases.* (PhD Thesis), RMIT University, Australia.

Sufi, F., Fang, Q., Khalil, I., & Mahmoud, S. S. (2009). Novel methods of faster cardiovascular diagnosis in wireless telecardiology. *IEEE Journal on Selected Areas in Communications, 27*(4), 537-551.

Sufi, F., & Khalil, I. (2008). Enforcing secured ecg transmission for realtime telemonitoring: A joint encoding, compression, encryption mechanism. *Security and Communication Networks, 1*(5), 389-405.

Sufi, F., & Khalil, I. (2011a). Diagnosis of cardiovascular abnormalities from compressed ECG: A data mining-based approach. *IEEE Transactions on Information Technology in Biomedicine, 15*(1), 33-39.

Sufi, F., & Khalil, I. (2011b). Faster person identification using compressed ECG in time critical wireless telecardiology applications. *Journal of Network and Computer Applications, 34*(1), 282-293.

Sufi, F., Khalil, I., & Mahmood, A. N. (2011). A clustering based system for instant detection of cardiac abnormalities from compressed ECG. *Expert Systems with Applications, 38*(5), 4705-4713.

Szczepański, A., & Saeed, K. (2014). A mobile device system for early warning of ECG anomalies. *Sensors, 14*(6), 11031-11044.

Tai, S. (1991). Slope—A real-time ECG data compressor. *Medical and Biological Engineering and Computing, 29*(2), 175-179.

Tang, W., He, H., & Tu, X. M. (2012). *Applied categorical and count data analysis*: CRC Press.

Tarvainen, M. P., Niskanen, J., Lipponen, J. A., Ranta-Aho, P. O., & Karjalainen, P. A. (2014). Kubios HRV–heart rate variability analysis software. *Computer Methods and Programs in Biomedicine, 113*(1), 210-220.

Task Force of the European Society of Cardiology. (1996). Heart rate variability: Standards of measurement, physiological interpretation, and clinical use. *Circulation, 93*, 1043-1065.

Texas Instruments. (2015a). CC2420. Retrieved from http://www.ti.com/product/cc2420

Texas Instruments. (2015b). Download CCS. Retrieved from http://processors.wiki.ti.com/index.php/Download_CCS

Thong, T., Li, K., McNames, J., Aboy, M., & Goldstein, B. (2003). Accuracy of ultra-short heart rate variability measures. *Proceedings on the 25th Annual International Conference of the Engineering in Medicine and Biology Society* (pp. 2424-2427). Cancun, Mexico, IEEE.

Tsipouras, M. G., & Fotiadis, D. I. (2004). Automatic arrhythmia detection based on time and time–frequency analysis of heart rate variability. *Computer Methods and Programs in Biomedicine, 74*(2), 95-108.

Tsipouras, M. G., Fotiadis, D. I., & Sideris, D. (2005). An arrhythmia classification system based on the RR-interval signal. *Artificial Intelligence in Medicine, 33*(3), 237-250.

Tu, C., & Koh, W. Y. (2017). A comparison of balancing scores for estimating rate ratios of count data in observational studies. *Communications in Statistics-Simulation and Computation, 46*(1), 772-778.

Vaage-Nilsen, M., Rasmussen, V., Jensen, G., Simonsen, L., & Mortensen, L. S. (2001). Recovery of autonomic nervous activity after myocardial infarction demonstrated by short-term measurements of SDNN. *Scandinavian Cardiovascular Journal, 35*(3), 186-191.

Valvbrde, E., Quinteiro, R. A., Bertran, G. C., Arini, P. D., Glenny, P., & Biagetti, M. O. (1998). Influence of filtering techniques on the time-domain analysis of signal-averaged p wave electrocardiogram. *Journal of Cardiovascular Electrophysiology, 9*(3), 253-260.

Voss, A., Schroeder, R., Caminal, P., Vallverdú, M., Brunel, H., Cygankiewicz, I., . . . De Luna, A. B. (2010). Segmented symbolic dynamics for risk stratification in patients with ischemic heart failure. *Cardiovascular Engineering and Technology, 1*(4), 290-298.

Voss, A., Schulz, S., Schroeder, R., Baumert, M., & Caminal, P. (2009). Methods derived from nonlinear dynamics for analysing heart rate variability. *Philosophical Transactions of the Royal Society of London A: Mathematical, Physical and Engineering Sciences, 367*(1887), 277-296.

Vu, T. H. N., Park, N., Lee, Y. K., Lee, Y., Lee, J. Y., & Ryu, K. H. (2010). Online discovery of heart rate variability patterns in mobile healthcare services. *Journal of Systems and Software, 83*(10), 1930-1940.

Wang, J., Chiang, W., Hsu, Y., & Yang, Y. (2013). ECG arrhythmia classification using a probabilistic neural network with a feature reduction method. *Neurocomputing, 116*, 38-45.

Wang, J., Chiang, W., Yang, Y., & Hsu, Y. (2011). An effective ECG arrhythmia classification algorithm. *Proceedings on the 7th International Conference on Intelligent Computing* (pp. 545-550). Zhengzhou, China, Springer.

Wang, J., & Wang, J. (2016). Forecasting energy market indices with recurrent neural networks: Case study of crude oil price fluctuations. *Energy, 102*, 365-374.

Wang, Y., Zhao, X., Oneil, A., Turner, A., Liu, X., & Berk, M. (2013). Altered cardiac autonomic nervous function in depression. *BMC psychiatry, 13*(1). doi:https://doi.org/10.1186/1471-244X-13-187

Wang, Z., Ma, S., Zappitelli, M., Parikh, C., Wang, C., & Devarajan, P. (2016). Penalized count data regression with application to hospital stay after pediatric cardiac surgery. *Statistical Methods in Medical Research, 25*(6), 2685-2703.

Wasilewski, J., & Poloński, L. (2012). *ECG signal processing, classification and interpretation:* Springer.

Wenyu, Y., Gang, L., Ling, L., & Qilian, Y. (2003). ECG analysis based on PCA and SOM. *Proceedings on the International Conference on Neural Networks and Signal Processing* (pp. 37-40). Nanjing, China, IEEE.

Widjaja, D., Vlemincx, E., & Van Huffel, S. (2012). Multiscale principal component analysis to separate respiratory influences from the tachogram: Application to stress monitoring. *Proceedings on the Computing in Cardiology* (pp. 277-280). Krakow, Poland, IEEE.

Winkelmann, R. (2013). *Econometric analysis of count data*: Springer Science & Business Media.

Wolf, M., Varigos, G., Hunt, D., & Sloman, J. (1978). Sinus arrhythmia in acute myocardial infarction. *The Medical Journal of Australia, 2*(2), 52-53.

Xhyheri, B., Manfrini, O., Mazzolini, M., Pizzi, C., & Bugiardini, R. (2012). Heart rate variability today. *Progress in Cardiovascular Diseases, 55*(3), 321-331.

Yen, T., Chang, C., & Yu, S. (2013). A portable real-time ECG recognition system based on smartphone. *Proceedings on the 35th Annual International Conference of the Engineering in Medicine and Biology Society (EMBC)* (pp. 7262-7265). Osaka, Japan, IEEE.

Yochum, M., Renaud, C., & Jacquir, S. (2016). Automatic detection of P, QRS and T patterns in 12 leads ECG signal based on CWT. *Biomedical Signal Processing and Control, 25*, 46-52.

Yu, S., & Chou, K. (2008). Integration of independent component analysis and neural networks for ECG beat classification. *Expert Systems with Applications, 34*(4), 2841-2846.

Zhang, Y., Liu, C., Wei, S., Wei, C., & Liu, F. (2014). ECG quality assessment based on a kernel support vector machine and genetic algorithm with a feature matrix. *Journal of Zhejiang University SCIENCE C, 15*(7), 564-573.

Zhang, Z., Dong, J., Luo, X., Choi, K., & Wu, X. (2014). Heartbeat classification using disease-specific feature selection. *Computers in Biology and Medicine, 46*, 79-89.

Zhang, Z., Jung, T., Makeig, S., & Rao, B. D. (2013). Compressed sensing for energy-efficient wireless telemonitoring of noninvasive fetal ECG via block sparse Bayesian learning. *IEEE Transactions on Biomedical Engineering, 60*(2), 300-309.

Zhao, X., Tong, X., & Sun, J. (2013). Robust estimation for panel count data with informative observation times. *Computational Statistics & Data Analysis, 57*(1), 33-40.

Zhou, F., Jin, L., & Dong, J. (2017). Premature ventricular contraction detection combining deep neural networks and rules inference. *Artificial Intelligence in Medicine, 79*, 45-51.

Zidelmal, Z., Amirou, A., Ould-Abdeslam, D., & Merckle, J. (2013). ECG beat classification using a cost sensitive classifier. *Computer Methods and Programs in Biomedicine, 111*(3), 570-577.

Zigel, Y., Cohen, A., & Katz, A. (2000). The weighted diagnostic distortion (WDD) measure for ECG signal compression. *IEEE Transactions on Biomedical Engineering, 47*(11), 1422-1430.